



Durham E-Theses

Emission of ionising radiation during spark discharge

Bainbridge, G. R.

How to cite:

Bainbridge, G. R. (1953) *Emission of ionising radiation during spark discharge*, Durham theses, Durham University. Available at Durham E-Theses Online: <http://etheses.dur.ac.uk/9231/>

Use policy

The full-text may be used and/or reproduced, and given to third parties in any format or medium, without prior permission or charge, for personal research or study, educational, or not-for-profit purposes provided that:

- a full bibliographic reference is made to the original source
- a [link](#) is made to the metadata record in Durham E-Theses
- the full-text is not changed in any way

The full-text must not be sold in any format or medium without the formal permission of the copyright holders.

Please consult the [full Durham E-Theses policy](#) for further details.

Presented to Dr. W. A. Prowse,
with the compliments of
G. R. Bainbridge.

EMISSION OF IONISING RADIATION DURING SPARK DISCHARGE.

BY

G. R. BAINBRIDGE.

Being an account of work carried out at the University of Durham during the three years ending in September 1952.

Thesis submitted to the University of Durham for Ph.D. degree examination.

ACKNOWLEDGMENTS.

The author wishes to thank Professor J. E. P. Wagstaff and the staff of the Department of Physics, South Road, Durham, for the facilities and advice made available during the course of the investigation.

He is indebted to Dr. W. A. Prowse for his patient guidance and invaluable criticism while acting as research supervisor.

Finally, he wishes to record his gratitude to the Armaments Research Establishment for the loan of the high speed oscillograph used in the experiments.

CONTENTS.

i.

Acknowledgments.

Contents.

List of Figures.

List of Tables.

	Page.
<u>Section 1. Historical Survey.</u>	
1.1. Introduction.	1.
1.1.1. Nature of the problem.	3.
1.1.2. Summary of previous theoretical and experimental work on photo-ionisation in gases as a contribution to electrical breakdown.	4.
1.1.3. Indication of some of the data required for a better understanding of the spark mechanism.	23.
<u>Section 2. The Apparatus.</u>	
2.1. The experimental problem.	25.
2.1.1. General experimental requirements.	25.
2.1.2. The short test pulse and gap irradiation.	28.
2.2. Experimental arrangements and apparatus.	32.
2.2.1. Layout of apparatus.	32.
2.2.2. The triggering pulse circuit.	34.
2.2.3. The production of high voltage pulses of short duration.	35.
2.2.4. The circular variable delay lines.	38.
2.2.5. The test spark gap and the irradiator spark gap arrangement in the test chamber.	42.
2.2.6. The counting circuits.	48.
2.2.7. The loop detector unit and the counting of weak sparks.	50.
<u>Section 3. Measurement of the sparking probability in the test gap.</u>	55.
3.1. Mechanisms which might be stimulated by the irradiator spark and operate to increase the probability of sparking in the test gap.	55.

CONTENTS.

11.

	Page.
3.2. Test procedure and mechanical count records in the early experiments in air.	58.
3.2.1. Test procedure.	58.
3.2.2. The general shape of the test curves.	61.
3.2.3. The effect of overvoltage on sparking probability.	64.
3.2.4. The effect of test pulse timing on the graphs of sparking probability against irradiator pulse time.	65.
3.2.5. The effect of irradiator pulse timing on the graphs of sparking probability against test pulse time.	69.
3.2.6. The effect of introducing resistance in series with the test gap.	69.
3.2.7. The effect of introducing resistance in series with the irradiator gap.	75.
3.2.8. The effect of the termination of the delay line on sparking probability.	79.
3.2.9. The effect of the pulse forming condenser on sparking probability.	80.
3.3. Mechanical count records in gases.	82.
3.3.1. Conclusions from the early experiments.	82.
3.3.2. Pre-set electrode arrangements and electrical circuit constants in experiments with gases.	84.
3.3.3. Dry air.	84.
3.3.4. Nitrogen.	90.
3.3.5. Oxygen.	95.
3.3.6. Hydrogen.	99.
3.3.7. The facility for sparking of the gases tested with the same experimental conditions.	103.
<u>Section 4. Photographs of test gap sparks.</u>	
4.1. Introduction.	107.
4.1.1. Dry air spark photographs.	110.
4.1.2. Nitrogen spark photographs.	116.
4.1.3. Oxygen spark photographs.	118.
4.1.4. Hydrogen spark photographs.	120.
4.1.5. Summary of spark photograph phenomena.	122.

	Page.
<u>Section 5. Data obtained using the high speed oscilloscope.</u>	
5.1. Methods of recording the shape and duration of the test pulse used in the sparking probability experiments.	125.
5.1.1. Data required.	125.
5.1.2. The oscillograph.	125.
5.1.3. Recording methods.	126.
5.1.4. The shape and duration of the pulse on the delay line.	133.
5.2. Determination of the time taken for a wave to travel down the delay line and the delay incurred by one LC section.	138.
5.2.1. Theoretical consideration of the oscillations on the artificial delay line.	138.
5.2.2. Value of the delay time for 109 LC units. Oscillographic determination.	142.
5.3. Check on the length of the delay line by a resonance method.	148.
5.4. Correspondence of the oscillographically recorded traces of line oscillations with those by graphical construction.	151.
5.5. Determination of the attenuation constant for a voltage pulse travelling down the delay line.	155.
<u>Section 6. Measurement of the absorption coefficient for the active radiation in argon, air, oxygen, nitrogen and hydrogen.</u>	
6.1. Introduction.	159.
6.1.1. Apparatus and method.	161.
6.1.2. Theory of the method of measuring absorption coefficients.	163.
6.1.3. Absorption coefficient for argon.	165.
6.1.4. Absorption coefficients in air, nitrogen, oxygen and hydrogen.	171.
6.1.5. Summary of absorption coefficient results.	174.
<u>Section 7. Discussion of the results of experiments.</u>	
7.1. The broad theory of spark initiation.	178.
7.2. Time lags before sparking.	182.

CONTENTS.

iv.

	Page.
7.3. The time lag test curves and pulse length.	185.
7.4. Effect of radiation or ionisation in the test gap.	187.
7.5. The expected effect of time of irradiation on sparking compared with that observed.	188.
7.6. The unexpected failure of irradiation.	192.
7.6.1. Occasional appearance of finite sparking probability for widely separated pulses.	193.
7.7. Processes of removal of electrons from the gap.	194.
7.8. Processes of electron production that might be initiated by photons in the gas.	196.
7.9. The action of the applied field and photons together.	200.
7.9.1. The release of electrons and recapture.	200.
7.9.2. Release of photo-electron only if an electric stress is also applied.	204.
<u>Appendix 1.</u> High voltage supply unit.	207.
<u>Appendix 2.</u> Ancillary vacuum plant.	209.
<u>Bibliography.</u>	217.

List of Figures.

v.

	Page.
1. Ionising potentials and expected threshold ionising wavelengths for some of the common gases.	8.
2. Layout of apparatus.	31.
3. Triggering pulse circuit.	33.
4. Pulse forming and delay circuits.	36.
5. Arrangement of the artificial delay lines, (plate).	39.
6. Two delay line sections.	40.
7. a) Test gap, b) Irradiator gap, c) Experimental arrangement of a) and b).	43.
8. a) Mounting chassis, b) Test chamber.	44.
9. Basic thyratron counter circuits.	47.
10. Detector circuits for spark counters.	48.
11. Variation of sparking probability (P) with irradiator pulse time for a fixed test pulse time. Effective pulse times are indicated for applied voltage 24 Kv.	60.
12. Variation of P with test pulse time for fixed irradiator pulse time. Effective pulse times are indicated for applied voltage 24 Kv.	62.
13. Variation of sparking probability with irradiator pulse time for fixed test pulse times.	67.
14. Variation of sparking probability with test pulse time for fixed irradiator pulse times.	71.
15. Variation of P with irradiator pulse time for fixed test pulse time. The effect of resistance in series with the test gap is illustrated.	73.

List of Figures.

vi.

	Page.
16. Time changes introduced by inserting resistance in series with the test gap.	74.
17. Variation of P with irradiator pulse time for a fixed test pulse time. The effect of resistance in series with the irradiator gap is illustrated.	77.
18. Variation of P with irradiator pulse time for a fixed test pulse time. The effect of change in pressure is illustrated.	89.
19. Photographs of sparks formed in air.	111.
20. Photographs of sparks formed in air, etc.	112.
21. Photographs of sparks formed in air, nitrogen, oxygen and hydrogen under similar test conditions.	113.
22. Photographs of sparks formed in nitrogen.	115.
23. Photographs of sparks formed in nitrogen, etc.	117.
24. Photographs of sparks formed in oxygen.	119.
25. Photographs of sparks formed in hydrogen.	121.
26. Early warning pulse circuit for high speed oscillograph.	123.
27. Potential dividers.	132.
28. Choice of the best value of line termination.	135.
29. Test pulse used in the sparking probability experiments, (plate).	137.
30. The natural oscillation of a line in the absence of distortion but with attenuation.	141.

List of Figures.

vii.

	Page.
31. The nature of the repetitive pattern with $R_c = 0$ or infinity depends on the point of connection of the leads to the oscilloscope.	144.
32. The repetitive pattern of line oscillations for two points of connection of the oscillograph leads, as displayed using the medium and high speed time bases.	145.
33. The repetitive pattern of line oscillations for three different line lengths as displayed using the medium and high speed time bases.	146.
34. Typical set of measurements on the repetitive line oscillations to obtain the delay resulting from one LC section of the line.	147.
35. Determination of the length of a delay line of 160 LC units by a method of resonance detection.	149.
36. Addition of incident and subsequently reflected rectangular pulses to give the resultant C.R.O. trace.	155.
37. Determination of the attenuation constant.	157.
38. Apparatus for the determination of absorption coefficients.	160.
39. Showing the beam of photons restricted to the sensitive volume of gas between the electrodes.	164.
40. Absorption coefficient of argon. No change with applied voltage.	168.
41. Absorption coefficient of argon. Small change with gap length.	168.
42. Absorption coefficient of argon. Little change with irradiator timing.	170.

List of Figures.

viii.

Page.

43.	Absorption coefficient of air.	172.
44.	Expected experimental curve for $\log n_p/n = 0.454 t/t_g$.	184.
45.	Expected experimental curve for $100 n_p/n$ against time.	186.
46.	Expected experimental curve for $100 n_p/n$ against time with early irradiation of the gas.	189.
47.	Expected test curves, presuming 2 microsec. electron life.	191.

Appendix figures.

A1.	50 Kv. D.C. supply unit.	208.
A2a.	High vacuum system.	210.
A2b.	Bellows differential pressure gauge.	212.
A2c.	Calibration graph for the differential pressure gauge.	214.
A2d.	Movement detected circuit for bellows differential gauge.	216.

List of Tables.

ix.

Page.

1. Variation of P with irradiator pulse time for fixed test pulse times. 66.
2. Variation of P with test pulse time for fixed irradiator pulse times. 70.
3. Variation of P with irradiator pulse time for fixed test pulse time, The effect of resistance in series with the test gap is illustrated. 72.
4. Variation of P with irradiator pulse time for fixed test pulse time, The effect of resistance in series with the irradiator gap is illustrated. 76.
5. Variation of P with irradiator pulse time for fixed test pulse time. The effect of delay line termination is illustrated. 80.
6. Variation of P with irradiator pulse time for fixed test pulse time. The effect of line input condenser value is illustrated. 81.
7. Probability counts for dry air at six set pressures and applied voltage 24 Kv. 86.
8. Probability counts for dry air at six set pressures and applied voltage 20 Kv. 87.
9. Probability counts for nitrogen at five set pressures and applied voltage 24 Kv. 91.
10. Probability counts for nitrogen at five set pressures and applied voltage 20 Kv. 92.
11. Probability counts for nitrogen at five set pressures and applied voltage 16 Kv. 95.
12. Probability counts for oxygen at four set pressures and applied voltage 24 Kv. 97.

List of Tables.

	N.
	Page.
13. Probability counts for oxygen at four set pressures and applied voltage 20 Kv.	98.
14. Probability counts for hydrogen with applied voltage 24 Kv.	100.
15. Probability counts for hydrogen at four set pressures and applied voltage 20 Kv.	101.
16. Probability counts for hydrogen at five set pressures and applied voltage 16 Kv.	102.
17. Irradiator positions at which sparking probability of 0.5 was recorded in hydrogen, nitrogen, air and oxygen; 20 Kv. pulses.	104.
18. As for Table 17, 24 Kv. pulses.	105.
19. Experimental values for the absorption coefficients in the gases examined.	174.
20. Survey of work determining the absorption coefficients for photons in some gases.	176.

SECTION 1.Historical Survey.1.1. Introduction.

Photo-ionization in gases is of importance in studies of many forms of electrical discharge in gases, (Meek¹ 1940; Loeb and Meek² 1941; Weisaler³ 1943; Korff⁴ 1946; Craggs and Jaffe⁵ 1947; Frense and Jasinski⁶ 1950 and many others). In atmospheric problems too, at heights greater than 20 Km., where the short wavelength radiation of the sun is able to penetrate, the property of ionization of gas atoms and molecules by photons is of great interest, (Massey⁷ 1958; Sayers⁸ 1943; Appleton⁹).

The singular lack of experimental data on the photo-ionization of air and other permanent gases has been repeatedly indicated in the literature^{10,11,12,13}, a situation which contrasts with the volume of data accumulated from studies of the photo-electric effect in the alkali metal vapours¹⁰. This difference in the state of knowledge in the two allied branches of work is due mainly to the fact that the energy of the quantum needed for ionization in the alkali vapours is

* For this and subsequent references see the end of this work.

much less than that needed to ionise a gas atom in a single stage. Moreover, most of the early work on photo-ionisation in gases was restricted by the difficulty of obtaining a material, to serve as a window between the source of radiation and the gas to be examined, which would transmit the shorter wavelengths.

That the action of short wavelength radiation can be responsible for the high speed development and propagation of spark channels where the product of pressure of gas (p in mm. Hg.) and distance of electrode separation (d in cm.) exceeds 200 is well established in the literature. The actual mechanism in which the radiation takes an active part is by no means certain and will be discussed later in this work. No lower limit has been set for the time taken from the emission of a light quantum in one part of the developing spark channel to the completion of its action in another part of the gas. It was thought that a type of experiment should be devised in which the photo-electric process is allowed only a limited time to develop and complete its action in the gas. The present study of the possible use of the unidirectional

high voltage pulse of short duration, as applied to plane parallel electrodes in some of the common gases, was therefore undertaken.

1.1.1. Nature of the problem.

The aim of the work has been to develop high speed methods of test, believing that such methods would give information about a mechanism which occurs at speeds which, with sufficient applied electric stress, result in spark development in centimeter gaps in a time less than 10^{-7} sec.

The proposed scheme was to apply a direct high voltage pulse for a small fraction of a microsecond to a test gap, with gas pressure and electrode separation so arranged that a spark would hardly ever develop* completely in the duration of the pulse because of the rare natural appearance in the gap of a suitably placed triggering electron. By introducing the radiation from a naked spark, formed in the same gas, at a suitable time into the gas between the test electrodes the chance of a spark occurring because of the pulse should increase. A count of the increase in the number of sparks occurring for a given number of pulses

* See section on time lags in sparking.

applied to the test gap should be an indication of the success of the radiations incident in the stressed gas. An experiment has been conducted in which the time at which the radiations enter the gas was varied and the increase in the chance of a spark developing in the gap has been recorded for each particular time separating the irradiator voltage pulse and the pulse applied to the test gap. The careful way in which the radiations have been restricted to the volume of the stressed gas and not allowed to fall on the electrodes offers confirmation to the evidence, set out in the account of the literature which follows, that the effect of the photons can be of major importance in the spreading of electric discharge in gases.

1.1.2. Summary of previous theoretical and experimental work on photo-ionisation in gases as a contribution to electrical breakdown.

That the incidence of ultra-violet light on a spark gap facilitates the passage of a spark was discovered by Hertz in 1887¹⁴. This was followed by a number of investigations¹⁵ into the photo-electric property as applied to solids and

liquids. This study showed that a separation of charge occurred at the surface of the substance irradiated, the degree of separation depending on a) the substance examined, b) the wavelength and intensity of the incident light and c) the potential gradient near the surface of the substance.

For the atoms and molecules of a gas affected in a similar way by ultra-violet light the effect should be detected as an increase in the ionisation in the gas. It was shown by Lenard¹⁶ and C.T.R. Wilson¹⁷ that irradiation of a gas by intense ultra-violet light did produce new nuclei which were easily revealed in an expansion chamber experiment. But as the mobility of these nuclei was demonstrated to be less than that for small positive and negative ions the effect was attributed to the photo-electric action at the surface of small dust particles.

The first definite evidence that air can be photo-ionised is attributed to Hughes¹⁸, who filtered his dry air and irradiated it through a fluorite window. The resulting ions were shown to be of the same mobility as those produced by X-rays acting on the same gas; no expansion ratio of less

than 1.25 would show condensation nuclei in the cloud chamber, thereby demonstrating the absence of 'large' ions.

The lower wavelength limit of transparency for Hughes' fluorite specimen was never determined because it broke. On replacing the window with crystalline quartz he found no photo-ionisation of air. Using Lyman's data¹⁹ on the transparency of quartz and fluorite it appears that the experimentally determined threshold wavelength for the ionisation of air lies between 1250 Å and 1450 Å. Later workers^{20, 21, 22} confirmed this observation, noting that the radiations responsible for the ionisation of air, oxygen and nitrogen were lost entirely by absorption when passed through 1 cm. thickness²⁰ of oxygen at atmospheric pressure as well as the fluorite walls of the absorption cell. The ionisation currents measured in air, ^{oxygen,} nitrogen and carbon dioxide²² under the same conditions of illumination were proportional to the numbers 135, 100, 155 and 152 respectively.

The first study of a gas ionised by its own radiations was made by Mohler²⁵. At one end of a tube the electrons from a hot filament were driven through a gas at controlled speed.

The radiations from this controlled low pressure discharge were restricted to enter the gas alone in another section of the tube where the current between two electrodes was space-charge limited. The change in current as a result of the radiations was a measure of the ionisation produced in the gas for a known excitation level of the gas atoms and molecules in the controlled discharge. Only the excitation of the spark lines in the controlled discharge was found to give appreciable ionisation in the gas of the detector section of the tube, which was accepted as reasonable after consideration of the energies involved. Working at near atmospheric pressure J. Thomson²⁴ was able to show that photons from a heavy current hydrogen discharge are able to ionise hydrogen gas and suggested that ionisation might be completed in more than a single stage under these conditions.

Excluding the work of Mohler and Thomson all observers mentioned so far used fluorite windows between the source of radiation and the gas under test, the observation being made that the threshold ionising wavelength for the common gases lies between 1250 Å and 1450 Å. But the table

of ionising potentials, as determined by Mackay²⁵ and Morris²⁶ shown in figure 1, indicates that the corresponding threshold wavelengths should be lower than the shortest wavelengths transmitted even by fluorite. Photon effects other than the direct ionisation of the atom or molecule by absorption of a single quantum of energy must therefore be considered.

Fig. 1. Ionising potentials and expected threshold ionising wavelengths for some of the common gases.

Gas	Ionising Potential (V_1 in volts)	Threshold Wavelength (λ_1 in \AA units)
O ₂	12.5	990
N ₂	16.5	960
H ₂	13.8	780
CO ₂	14.5	860
NO	9.5	1300
H ₂ O	13.2	940

The threshold wavelength, λ_1 , has been calculated in each case presuming the quantum equation $eV_1 = h/\lambda_1$ to hold for photo-ionisation in gases.

Varney and Loeb²⁷ (1935) have attempted to check some of the

work of previous observers of photo-ionisation in gases using the balanced space charge method for the detection of any ionisation present. Using a spark in hydrogen as the source of radiation they were unable to measure ionisation present in any gas, except that attributable to electrostatic effects, when the radiation entered the gas through a fluorite window transmitting down to 1500 \AA . In a second experiment using apparatus similar to that of Mohler, strong photo-ionisation was detected for argon and xenon (and weak ionisation in nitrogen and air) by radiation arising in the same gases. No photo-ionisation was detected when the gas acting as the source of the radiations was excited to less than its ionising potential. In all gases the photo-ionising radiations were not transmitted when specimens of thin fluorite and quartz were inserted between the source and the test gas.

In assessing the earlier work Varney and Loeb have indicated possible alternative explanations of the observed photo-ionisation of gases by radiations transmitted by certain cuts of fluorite, which they themselves were not able to detect. They thought that Lenard¹⁶ might have been

observing as ionisation the electrostatic coupling between the source of radiation (a high frequency spark between aluminium electrodes) and detector of ionisation. The fluorite specimen used by Hughes¹⁸ might have been a rare specimen, porous to shorter wavelengths than estimated, or his failure to eliminate mercury vapour, or the products of sustained air discharges such as the oxides of nitrogen, from his apparatus could have provided in the test chamber a substance which is ionised by wavelengths above the 1300 Å fluorite transmission limit. Palmer²⁰ also unwittingly reduced the value of his work by allowing the presence of mercury vapour. The work of Oldenberg²³, who observed that a thin film of collodion 10^{-5} cm. thick, when placed between the light source and the gas, caused the entire fluorescence spectrum of normal and ionised nitrogen to disappear, would appear to favour the idea that a much shorter wavelength than 1300 Å is required to photo-ionise in the permanent gases. Though the property of photo-ionisation in some gases is firmly established in the literature since 1935 there is no definite experimental evidence of the actual threshold wave-

lengths for the individual gases.

Photo-ionisation in the volume of the gas between electrodes subject to a high direct voltage was one of a set of possible mechanisms considered by Brode and Neuman²⁹ (1928) which might lead to the unstable condition made manifest by the passage of a spark through the gas. It was there shown that, with certain simplifying assumptions, all of the suggested mechanisms could lead to general equations similar to that arrived at by Townsend³⁰ (1903). He had treated the development of sparking as the instability due to cumulative ionisation by collision of the positive ions and electrons with gas atoms. The general Townsend theory, which was later proposed² in an attempt to reconcile theoretical and experimental evidence, took the occurrence of a spark to indicate the failure of equilibrium conditions between the processes of production and removal to the electrodes of ions initiating in the gap. Possible ion production mechanisms for this general Townsend equation could include :-

1. Ionisation by positive ions, a) at the cathode,
b) in the gas.
2. Photo-ionisation by short wavelength quanta,

- a) at the cathode,
- b) in the gas.

Whatever the operative mechanism might be for the production of new ions, whether dependent on the cathode material or on the gas alone, formative time is required for the growth of unstable conditions in the gap. Measurements of formative time lags in slightly overvolted long gaps (pd greater than 200 mm. Hg. x cm.) were shown to be independent of cathode material² and inconsistent with the assumption that positive ions cross the gap during the formative stages of breakdown.

Pedersen³¹ (1925) estimated this formative time to be of the order of 10^{-7} sec. in centimeter gaps at atmospheric pressure in air. The works of Torok³², Beams³³, Tamm³⁴ and Rogowski³⁵ measured formative times of 10^{-8} sec., when 20 % overvoltages and cathode illumination were used. Dunnington³⁶, White³⁷, Tilles³⁸ and others³⁹ have added confirmatory weight of evidence in favour of times as short as 10^{-9} sec. with the gap sufficiently overvolted. A mechanism by which the spark could develop with a velocity approaching that of light is one

in which high energy quanta, produced by some as yet undetermined means in the developing spark channel, radiate into the surrounding gas, rapidly extending the zone of ionisation to bridge the gap.

Experimental evidence in favour of photo-ionising radiation as the active agent in the spreading of many forms of discharge has accumulated convincingly since 1930. It is believed to be an important feature in the operation of positive wire Geiger counters, as shown by Greiner⁴⁰ (1935). High energy photons arising in the gas in the intense field region near the positive wire were then believed to be little absorbed in the low pressure gas, to reach the negative cylinder and there release one photo-electron for every 10^3 to 10^4 photons incident³⁷. Recently Graggs, Jaffe⁵ and co-workers have shown that the spread of the Geiger counter discharge can occur in suitable gases when no photons could possibly reach the cathode, because of the experimental arrangement used. They attribute this effect to photo-ionisation in the gas itself.

Photo-ionisation in the gas has been studied by Gravath⁴¹ (in corona discharges in 1935) and Dechens⁴² (1930),

who showed that radiations emitted by the excited gas are heavily absorbed in air. Both investigators found the radiations to consist of two wavelength groups, one more penetrating than the other. The more heavily absorbed radiations penetrated only 1 mm. of air at atmospheric pressure, (absorption coefficient 10 cm.^{-1}), but ionised air strongly. The more penetrating radiations (absorption coefficient 2 cm.^{-1}) were calculated to be able to release, if incident on a brass surface, one photo-electron for every 10^5 normal electrons in the body of the gas where the photons originate.

Jones F. L.⁴⁵ has recently indicated that photo-ions created in the gas of the gap by radiation emitted from minute corona discharges occurring at microscopic points might have been the cause of the reduction of sparking potentials and time lags observed by Howell⁴⁴ (1939), for there the effect was independent of whether the roughened electrode was the anode or the cathode and so would depend on the electric field alone.

Trichel⁴⁵ and Kip⁴⁶ working with positive point to

plane corona discharges noted bursts of current to the point, irregular in amplitude and time of occurrence. These they believed to be triggered by photons emitted from the space charge left behind after a previous avalanche of electrons to the point. Even when the negative plane was remote from the point the bursts continued, indicating that the photons could be active in the gas alone. Flegler⁴⁷, Raether and Costa⁴⁸ obtained some interesting cloud track photographs of avalanches of electrons initiated in electric fields between parallel planes, where photons entered the gas. Absorption coefficients calculated for the ionising wavelengths in air, by counting the avalanches arising in centimeter lengths of the beam of radiation, correspond to those for the most penetrating radiation noted by Cravath and Dechene, 2 cm^{-1} at atmospheric pressure. Values of absorption coefficients for oxygen and hydrogen measured under the same conditions were calculated to be 5 cm^{-1} and 0.8 cm^{-1} respectively.

In an experiment by Prowse and Jasinski⁶ it was shown that an ultra-high frequency discharge between plane-parallel electrodes could be triggered by irradiation of the

inter-electrode gas with a fine pencil of ultra-violet light from a naked spark. A narrowing or waist in the middle of certain mid-gap air sparks, which occurred along the track of the irradiating pencil suggested that they started from there and developed simultaneously towards both electrodes. Measurement of the absorption coefficients for the radiations responsible for triggering the discharges in air and oxygen, worked out by several methods, was in fair agreement with the values obtained above^{40,41.}

An explanation of the stepped leader strokes in the lightning discharge, described by Schonland and Collens⁴⁹ (and by Allibone and Meek⁵⁰) has been attempted^{51,52.} on the basis that air is photo-ionised ahead of the developing streamer by radiation from parts of the air already highly ionised. In fact it appears likely that photo-ionising radiation as an active mechanism in spreading the discharge in the gas must be considered for all long sparks, (Cravath and Leeb⁵²), and also in cases where the electrodes are remote or otherwise unable to affect the discharge⁵³ because of the imposed experimental conditions.

Consideration of experimental evidence for the test gap conditions giving values of pd less than 200 mm.Hg. x cm. shows that the general Townsend theory is still tenable. There is not, however, much experimental evidence as yet to support the view that a Townsend mechanism can operate at higher values of pd . A recent paper of Jones F.L.⁷¹ and collaborators has examined the possibility, suggested as early as 1928³⁹, that photons active in the gas can give a secondary mechanism to satisfy the general Townsend equation. The equation derived,

$$I = I_0 \exp(\alpha d) / \{ 1 - [\exp((\alpha - \gamma)d) - 1] \phi \},$$

where ϕ is a combination of constants $\theta fg\gamma/(\alpha - \gamma)\alpha^*$, is of the same analytical form as the general Townsend equation when γ is some fraction of α . When γ is large the equation simplifies so that photo-ionisation in the gas introduces a constant factor, independent of gap length, by which the initial current through the gap is enhanced.

Detailed examination of the equation for large values of γ

- * θ is number of photons produced per cm. electron path.
- f is number leading to photo-ionisation.
- g is geometrical factor. γ is absorption coefficient.
- α is number of electrons produced per cm. electron path.
- d is gap length.

shows that the growth of current in the gap to the instability of sparking is not improved by photo-ionisation in the gas. Propagation of the discharge streamer in air seems most likely when a value of μ for ionising radiations less than 7.5 cm.^{-1} is used, (values of this order were obtained, e.g. by Raether, 1938; Cravath, 1935; Wynn Williams, 1926.), allowing new electrons to be liberated some distance from the source of photons in order to regenerate the initial electron avalanche. Under these conditions it is apparent that in short gaps the effect of photons reaching the cathode is going to be appreciable, but in long gaps the discharge streamer might progress by photo-ionisation of the gas alone.

The possible source of production in the gas of quanta with sufficient energy to ionise other gas atoms and molecules of the same gas has been considered recently by Hopwood¹². Of the processes examined, namely :-

1. Ionisation of atoms by electron collisions, with the removal of an electron from an inner shell and the emission of soft X-rays,
2. Excitation of positive ions by a second electron collision,

B.

and 3. Recombination of an electron and a positive ion, with a return of the electron to the ground state, that set out in 3. is shown to be most likely to satisfy the Meek⁵⁴ criterion for the propagation of a positive streamer. Such a recombination process would be most likely to occur when the advance of the electron avalanche is retarded by the growth of positive space charge, as for example when the electron avalanche approaches the anode in breakdown between electrodes; in this last case the density of positive ions at the tail of the electron avalanche is most likely to be sufficient to reduce the applied field to zero.

Working with slight overvoltages of a fraction of one percent applied to parallel plate electrodes, Fisher and Pederson⁵⁶ have obtained long delay times of 100 microseconds and over before eventual breakdown. The length of the delay was a function of overvoltage and plate separation; it was independent of the intensity of cathode illumination and gas pressure for values of pd more than 200. The association, in their experiments, of a statistical component with a formative time lag could arise from the possibility of success or

or failure to convert initial electron movement into a successful streamer-propagating avalanche. An electron avalanche might develop in part of the inter-electrode space where, because of the weakness of the electric field or the proximity of the positive electrode, the cumulative growth of ionisation is small. High energy photons emitted from the plasma of positive ions and electrons at the tail of the electron avalanche could possibly release new photo-electrons in the surrounding gas; but unless the field strength of the plasma is sufficient to cause a new electron avalanche (Loeb⁵⁷), or new avalanches (Loeb and Wijzman⁵⁸), to feed into and extend the plasma volume, the positive streamer will not develop. In this case a time delay would be introduced pending the production of a photo-electron (or other electron) in another part of the volume of the gap which gives the sufficient conditions for a successful avalanche. The eventual streamer-propagating avalanche could possibly owe its success to the fact that it travels in an excited atmosphere of gas atoms. Excited atoms could be created by photons of less than ionising energy from the previous unsuccessful avalanches. Though the transfer of ionisation from an unsuccessful avalanche to one which starts

the propagation of a successful streamer is actually a formative process, in measurement it will appear, together with the wait for a casual electron, as a statistical lag rather than a formative one, unless it is the invariable process.

Photographic evidence from many sources in the last thirty years supports the view that the gas ahead of the tip of the developing streamer (or leader stroke) is photo-ionised. Slepian and Torok^{59,60} applied chopped impulse voltage waves to sphere gaps and photographed the resulting suppressed discharges. By adjustment of the length of the delay line leading to an auxiliary gap in parallel with the test gap, the impulse voltage applied to the spheres was rapidly reduced to zero before the streamer had time to develop fully. Where the streamer crossed only part of the gap photographs showed that the remainder was bridged by a diffuse region, light purple in colour in air sparks. Flowers⁶¹ suggested that the hazy streaks observed by Dunnington⁶² in shorter gaps, at pressures near one atmosphere, might be of the same nature.

Koselkov^{63,64} has used a rotating camera technique to record the growth of streamers initiating breakdown in a point

to plane gap with 40 cm. electrode separation. His photographs show that the tip of the streamer is preceded by a luminous cloud some ten to twenty cm. in radius, stated to consist of minute filamentary streamers. The final leader stroke channel was less than 0.4 cm. wide. Using electrode systems similar to those of Kowalkov, photo-multipliers have been used by Saxe and Meek⁶⁵ to detect radiation in a zone approximately 20 cm. in diameter, which preceded the leader stroke. They showed that the velocity of streamer propagation in the gas was reduced by an increase in the resistance in the leads to the electrodes. About two microseconds separated the detection of the first diffuse radiation and the tip of the leader stroke.

The filamentary nature of the diffuse discharge has been described by Allibone⁶⁶ for the case of the corona developed at a positive point four feet from an earthed plane, when an impulse voltage just less than that required to give spark-over was applied. Further confirmation of the nature of the leader stroke is given in papers by Allibone and Meek⁶⁷, by Allibone⁶⁸ and by Loeb⁶⁹. Two mechanisms have been suggested tentatively to account for the luminous cloud¹⁵ observed in the positive point

discharges where the cathode is remote. The first of these requires the excitation of the volume of the gas by electrons drawn laterally into the space charge left behind positive streamers, where the residual density of ionisation is insufficient to encourage the succeeding discharges to follow the same path. The second possibility is that photo-excitation of the gas is caused by photons less strongly absorbed than those leading to the propagation of the streamer.

1.1.3. Indication of some of the data required for a better understanding of the spark mechanism.

In an experiment carried out by Prowse and Jasinski⁶, the short wavelength radiation from a partly developed spark in air was used to irradiate the gas, but not the electrodes, of a second spark gap. The probability of a spark developing in the second gap during the test pulse, with irradiation of the gas, was shown to exceed the chance of a spark for a similar pulse without irradiation. This was taken to indicate that energetic quanta are emitted from the early stages of spark formation which are able to penetrate up to 10 cm. of gas at atmospheric pressure. The radiation had an effect on the test gas which was thought to be the production by the photons of at least a casual electron to

trigger the test spark; this observation was supported by the work of previous investigators^{27,41,42.} and on general grounds by the study of Hemsalech⁷⁰ noting that the air lines of the spectrum appear in the spark track before those of the metal of the electrodes. To determine the true mechanism by which the radiations from the early stages of one unidirectional spark can create the requisite conditions for a spark in the gas between a second pair of electrodes further experiments are required.

It has been indicated¹³ that theoretical equations already deduced^{57,58,71.} cannot lead to the prediction of values for sparking potentials and formative time lags to fit experimentally determined values without reliable measurements of, for example :-

1. The source of the photons responsible for the spread of ionisation in the gas,
2. The particular wavelength regions responsible for photo-emission and photo-excitation of electrons in the atoms and molecules of individual gases,
3. The efficiency as ionising agents and the range of the photons active.

SECTION 2.The Apparatus.2.1. The experimental problem.2.1.1. General experimental requirements.

Although the experiments already discussed have demonstrated the presence of ionising radiation in the gap during spark discharge, there is no indication, other than the internal evidence of the spark itself, of the stage at which such radiation first makes its appearance, or of how long the emission lasts. If, for example, the radiation is the result of recombination processes between electrons and positive ions in the gas, these might be expected to persist after the completion, electrically and visibly, of an impulsive spark.

The present work deals with an attempt to examine the variation of emission of ultra-violet radiation with time during the early stages of spark discharge.

The intention was to develop an electrical circuit to give two pulses of direct high voltage so that the pulses could be moved on a time scale through one another. One pulse was to be applied to a test gap; the second pulse was to be applied

to give a spark in an irradiator gap, from which radiation could enter the gas of the test gap without striking the electrodes. By adjustment of the two pulses on the time scale, the effect on the sparking of the test gap could be studied with the radiation emitted a) earlier than, b) coincident with, and c) during the later stages of the test pulse.

The effect of the radiation incident in the test gas was shown as an increase in the number of sparks developed in the test gap for a given number of trial pulses. The parameter used to gauge the effect of the radiation at a set irradiator pulse time relative to the starting time of the test pulse was termed the sparking probability of the test gap. This is defined as the fraction of the test pulses applied to the electrode system which result in a discharge; sparking probability will be indicated by the letter P.

As the effect of the radiation was expected to be greater at higher pressures² conditions of test were limited to electrode systems with a value of pd greater than 200 mm. Hg. x cm. The direct voltage applied to the test gap was greater than that which would give a spark if it were maintained indef-

indefinitely, but in the duration of the pulse no spark occurred for a large number of trials without irradiation of the test gas,

With the radiation entering the test gas much earlier (e.g. by several microseconds) than the start of the test pulse no change in the sparking probability was expected. For radiation entering the test gas more in coincidence with the test pulse time an increase in P should occur. With the radiation entering the test gas in the later stages of the test pulse the value of P was expected to fall off again as the time left after the irradiator pulse for the development of a spark in the test gap became shorter. For the range of times of irradiation between the early and late limits where no effect could be recorded, the size of the increase in P should be an indication of the value of the radiation, arising in the gas itself, at various stages of the applied test voltage pulse.

The initial problems were to devise arrangements by means of which :-

1. A test voltage greater than the minimum sparking potential could be rapidly, (instantaneously if possible), applied to the electrodes of the test gap, maintained there for

a small fraction of a microsecond and then equally rapidly removed ;

2. Short wavelength radiation of the type believed to be active in the developing spark channels could be produced and introduced into the test gas ;

3. The relative timing of the irradiator and the test voltage pulse could be adjusted and easily measured ;

4. Sparking probability could be measured for each condition of irradiation of the test gas ;

5. The inter-electrode gas and pressure could be adjusted; the vacuum system required had to be free from dust and unwanted gaseous contamination, while the pressure had to be easily measured using gauges which would not introduce mercury vapour into the test chamber.

2.1.2. The short test pulse and gap irradiation.

The choice of an unusually short duration pulse for the tests, to be of as near rectangular form as possible, was made so that the degree of accuracy in the subsequent measurements of sparking probability would be high. The many advantages of this form of voltage application become apparent when the time lags involved in sparking are considered. The time lag of a

spark discharge may be defined as the interval between the attainment of normal breakdown potential and the beginning of the rapid fall in potential across the gap as the gap breaks down. It may in general be divided into two parts, 1. a statistical time lag, being a wait for the particular triggering event in the sensitive volume of the gap and 2. a formative time lag required for the development of the discharge subsequent to the triggering event. With sustained voltages near to the minimum sparking value the total time lag can be of order 10^{-4} sec.⁵⁶, (a recent paper by Llewellyn Jones and Morgan¹¹¹ indicated that with carefully prepared 'conditioned' electrodes in pure gas the lag might be of the order of a minute even with large overvoltage), while with large overvoltage and/or electrode irradiation the total lag is reduced to less than 10^{-8} sec. (see references 32 to 39).

With an impulsive breakdown stress lasting less than a microsecond the statistical lag becomes of particular importance, for even with high overvoltages, unless this lag is short compared with the duration of the pulse, the sparks which develop will be few. The naturally produced casual electron or other chance triggering event might be relatively rare; in

this case the sparking probability due to background events becomes more negligibly small the shorter the test pulse.

The detailed nature of the triggering event introduced by the incidence of suitable photons in the gas of an overvoltage gap is not known. For the radiation to be introduced into the gas at a definite time relative to the time of application of the test pulse the irradiator has also to be pulse operated. The quickest type of irradiator which can be tripped into action is the overvoltage, pre-ionised spark gap; operating this in the same gas as the test gap the correct type of radiation for the experiments is made available. A short duration pulse applied to the irradiator at least defines the earliest possible time at which the irradiating photons can act; no precise limits can, however, be set for the actual duration of emission of the effective wavelengths, for these might come at a particular time in the development of the irradiator spark or over an extended period.

The time for which there is a possibility of photons emerging from the irradiator gap will be termed the effective irradiator pulse duration, which is chosen for purposes of

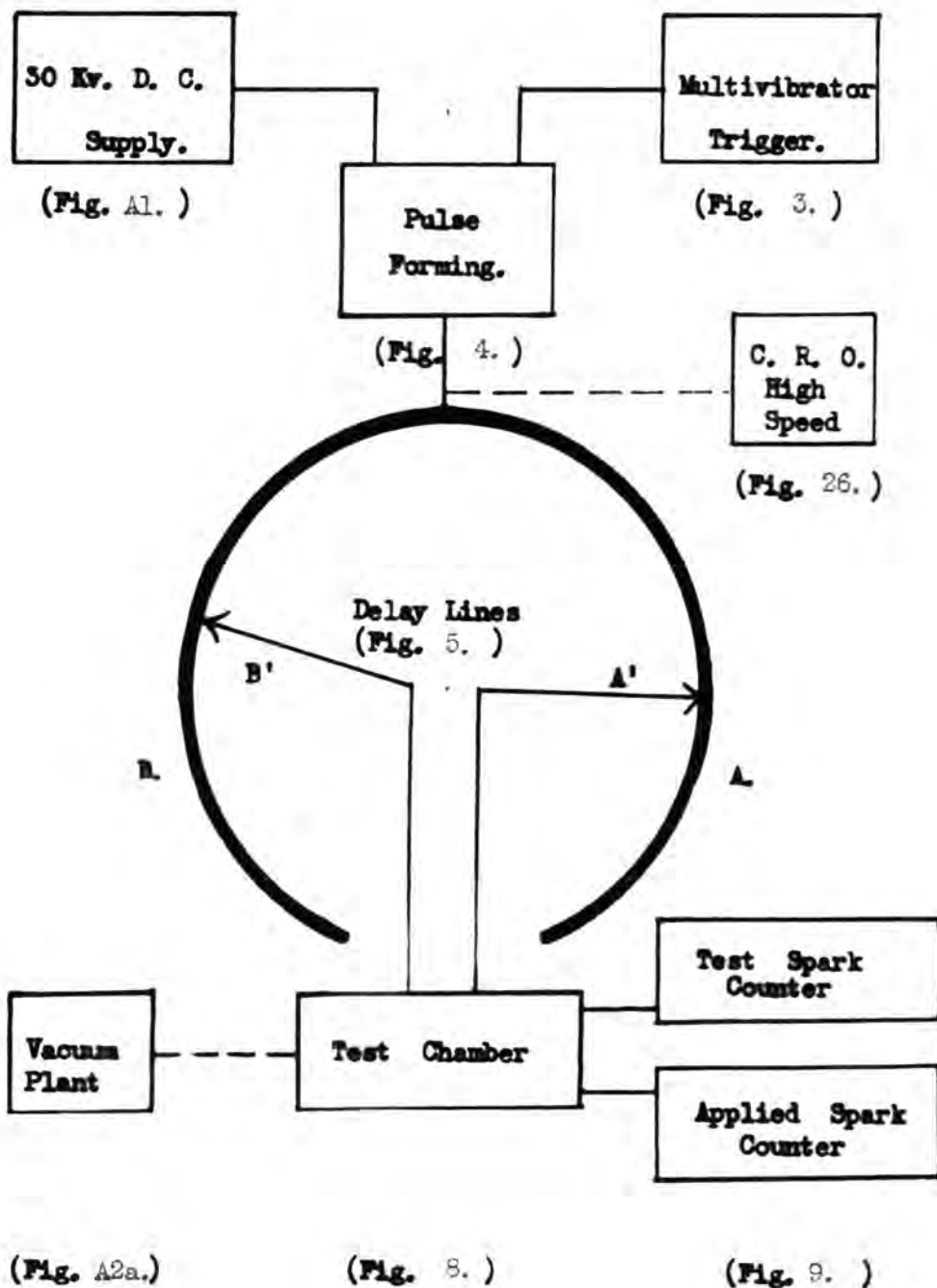
Fig. 2. Layout of Apparatus.

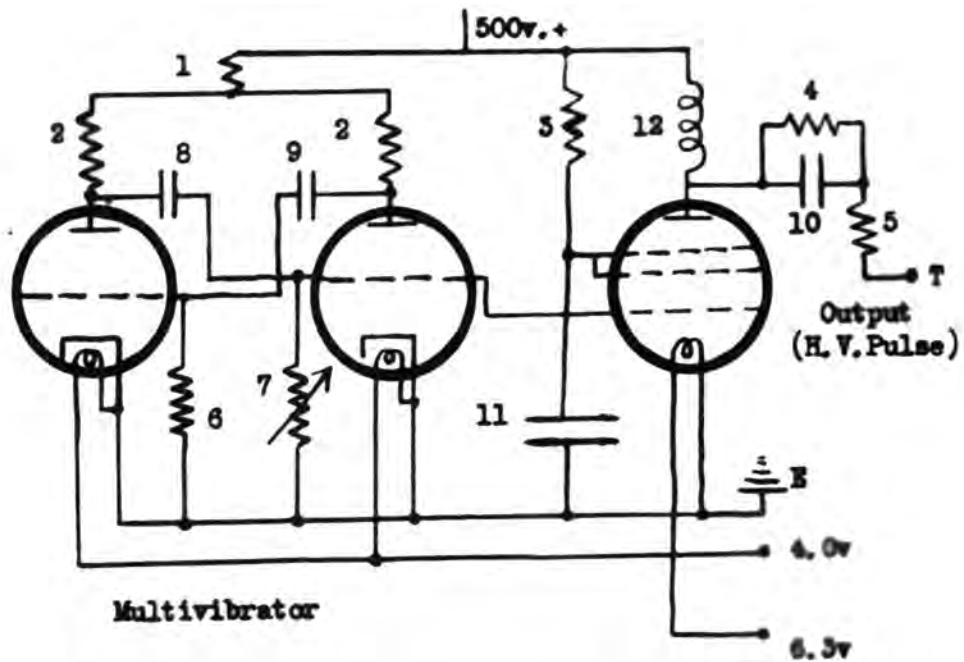
illustration quite arbitrarily. It must include the time from the rise of the irradiator pulse to the minimum voltage for the irradiator gap to spark over to the time when the last photons which can be effective in the test gas are emitted; this last time might be after the removal of the potential difference across the irradiator gap.

The effective test pulse time is simply the time for which the voltage applied to the test electrodes is in excess of the minimum sparking voltage required in a sustained trial. The shorter the duration of the test and irradiator pulses the smaller the range of times for which the effective pulses overlap and so the more nearly should the time of, or reason for, any sudden change in sparking probability be fixed.

2.2. Experimental arrangements and apparatus

2.2.1. Layout of apparatus.

The block diagram of figure 2 illustrates the layout of the units built to achieve the test requirements set out in 2.1. above. A pulse forming unit was supplied from a source of direct high voltage giving from 3 to 30 Kv., (see appendix 1). Pulses were triggered at regular intervals by the multivibrator circuit

Fig. 3. Triggering Pulse Circuit.

V1 (ML4)

V2 (ML4)

V3 (PT15)

1	15k	4	5m	7	5m	10	0.5uf
2	100k	5	10k	8	0.5uf	11	4uf
3	100k	6	250k	9	0.5uf	12	60H

Pulse output to trigatron at T.

giving a pulse repetition rate of 15 per minute or more as preset. From a delay line system, designed to divide each pulse into two channels, A and B, one pulse was picked off along leads A' and fed to the test electrodes; the second pulse, travelling via leads B', acted as a source of supply of energy for the irradiating system in the same enclosure as the test gap. The time separating the two pulses was adjustable by a choice from the multiple connections possible on the two arms of the delay line.

Variation of gas type and pressure were achieved by means of the ancillary vacuum plant, (appendix 2), to which the test chamber was directly connected.

Sparking probabilities were measured by using electro-mechanical counting circuits inserted to detect spark discharge of the test gap and each trial voltage applied there.

The high speed oscilloscope was used to determine the time taken for a voltage pulse to travel the length of the artificial delay line and to assess the duration of the pulses used.

2.2.2. The triggering pulse circuit.

The triggering unit was used to deliver regular trains

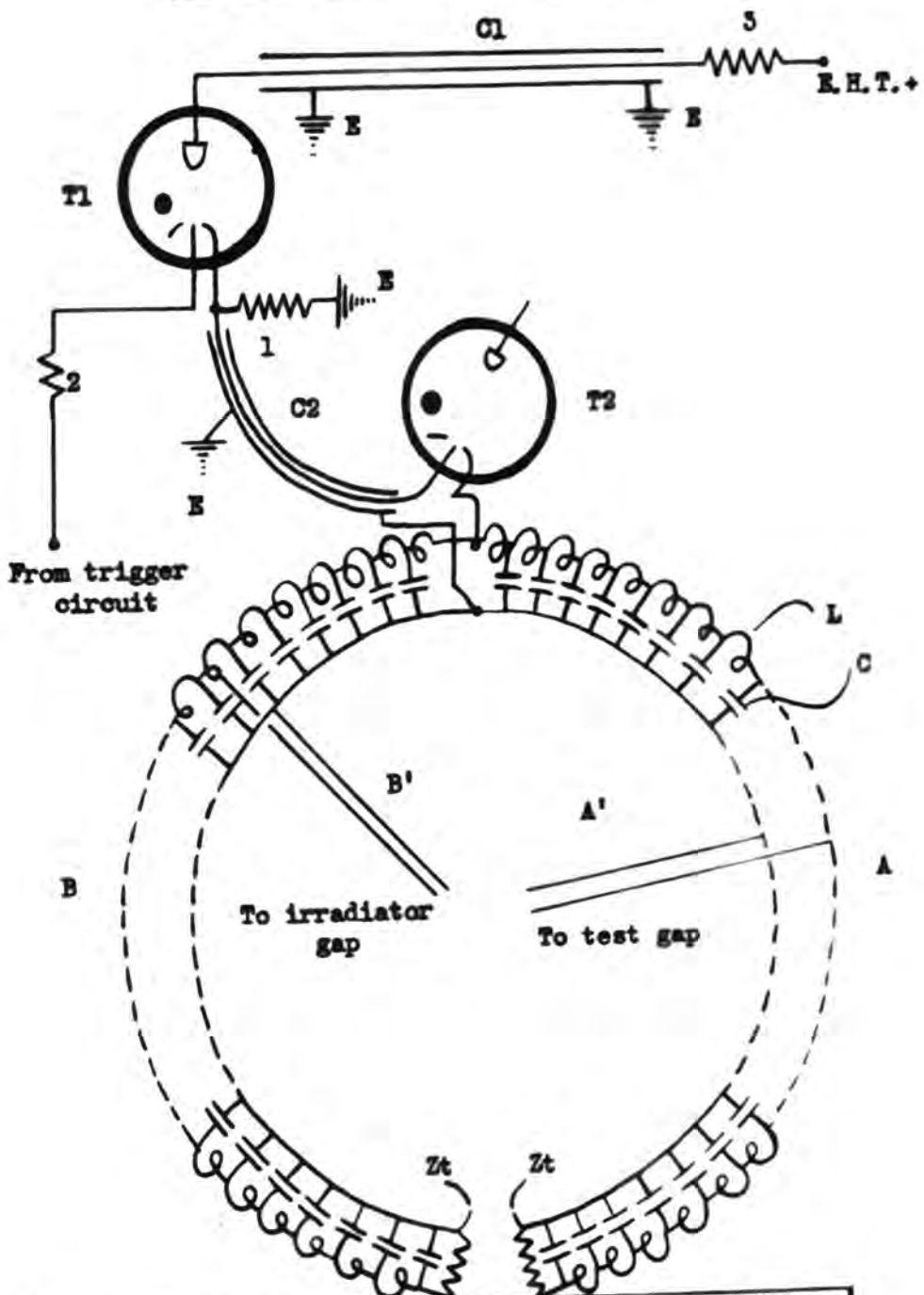
of pulses at rates adjustable from 15 to 35 per minute. Too low a repetition rate would reduce the number of trials possible in a given run with steady experimental conditions and so reduce accuracy, while too high a rate would not allow products of spark discharge to clear from the gap between pulse trials.

The multivibrator circuit, figure 3, operated so that each time the grid of valve V2 ran negative the electron flow through an inductively-loaded-anode pentode, V3, was cut off. The resulting voltage surge, either across the inductance of 60 henries or across the pentode, was sufficient if applied to the minor gap of a trigatron (3 electrode spark gap) to give a triggering spark there.

2.2.3. The production of high voltage pulses of short duration.

To achieve an accurate determination of the time at which the radiation became effective in the gas and to avoid the onset of breakdown due to natural causes, as indicated in 2.1.2. above, as short a pulse duration as practical was required. The ideal pulse had also to have a rectangular envelope to give the highest resolution in the timing measurement. The pulse forming circuit designed, figure 4, was simple in construction

Fig. 4. Pulse forming and delay circuit.



C1	300 uf	T1	CV 125	1	2k	C	5.5 uf
C2	150 uf	T2	CV85	2	10k	L	0.1 uh
				5	10k	Zt	120 ohms

and reasonable in operation. A coaxial cable condenser C1 was continually charged by a current, limited to less than a milli-amp, by a liquid resistor of Gemant⁷² type, flowing from the E. H. T. direct voltage unit (appendix 1). The interval between triggering pulses was sufficient for C1 to be fully charged to any desired voltage between 12 and 24 Kv., the limits of operation of the trigatron valve. When a spark in the minor gap of the trigatron T1 occurred the condenser C1 discharged through the major gap of the trigatron and resistance 1 to earth. An impulsive voltage developed across the resistance travelled as a wave along the coaxial condenser cable C2. The short high pressure nitrogen gap at the cable termination was heavily overvolted by the incident pulse and broke down after a short delay, giving a sharpened pulse of duration 10^{-7} sec. * The actual rise times and fall times of this pulse were not negligible, as ideally they should be, but, as the pulse proved satisfactory in the subsequent exploratory experiments, discussion of its exact form will be left until the section of the work on oscillographic measurement.

The minor gap of a CV 85 trigatron valve, which was

* Oscillographic measurement.

used as this pulse sharpening gap could have been improved upon by the special manufacture of an extremely short length gap (down to 0.001 inch) in nitrogen at 50 atmospheres pressure; which Fletcher⁷⁵ used to get pulses with rise times as small as 0.3×10^{-9} sec. Much of the improvement in pulse rectangularity would have been subsequently lost in the delaying circuits essential to this experiment and so the highly specialised gap was not warranted.

The condenser C1 served the additional purpose of link between the remote E.H.T. rectifying system and the pulse forming unit. C2 linked the pulse forming unit to the delay lines so that the sharpened pulse was fed directly through T2, situated at the junction of the two parts of the line. This arrangement can be clearly seen in the photograph of the delay lines in figure 5.

2.2.4. The circular variable delay lines.

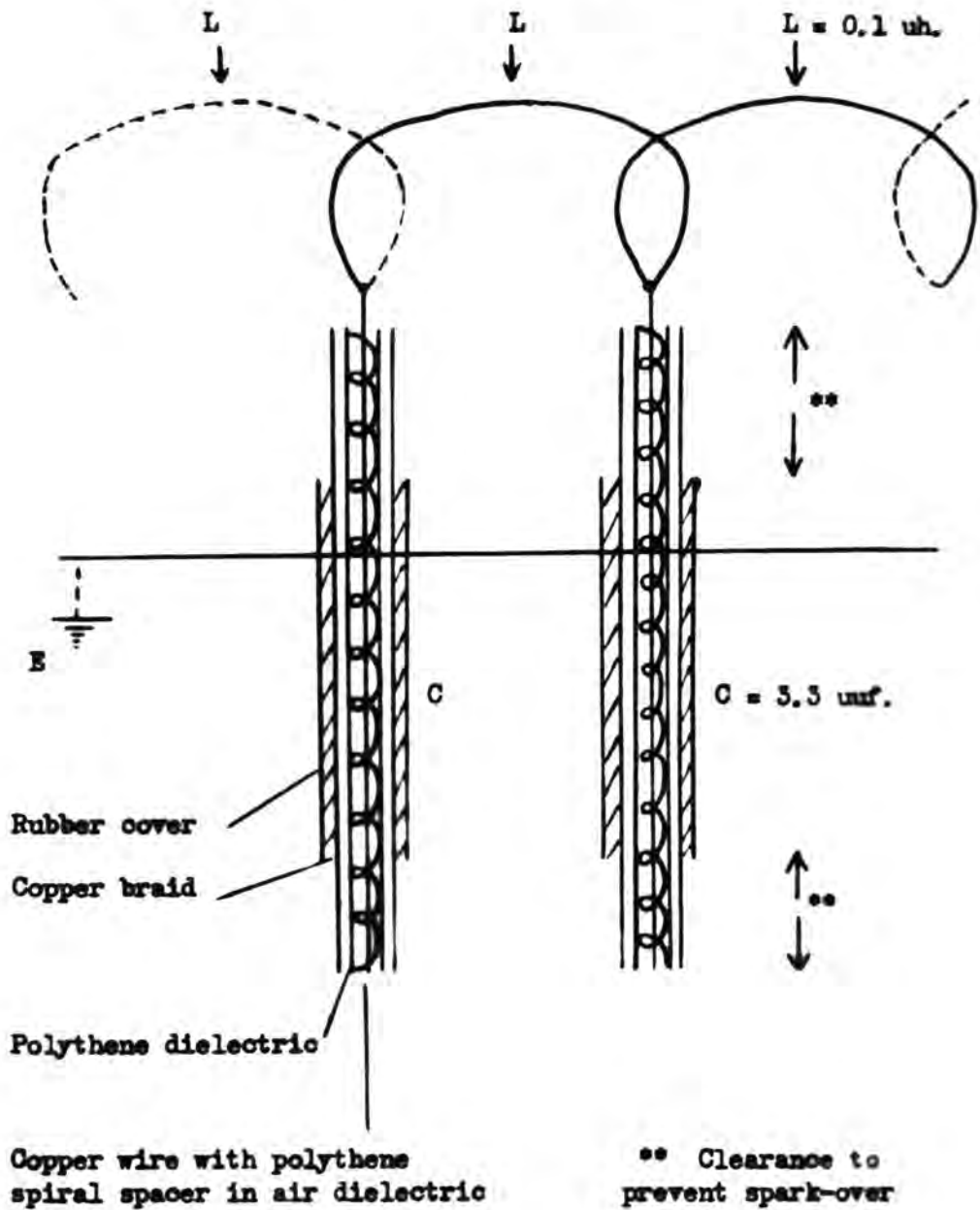
The sharpened pulse from T2 entered two artificial delay lines in parallel round a circle four feet in diameter. Each line was measured* to be 0.08 microsec. in delay time length and consisted of 109 units of inductance and capacitance

* Oscillographic measurement.

Fig. 5. Arrangement of the artificial delay lines.



- | | |
|-------------------------------------|----------------------|
| 1. Delay line. | 2. High speed C.R.O. |
| 3. Pulse forming and trigger units. | 5. Lead to E.H.T. |
| 4. Vacuum plant. | |

Fig. 6. Two Delay Line Sections.

arranged as in figure 4, (photograph figure 5). Each inductance was a single open turn of 16 gauge copper wire, one inch in diameter, giving an inductance of average value 0.1 microhenry, which acted as a link between successive capacitance elements. These capacitances were made to an average value of 3.3 micro-microfarads from low loss, part air dielectric, coaxial cable. The outer braiding of the condensers was stripped back to prevent spark-over at the ends. A pair of inductance-capacitance unit sections is illustrated in figure 6.

Such a delay line was calibrated as a scale for the measurement of pulse delay time. It was terminated by its characteristic impedance to cut out unwanted reflected voltage waves. Leads were taken from the delay line A to the test electrodes along an open pair of parallel wires A'. From delay line B similar leads B' fed the voltage pulse to the irradiator mechanism. Thus the points of connection of the "clock pointer" arms A' and B', on the delay lines A and B respectively, arranged the time interval separating the irradiator and test pulses when they arrived at their electrode systems. This arrangement of the two arms gave the possibility of having

the irradiator system operating in time a) earlier than, b) coincident with, or c) later than the application of the test pulse, as required.

2.2.5. The test spark gap and the irradiator spark gap arrangement in the test chamber.

The photographs of figure 8 show the Pyrex glass test chamber with special ends and the mounting chassis for the test gap, irradiator gap and collimator which the chamber enclosed. Figure 7 shows additional detail of the chassis mountings.

The electrodes used for the test gap consisted simply of a pair of 0 B.A. brass screws the ends of which were made plane and polished. These were inserted in a Tufnol block so that the distance apart of the smoothed ends was adjustable. The arrangement is shown in figure 7a.

In figure 7c is shown the arrangement of the irradiator spark gap and collimator to provide a fine beam of radiation restricted to the gas in the centre of the test gap. The line of centres of the test gap electrodes was at right angles to the line of centres of the irradiator electrodes. The collimator consisted of two adjustable knife edged optical slits of steel.

Fig. 7. a) Test Gap b) Irradiator Gap
c) Experimental Arrangement of a) and b).

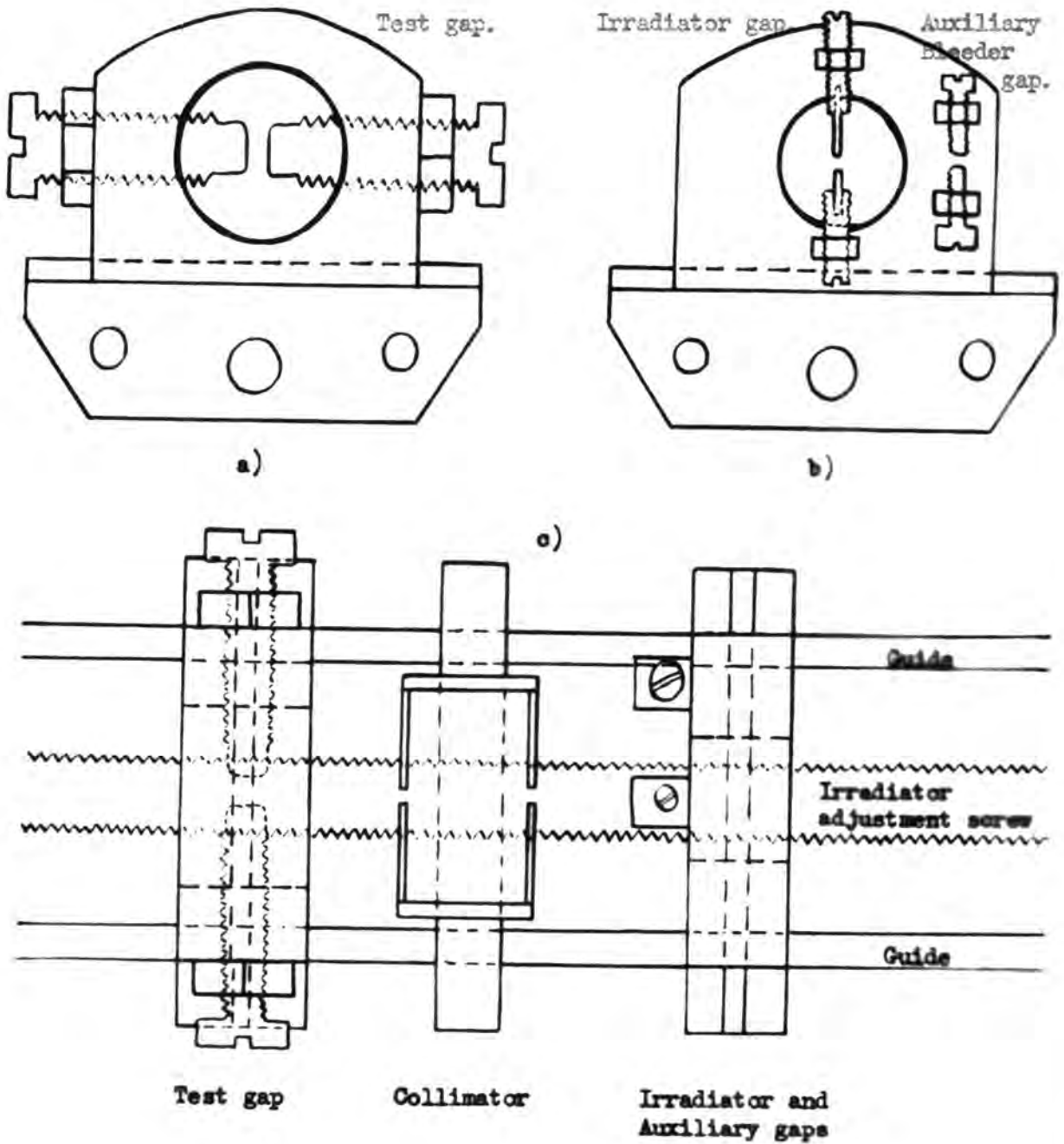
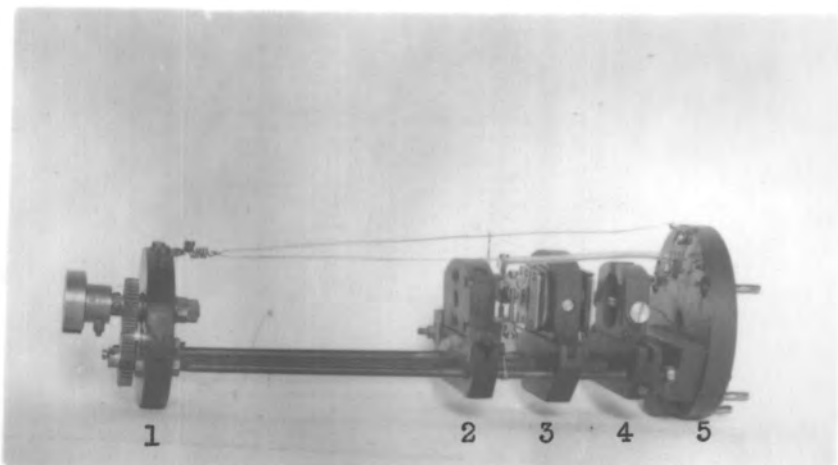
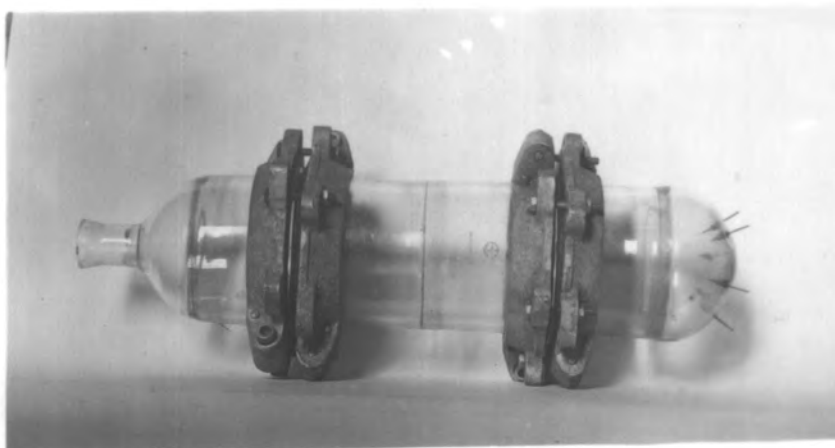


Fig. 8 . a) Mounting chassis.
b) Test chamber.



a)

1. Irradiator-to-test-gap distance adjustment.
2. Irradiator and auxilliary spark gaps.
3. Collimating slits.
4. Test gap.
5. Plug for lead connections.



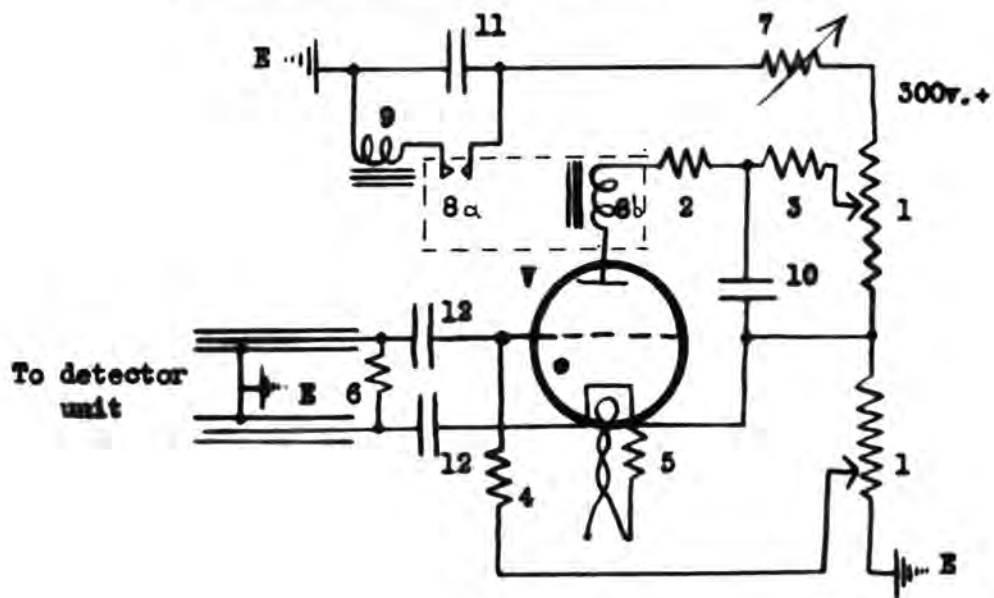
b)

These were mounted at a distance of 2 cm. apart on a brass ring supported on a Tufnol chassis. To prevent drift of electrons from the irradiator to the test gap, (and also of photo-electrons which might be released from the edges of the metal slits), the collimator was connected to the positive electrode of the test gap.

The irradiator gap was first constructed in a similar way to the test gap using in this case 6 B.A. brass screws for the electrodes. Two conditions had to be satisfied by the irradiator arrangement, namely, a) the approximate line of the spark channel had to be in line with the collimator slits, b) the electrode separation had to be small so that, with high percentage of the gap, unit sparking probability could be assured. The first attempts to satisfy these conditions resulted in discharges which pitted the electrodes, giving irregular sparking after several hundred trials. This difficulty was overcome by inserting one mm. tungsten wires in the brass irradiator screws and grinding each tungsten to a plane end (figure 7b). The allowed minimum distance of separation of the irradiator electrodes was limited by the need to have a volume of gas in which the processes

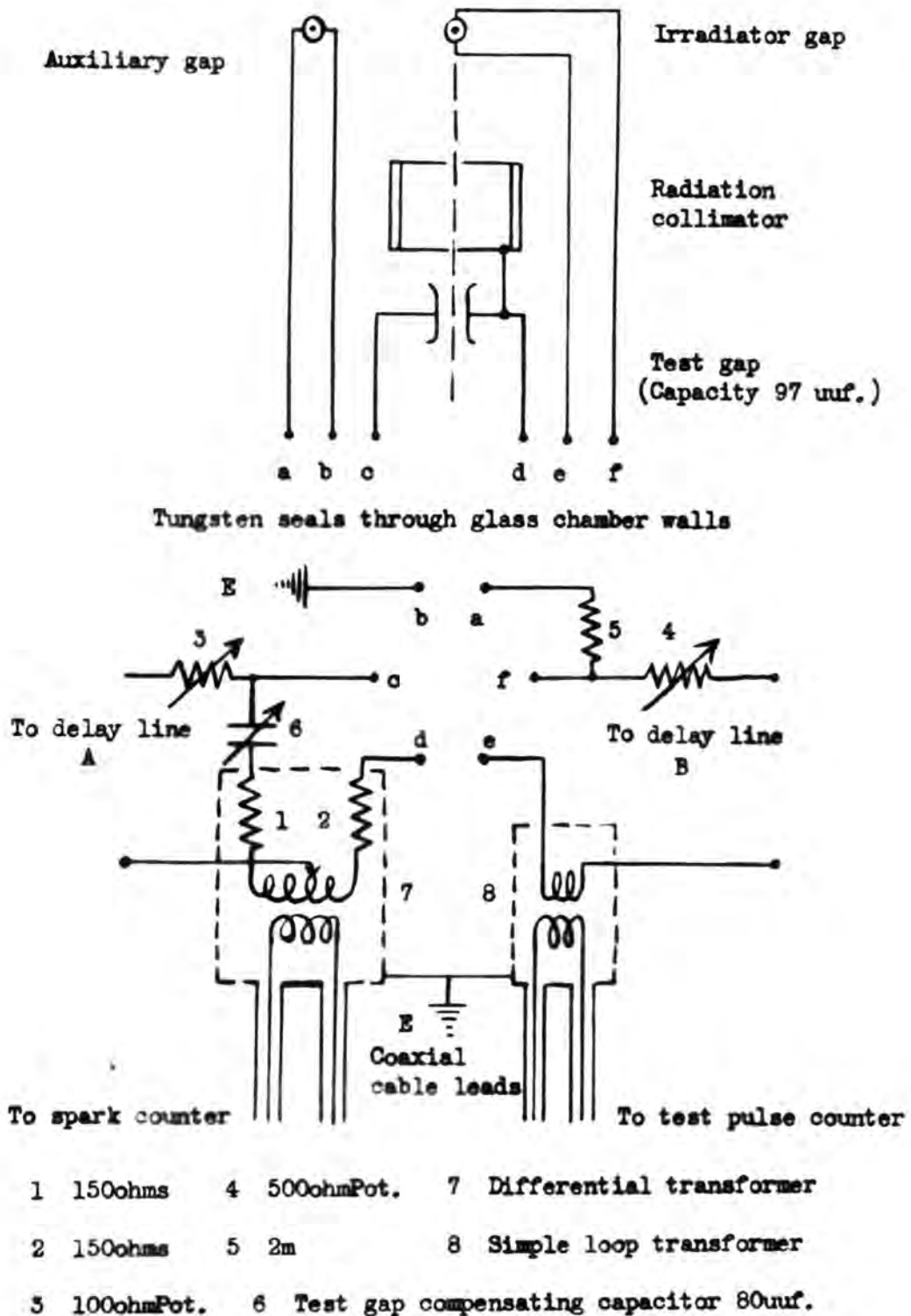
leading to the emission of high energy quanta could develop; a compromise arrangement had therefore to be reached between the requirement of this last condition and that of b) above. An auxiliary 'bleeder' spark gap was used, fed with the same pulse as the irradiator gap by way of a 2 megohm resistance, figure 10; the overvoltage of this gap was such that each pulse applied to it gave a spark which irradiated the gas and the electrodes of the irradiator gap. This arrangement ensured an adequate supply of ionisation in the irradiator gap to give unit probability of sparking there. At the same time only a small fraction of the whole irradiator pulse energy was taken by the bleeder spark. No radiation from this bleeder spark gap could pass the collimator slits as the bleeder electrodes were offset at right angles from the line joining irradiator and test gaps. Only radiation from the main irradiator spark could be responsible for the photo-electric action in the test gas.

The voltage pulses for the test gap, irradiator gap and auxiliary gap entered the test chamber each by separate tungsten leads sealed through the glass of the end wall. The other end wall of the chamber was connected to the vacuum plant

Fig. 9. Basic Thyatron Counter Circuit.

V Thyatron GT1C							
1	100kPot	4	120k	7	30k	10	2uf
2	1k	5	5k	8	Relay	11	4uf
3	100k	6	150ohms	9	Counter	12	75pf

Fig. 10. Detector circuits for spark counters.



by a flexibly mounted brass cone fitting a ground glass socket. By rotating the cone the irradiator adjustment screw, (figures 7c and 8a), could be made to set the distance separating the irradiator and test gaps as desired. Parallel wire leads above the mounting chassis, (figure 8a), ensured the continued connection of the pulse leads to the gaps as they were moved.

2.2.6. The counting circuits.

The parameter by which the effect of the radiation entering the test gas was to be assessed was the probability of a test gap spark. To determine this quantity a measurement had to be made of a) the number of pulse trials made in the test gap during which the gas there was irradiated and b) the number of those pulses which resulted in a spark. The delay line arrangement in this experiment was such that the number of applied pulses, a), was the same as the number of sparks which occurred in the irradiator gap and so a count of the latter sparks was made.

Even the most fully developed sparks were such that the current through the gap could only continue for a fraction of a microsecond, set by the duration of the applied pulse.

The small total charge flow and the short time for which it was available made the use of a direct mechanical counter impossible.

The method adopted was to insert in the negative lead to the spark gap a detector unit, which in its simplest form consisted of a resistance of the order of 100 ohms, sufficient to reduce the speed of application of the voltage pulse, as shown later, but not to distort the trend of results. In the event of a spark in the gap the positive voltage pulse developed across the detector was applied to the grid of a thyatron, (figure 9). The subsequent discharge of condenser 10 through the valve and the winding of relay 8b closed the relay contacts 8a and recorded a count on the mechanical counter 9.

2.2.7. The loop detector unit and the counting of weak sparks.

To count separately sparks occurring in the irradiator and test gaps two sets of counting apparatus, each of the fundamental pattern set out in the previous section, had to be constructed. Care had to be taken to ensure that false counts could not be recorded in either set of apparatus in any of the following ways :-

1. By electrical connection of any kind between the counting systems;
 2. By electrostatic coupling from the pulse forming and delay line circuits to the counters;
 3. Due to surges of voltage along the earth line following any heavy electrical discharge in the room;
 4. By displacement current through the spark gap capacitance when a spark did not develop during an applied pulse.
- The difficulties of 1. and 2. were overcome by housing each counter system from the detector unit onwards in a separate metal enclosure which was independently earthed. The detector units were developed so that no direct wire linked the spark gap to its respective counter. The surges along the earth line, (3), were not able to cause the unbalance of the thyratron needed for a count provided all of the earth leads of a counter were made first directly to a single point and from there one lead was taken to the common earth at the screening case.

To differentiate between displacement current and spark current through the irradiator gap a simpler method was possible than in the case of the test gap. The reason for

this lay in the different nature of the sparks formed in the two gaps.

Sparks through the irradiator gap were always fully developed because the gap was always pre-ionised and heavily overvolted. A simple loop transformer consisting of four half inch diameter turns of wire in primary and secondary (figure 10) acted as a reliable detector for a spark. The detector signal output was sufficient when a spark occurred in the irradiator gap to operate the thyratron counter in a low sensitivity setting; the displacement current through the irradiator gap and the loop transformer primary, on the rare occasions when no spark developed, gave an insufficient detector output signal to record a count.

Weak sparks, which occurred frequently in the test gap for certain irradiator conditions discussed later, were more difficult to count, since for them the order of current through the gap was comparable with capacitive displacement currents as a result of a test pulse for which a spark did not develop. The simple loop detector transformer and thyratron counter were unable to differentiate between the two types of

signal here. A differential transformer bridge circuit was therefore devised, as shown in the lower left hand corner of figure 10; two of the arms consisted of the opposed windings of the transformer, the third arm contained the test gap (95 micro-microfarad) and the fourth arm a variable capacitance of the same order. Also in the third and fourth arms resistances of 150 ohms were included to prevent the natural oscillations which might start in the circuit. When a test pulse was applied across the input terminals of the bridge, and a spark developed in the test gap, only the difference between the spark current and the displacement current through C6 gave a signal in the output winding of the differential transformer. It was found necessary to amplify this signal before it could be applied to trigger the thyratron counter set sensitively. A single stage of amplification with a gain of about 100 was used and then the counter sensitivity required was not high. When no spark developed in the test gap the difference current in the output transformer of the bridge circuit was insufficient to record a count.

While this arrangement was satisfactory for cond-

conditions of irradiation where a medium strength test spark was triggered in the test gap, for certain conditions of irradiation extremely weak sparks and sometimes merely diffuse glows appeared. These were hardly visible in the test gap except when the room was darkened. They were not recorded as counts, even with the bridge arrangement, which suggested that the spark current in these cases was not measurably different from the displacement current when a spark did not develop. Later photographing of the test gap in test conditions where these weak or incipient sparks occurred yielded interesting information about their form.

In counts of sparking probability recorded mechanically it must be borne in mind that a spark counted was a count of a condition arising in the test gap, where visible light was produced and a sufficient difference current through the arms of the bridge circuit to provide a detectable signal for the later stages of the counter.

SECTION 3.Measurement of the sparking probability in the test gap.3.1. Mechanisms which might be stimulated by the irradiator spark and operate to increase the probability of sparking in the test gap.

In this account it will be assumed that it is the direct effect of radiation produced in the initial stages of breakdown of the irradiator gap which, if it arrives at a suitable time relative to the test pulse, gives the conditions in the test gas for breakdown there. It has been observed by Hemsalech⁷⁴ and others that the air lines appear chiefly in the initial stages of a spark; the velocity of diffusion of the metal vapour of the electrodes into the gap, of the order of 10^5 cm./sec.⁷⁵ is too low for the radiations of the metal arc lines to be emitted in the duration of the impulsive stresses used here. In the present work a change in the metal of the irradiator electrodes from brass to tungsten did not change the form of the test curves of P against irradiator timing; only a slight shift of the curves as a whole occurred which was accounted for by the change in the electrical circuit conditions

made at the same time. This is in keeping with the assumption that only the air lines are active in the radiation here.

Certain effects of the irradiator spark which might influence the probability of test gap sparking apart from photo-electric effects in the test gas were checked before proceeding to the main experiment. These, together with tests used by Prowse and Jasinski⁷⁶ in their investigation of similar effects which triggered microwave sparks, are considered below:-

1. Electrostatic coupling between the irradiator and test gaps. Even when the two spark gaps were separated by 1 cm., if the irradiator beam was cut off from the test gas by a thin strip of polythene or paper the sparking probability always returned to the set zero.

2. Photo-emission from the electrodes. The electrodes of the test gap and the collimator slits were set in every experiment here so that the direct light from the irradiator spark could not impinge on the test electrodes. The incipient spark streamers photographed and discussed later in this work do not appear in every case to reach the electrodes but seem to spread

from the centre of the gap.

3. The emission of solid particles from the irradiator spark. In the earlier experiments of Prowse and Jasinski⁷⁶ three films showing interference colours were prepared, having approximately equal mass per unit area but were different in chemical composition. The films were placed in turn between a naked spark and the gas in a microwave resonator which it irradiated. A difference between the sparking probability of the resonator recorded when the radiations passed through nitro-cellulose and cellulose nitrate was attributed to a difference in transparency of the two films for short wavelength radiations. In the present experiments it seems most likely that no charged particles could have passed through the collimator slits while the test pulse was applied, for during that time the collimator was at the potential of the positive electrode. In the later work on absorption coefficients^{*}, where a steel irradiator was used, an effect on the sparking probability was observed with the test gap up to 50 cm. away from the irradiator at atmospheric pressure in some gases. This effect was not reduced by a magnetic field estimated at 4000 oersteds applied across

* See page 159.

the track of the radiation close to the collimator; particles of the charge and mass of the proton would have to be emitted with a velocity approaching that of light to penetrate the magnetic field and the collimator apertures.

4. Mercury vapour and dust particles. In all of the work filtered dry air or commercial cylinder gases were used; mercury vapour and impurities, other than the inevitable vapours of good quality stop-cock greases, were deliberately kept out of the vacuum system*. Dust particles from the electrodes, arising in vigorous sparks, can never be guaranteed completely eliminated. However, the lack of any change in the sparking probabilities observed after changing the waiting time between pulse trials 2 sec. to 3 minutes (manual tripping of the pulse forming unit) suggests that particles, if present, do not play any more effective part in the triggering of the discharges than residual ions from previous trials.

3.2. Test procedure and mechanical count records in the early experiments in air.

3.2.1. Test procedure.

In all of these preliminary experiments the test

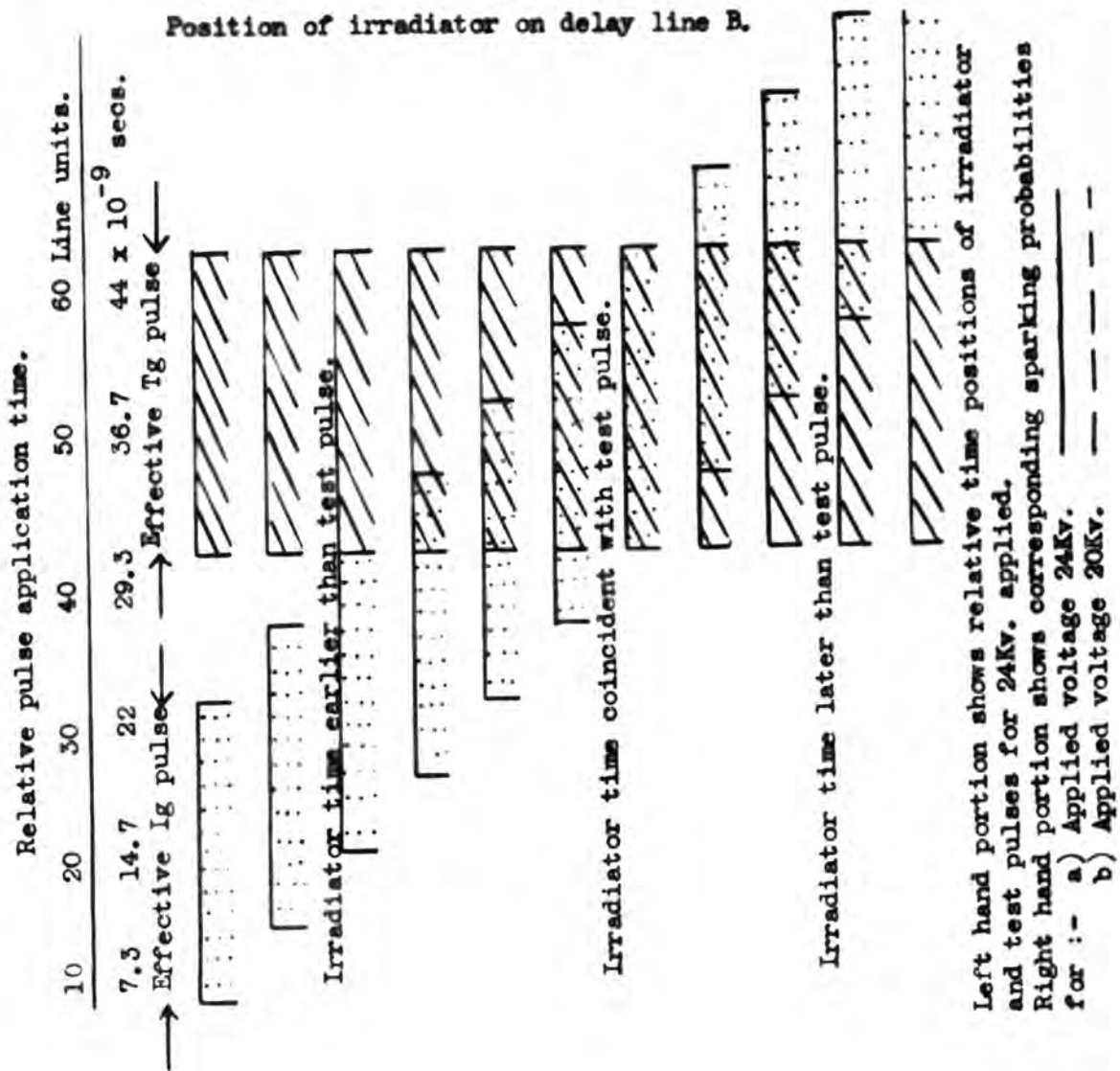
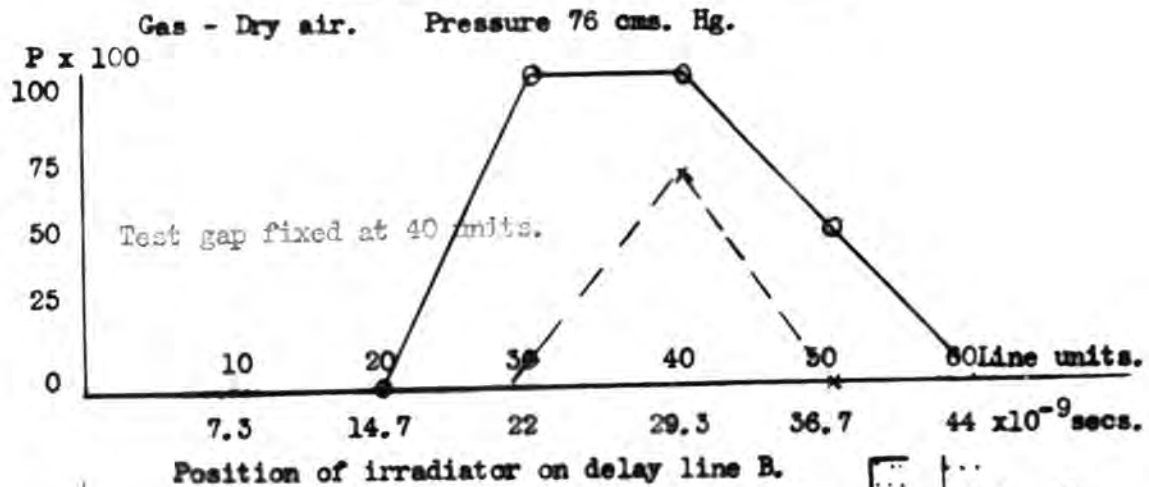
* Appendix 2.

chamber was filled with filtered dry air at atmospheric pressure, unless otherwise stated.

High voltage pulses of a chosen value more than 12 Kv., the lower limit set by the pulse forming trigatron, were applied at three second intervals to the circular delay lines, (figure 4). A setting of the irradiator gap size was made to give a spark there for every applied high voltage pulse drawn from the delay line B, at the desired working pressure. Next the test gap was gradually opened until, in the absence of all external ionising agencies and with the irradiator leads short circuited, a similar high voltage pulse drawn from delay line A would not give any spark in that gap; but so that a radium capsule brought to the walls of the glass enclosing chamber increased the sparking probability to more than one half. The radium was then removed and the sparking probability of the test gap was examined for :-

1. Set time positions on the delay line A of the test gap pulse leads, while the point of connection of the irradiator gap pulse leads was moved in time down delay line B;
2. Set irradiator pulse time positions while the test pulse

Fig. 11. Variation of sparking probability with irradiator pulse time for fixed test pulse time. Effective pulse times are indicated for applied voltage 24Kv.



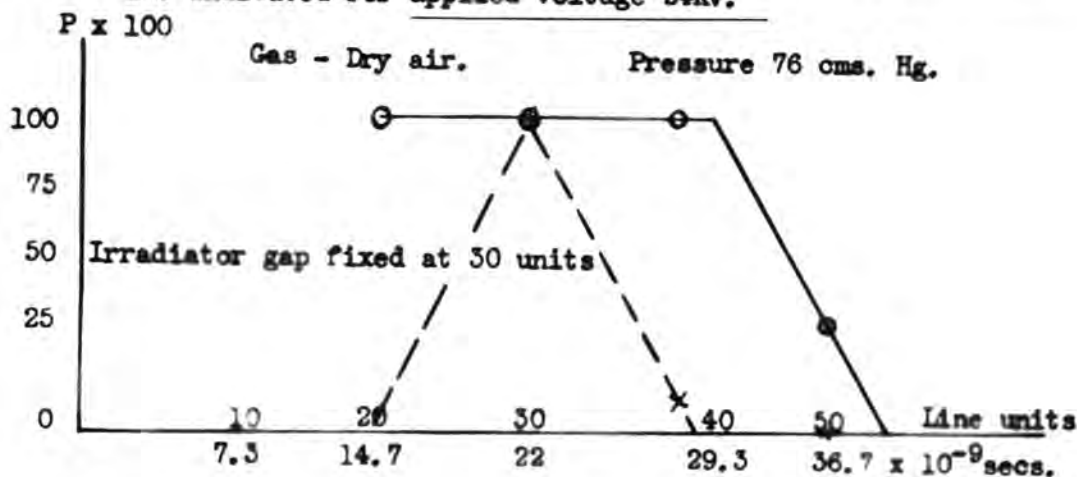
was moved in time through the irradiator pulse.

The distance in the chamber that the radiation had to penetrate to reach the test gap from the irradiator was constant throughout the experiments, as were the aperture sizes and position of the collimator.

3.2.2. The general shape of the test curves.

Typical diagrams showing the way in which the sparking probability of the test gap, P , varied with irradiator gap pulse timing on the delay line for 1. above are included in figure 11. The time scale has been set out in two forms; 'line units' represent the number of LC sections, measured from the input to the delay line, at which the irradiator connections were made; the 'seconds' scale gives the time after the pulse entered the delay line system at which the leading edge of the pulse was applied to the electrodes. To obtain these times the delay line had to be calibrated, as described later. The relative positions of the test and ^{irradiator} pulses in time, irradiator early or late, is shown for each line setting at which a count of P was made. The effective time for each pulse (i.e. the time for which adequate ionisation in the gap can lead to the instability of sparking) is arbitrarily taken, for 24 Kv. pulses,

Fig. 12. Variation of sparking probability with test pulse time for fixed irradiator pulse time. Effective pulse times are indicated for applied voltage 24Kv.



60 Line units
44 x 10⁻⁹ secs.

50
36.7

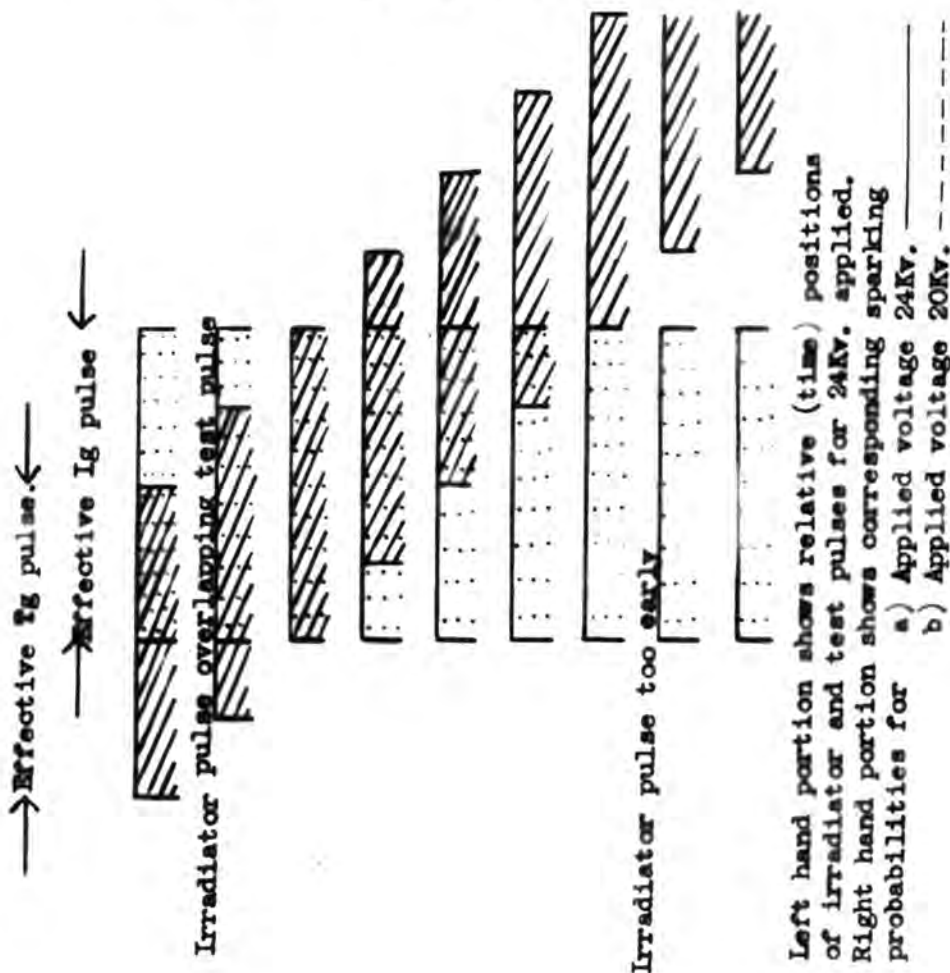
40
29.3

30
22

20
14.7

10
7.3

Position of test gap on delay line A



as the time for which the pulse as recorded on the high speed oscilloscope* was in excess of 0.95 of the peak voltage. For the pulse, of total duration 0.35 microsec. this effective time is 0.014 microsec., approximately equal to the delay caused by 20 sections of the delay line. It will be noticed that the sparking probability was in excess of zero for settings where the effective irradiator and test pulses overlap.

The typical diagram for a set of counts with fixed irradiator pulse time, and test pulse moved through irradiator pulse time, is in figure 12. Here the test (T_g) pulse was never sufficiently early for the effective irradiator (I_g) and test pulses not to overlap. The observed value of P was always in excess of zero, except when the test pulse was much later than the irradiator pulse, more than 50 units from the input to the delay line.

The general trend of the graphs of figures 11 and 12 suggests that there is a definite limit to the time by which the irradiator can be earlier than the start of the test pulse if increase in the value of P is to be effected:-

1. For 24 Kv. pulses the irradiator pulse time had not

* See page 137.

to be more than 20 line units earlier than, or more than 20 units later than, the start of the test pulse to give an increase in P.

2. For 20 Kv. pulses the time limits for successful irradiation were 10 line units on either side of the start of the test pulse.

3.2.5. The effect of overvoltage on sparking probability.

The probability curve of figures 11 and 12 shows that the values of P for 20 Kv. applied pulses were generally less than those for 24 Kv. pulses. Only when the irradiator and test pulses coincided in time, in figure 12 at 50 units, was the probability recorded for both voltages alike, being then unity. This is explained by considering that the effective pulse time for the lower peak voltage is shorter than for the 24 Kv. peak voltage and so, in consequence, is the range of times for which the effective irradiator and test pulses overlap. It is not thought that the diminished voltage applied to the irradiator resulted in a sufficient reduction in intensity, or change in type of the effective radiation, to account alone for the considerable reduction in P observed in

many cases. Even with the lower pulse voltages the irradiator was always heavily overvolted. Later measurements made of absorption coefficients* for the radiation, using this same parameter of sparking probability, did not disclose any measurable difference in the coefficient obtained for different overvoltages of the irradiator and test gaps. This supports the view that the type of radiation does not change with overvoltage for the range of pulses used. It is possible, however, that if the stress in the gas and photons are needed at the same time to release electrons, the duration of the test pulse will considerably affect P.

3.2.4. The effect of test pulse timing on the graphs of sparking probability against irradiator pulse time.

The table 1. (page 66) shows experimental values obtained for P when a fixed position was taken for the test gap leads on delay line A, (e.g. a. 20 line units, or 14.7×10^{-9} sec., from the line input), and positions of the irradiator gap leads were taken at 10, 20, 50 etc. units from the input to delay line B. P is given in each case as a percentage and unit value of P, (100 %), is indicated by +. The table includes

* See page 159.

Table 1. Variation of P with irradiator pulse time for fixed test pulse times.

Gas - Dry air. Pressure 76 cm. Hg. 100% indicated by +.

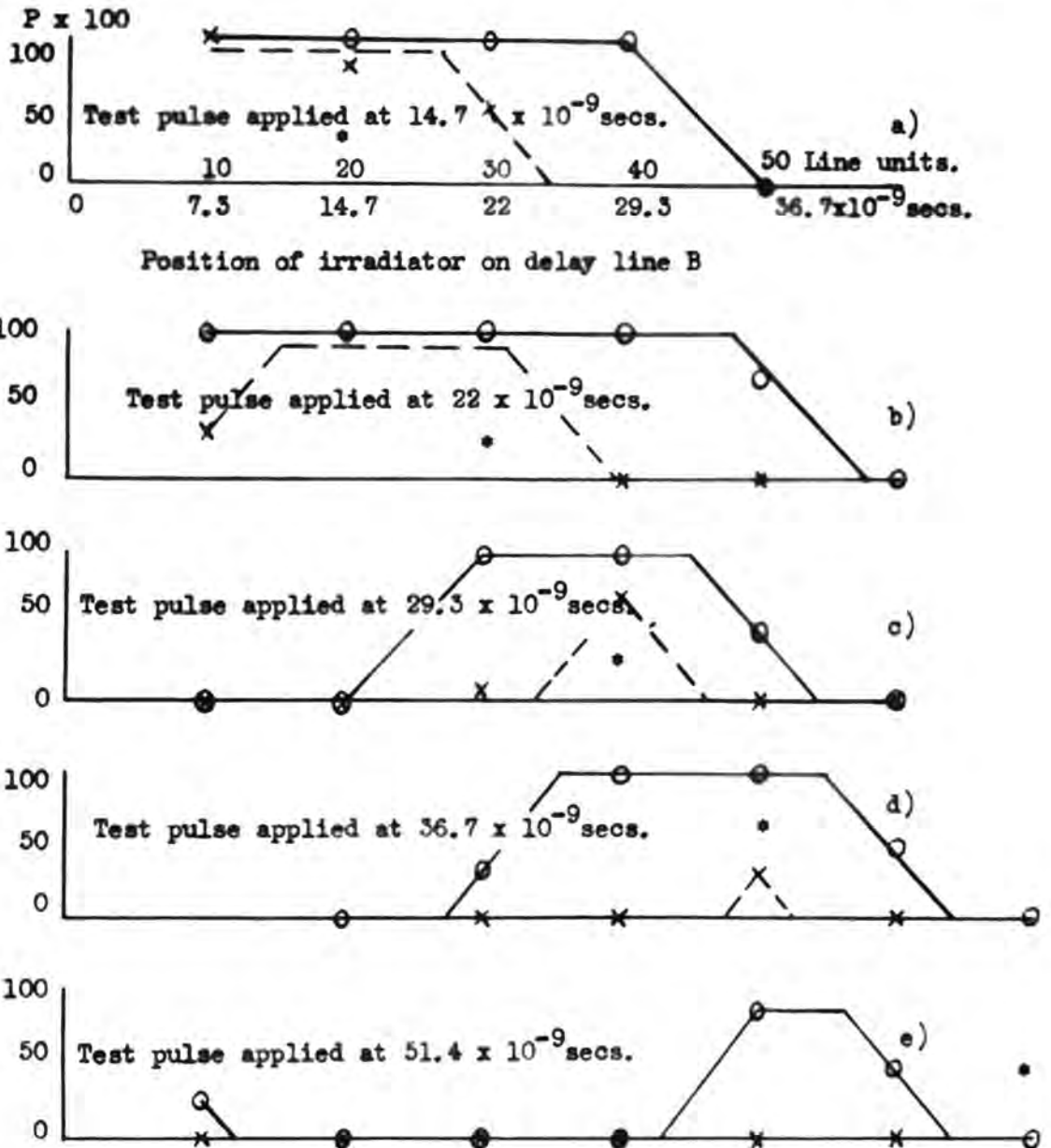
Graph Fixed test pulse Position of irradiator on delay line B.
time. (line units)

	Line units.	$\times 10^{-9}$ sec.	P x 100						
			10	20	30	40	50	60	70
24 Kv.									
a.	20	14.7	+	+	+	+	0	0	0
b.	30	22.0	+	+	+	+	65	0	0
c.	40	29.3	0	0	+	+	50	0	0
d.	50	36.7	0	0	35	+	+	30	0
	60	44.0	No count taken.						
e.	70	51.3	0	0	0	0	85	50	0
20 Kv.									
a.	20	14.7	+	80	50	0	0	0	0
b.	30	22.0	35	+	+	0	0	0	0
c.	40	29.3	0	0	10	70	0	0	0
d.	50	36.7	0	0	0	0	30	0	0
	60	44.0	No count taken.						
e.	70	51.3	0	0	0	0	0	0	0

the results for 24 and 20 Kv. pulses. These results are illustrated in figure 13, where each fixed test pulse time a., b., c., has its own graph of P against irradiator time for the two pulse voltages, 24 Kv. (full line) and 20 Kv. (broken line).

Fig. 13. Variation of sparking probability with irradiator pulse time for fixed test pulse times.

Gas - Dry air. Pressure 76 cms. Hg. Applied volts a) 24Kv. ---
b) 20Kv. ---



Time of test pulse application indicated by *
Experimental values are shown in fig. table 1.

Graphs are of the form already described for figure 11 in sections 3.2.1. The approximate centre of the area covered by the graphs is generally at the fixed test pulse time. As the fixed time for the test pulse was taken later on the delay line the irradiator times for which P rose to a finite value also occurred at later times. The total range of irradiator times for which a finite value of P was recorded was diminished as later positions of the test pulse time were taken. This is attributed to the reduction in test pulse voltage by the attenuating effect of the delay line, with a consequent reduction in overvoltage for the later times and smaller effective pulse duration. After travelling a number n sections of the line the peak voltage of the pulse, which at the input was of the value V_0 , is estimated to have been reduced to a value given by $V_n = V_0 \exp.(-kn)$, where k is a constant 0.0028 determined from oscillographic data (page 155).

When the test pulses were drawn from delay line B and the irradiator pulses from delay line A the same set of graphs was obtained, indicating that the delay lines were symmetrical as designed.

The change in the time separating the irradiator and the test pulses which had to be made to effect a change in P of unity, here of order 7×10^{-9} sec. might be of significance as it was not the same in the different gases used.

3.2.5. The effect of irradiator pulse timing on the graphs of sparking probability against test pulse time.

The experimental values of table 2 (page 70) were obtained when fixed line positions for the irradiator leads were taken and the test pulse time was moved through irradiator pulse time, using 24 Kv. pulses. For each setting of irradiator pulse time a small range of test pulse times on either side, early and late, of the fixed time gave a finite P . The results are illustrated in figure 14, and again it is seen that, with fixed irradiator pulse time remote from the input to the delay line, the range of test pulse times for which P was greater than 0 is less than for an early fixed irradiator pulse time. For each particular irradiator pulse time the value of P fell to zero when the test pulse was more than 20 units later.

3.2.6. The effect of introducing resistance in series with the test gap.

The resistance normally in series with the test gap

Table 2. Variation in P with test pulse time for fixed irradiator pulse times.

Gas - Dry air. Pressure 76 cm.Hg. Applied voltage 24 Kv.

Graph Fixed irradiator pulse time. Position of test pulse on delay line A. (line units)

	Line units.	$\times 10^{-9}$ sec.	20	30	40	50	70
			P x 100				
a.	10	7.5	+	+	0	0	0
a.	20	14.7	+	+	0	0	0
b.	30	22.0	+	+	+	35	0
c.	40	29.3	+	+	+	+	0
d.	50	36.7	0	65	50	+	85
e.	60	44.0	0	0	0	50	50
f.	70	51.3	0	0	0	0	0

Some data
on table 1
fold

No count was taken for test pulse position 60
100 % indicated by +.

was one of 150 ohms. This was situated in the spark detector circuit as shown in figure 10 where it is numbered resistance

2. There were three reasons for the value chosen, namely :-

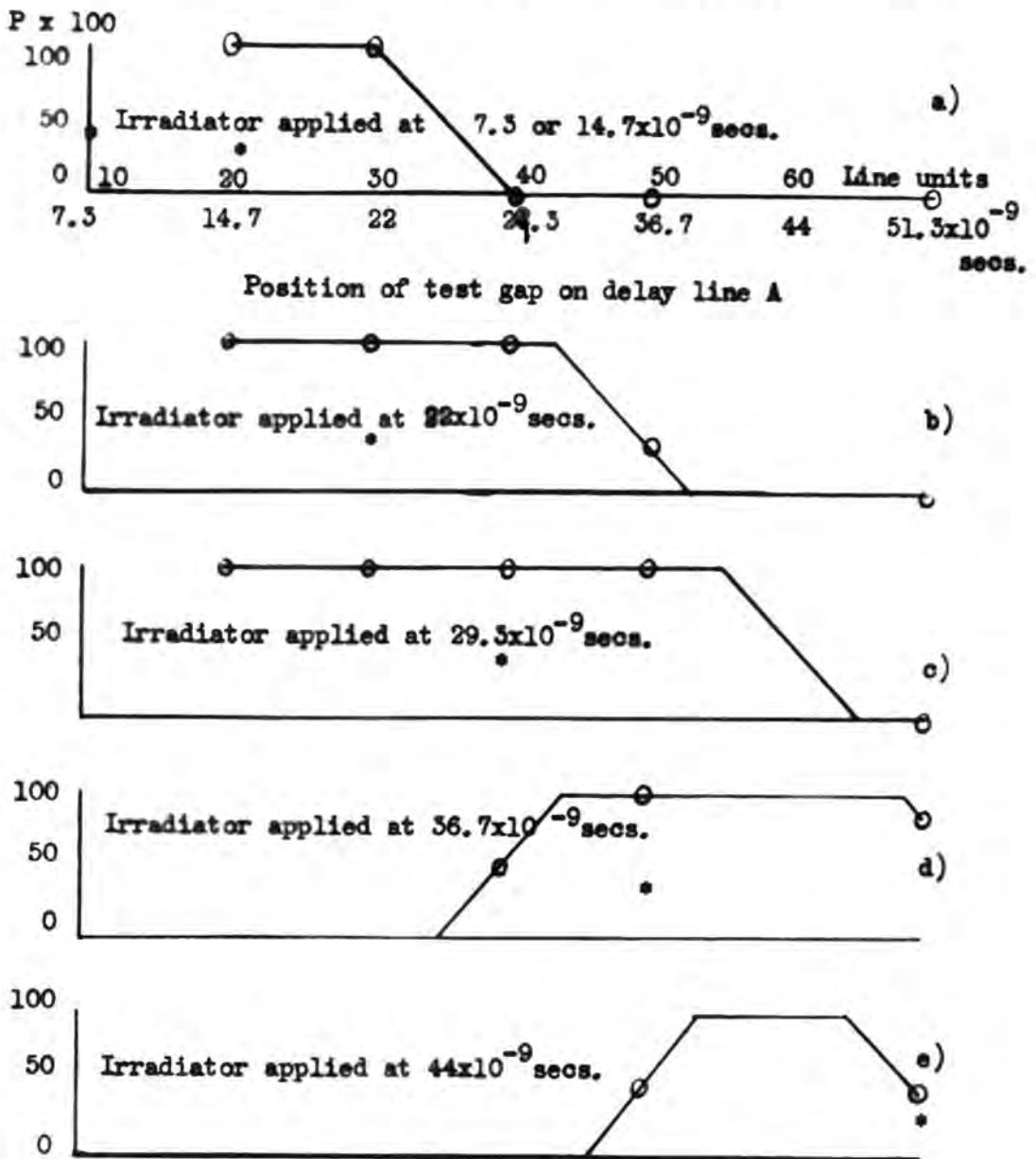
1. It was sufficiently small to permit the quick discharge of the test gap capacitance once the breakdown had started,

2. It would act as a deterrent to the natural oscillation of the detector bridge circuit, and

3. 150 ohms was near enough to the characteristic impedance of the delay line to prevent reflection after breakdown.

Fig. 14. Variation of sparking probability with test pulse time for fixed irradiator pulse times.

Gas - Dry air. Pressure 76 cms. Hg. Applied volts 24Kv.



Time of irradiator pulse application *
Experimental values are shown in fig. table 2.

In figure 10 the resistance S was generally set at zero. The inclusion of it in the circuit was made so that the effect on sparking probability of resistance in series with the test gap could be examined. The resulting values of P , when irradiator time was moved through a fixed test pulse time, using values of series resistance 150, 175, 200, 225 ohms in turn, are shown in table 3 and are illustrated in figure 15.

Table 3. Variation of P with irradiator pulse time for fixed test pulse time. The effect of resistance in series with the test gap is illustrated.

Gas - Dry air. Pressure 76 cm. Hg. Applied volts 24 Kv.
Resistance in series with the irradiator gap is 0 ohms.
Test pulse leads are connected at 30 line units.

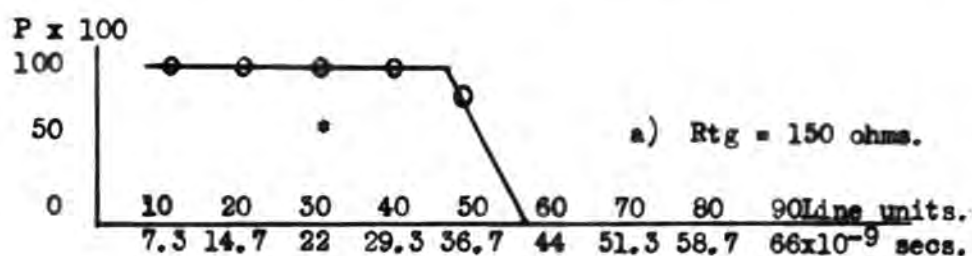
Graph.	Resistance in test lead.	Position of irradiator on delay line B. (line units)								
		10	20	30	40	50	60	70	80	90
	ohms.	P x 100								
a.	150	+	+	+	+	65	0	0	0	0
b.	175	0	95	+	+	+	+	25	0	0
c.	200	0	0	+	+	+	+	+	75	15
d.	225	0	0	0	+	+	+	+	+	+

100 % indicated by +.

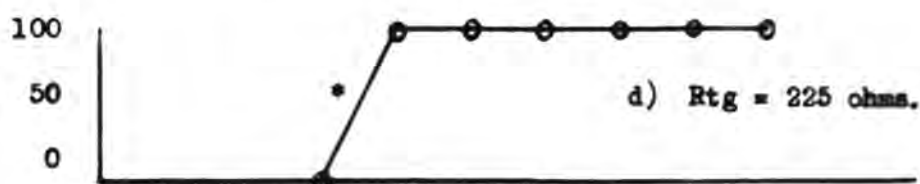
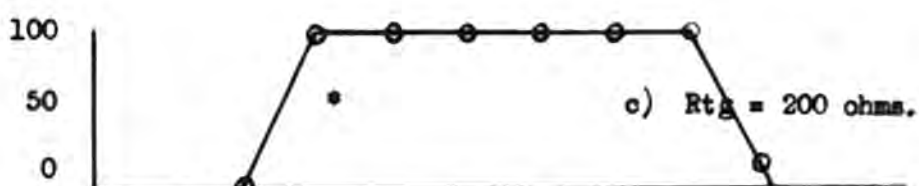
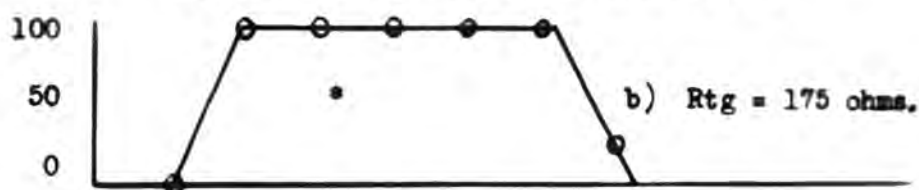
An increase in the resistance in series with the test gap is seen to result in a movement of a given value of

Fig. 15. Variation of sparking probability with irradiator pulse time for fixed test pulse time. The effect of resistance in series with the test gap is illustrated.

Gas - Dry air. Pressure 76 cms. Hg. Applied volts 24Kv.



Position of irradiator on delay line B.



P values are taken from fig. table 3.

Time of application of the test pulse is at 30 line units.*

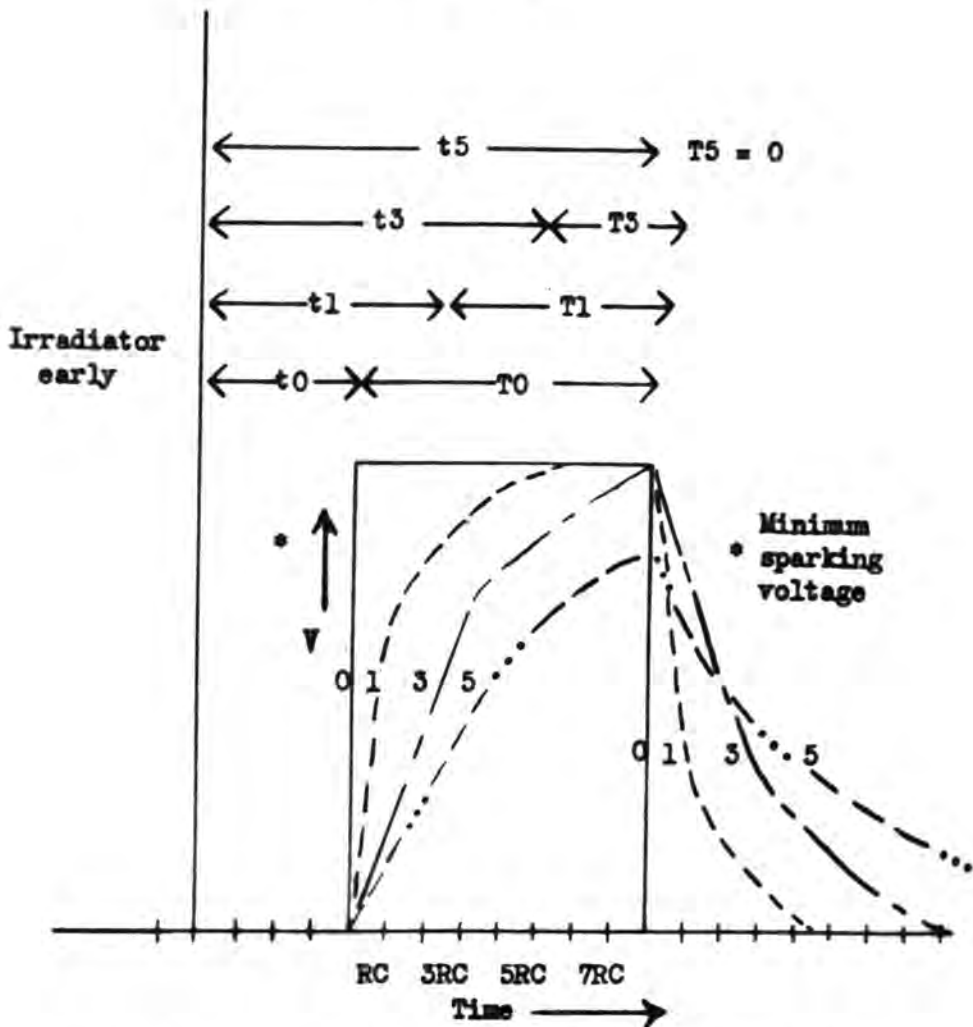
Resistance in series with the irradiator gap is 0 ohms.

Resistance in series with the test gap is:-

a) $R_{tg} = 150$ b) $R_{tg} = 175$ c) $R_{tg} = 200$ d) $R_{tg} = 225$ ohms.

As resistance is added in series with the test gap a given value of P is moved to a later irradiator time.

Fig. 16. Time changes introduced by inserting resistance in series with the test gap.



Curves 0,1,3,5, indicate voltage across the test gap at a given time for a pulse of duration $5RC$ secs. applied through series resistances:-

0) $R_{tg.} = 0$ 1) $R_{tg.} = R$ 3) $R_{tg.} = 3R$ 5) $R_{tg.} = 5R$ ohms.

Effective test pulse durations are respectively:-

0) T_0 1) T_1 3) T_3 5) T_5 .

The time separating the fixed early irradiator and the effective test pulse is shown to increase with $R_{tg.}$. This time is shown for:-

0) t_0 1) t_1 3) t_3 5) t_5 .

P to a later irradiator pulse time. This can be explained if the RC times of the test gap, given by the product of the series resistance and the capacitance associated with the test gap are considered.

The measured capacitance of the test gap was 97 micro-microfarads. On introducing an additional series resistance of 25 ohms the change in RC value is 2.42×10^{-9} sec. Each probability value is seen to have moved about 8×10^{-9} sec. or ten line units. The movement is repeated for each succeeding increment of 25 ohms until the resistance is high enough to prevent the sparking voltage from being reached during the test pulse.

Figure 16 illustrates the successive time changes involved. For the purpose of demonstration in this figure a hypothetical rectangular pulse has been applied to a resistance-capacitance circuit similar to that associated with the test gap. The times indicated, t_0 , t_1 , t_3 , and t_5 in the diagram are those between the fixed irradiator pulse time and the start of the effective test pulse times for test gap series resistances of 0, R, 3R, and 5R ohms respectively. The effective test pulse

time is also seen to decrease slightly with each increment in series resistance, until finally, with sufficient resistance the minimum voltage required for a spark is not reached in the duration of the rectangular applied pulse.

3.2.7. The effect of introducing resistance in series with the irradiator gap.

A similar effect of change in sparking probability was obtained when resistance was included in the irradiator gap lead, (resistance 4 in figure 10).

Table 4. Variation of P with irradiator pulse time for fixed test pulse time. The effect of resistance in series with the irradiator gap is illustrated.

Gas - Dry air. Pressure 76 cm. Hg. Applied volts 24 Kv.
Resistance in series with the test gap is 150 ohms.
Test pulse leads are connected at 30 line units.

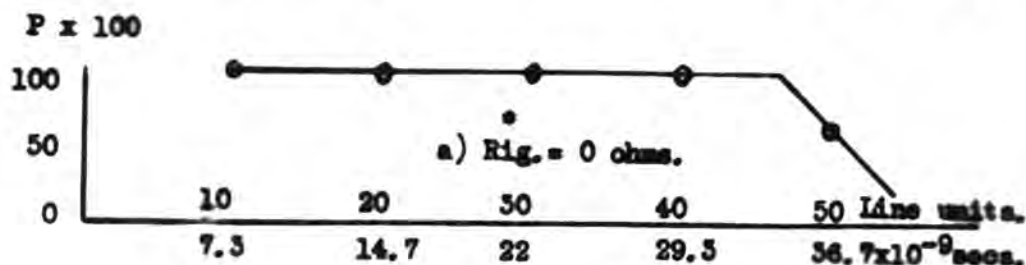
Graph. Resistance in Position of irradiator on delay line B.
irradiator lead. (line units)

	ohms	10	20	30	40	50
a.	0	+	+	+	+	65
b.	66	+	+	+	50	0
c.	132	+	60	20	0	0
d.	198	+	10	0	0	0

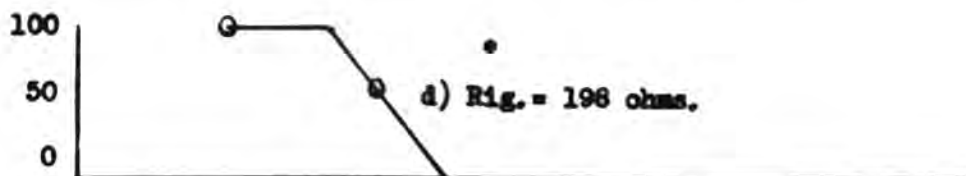
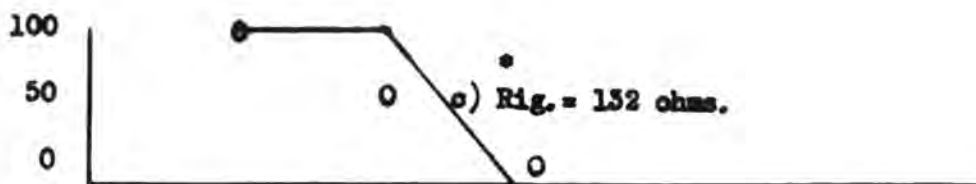
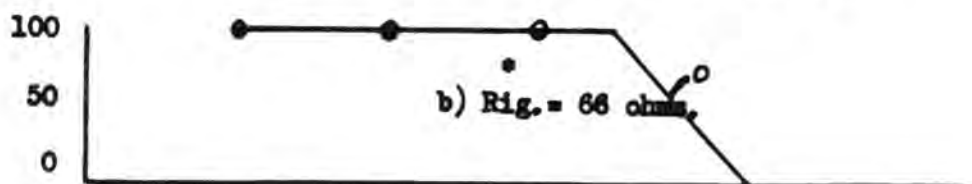
100 % indicated by +.

Fig. 17. Variation of sparking probability with irradiator pulse time for fixed test pulse time. The effect of resistance in series with the irradiator gap is illustrated.

Gas - Dry air. Pressure 76 cms. Hg. Applied volts 24KV.



Position of irradiator on delay line B.



P values are taken from fig. table 4.

Time of application of test pulse is at 30 line units.*

Resistance in series with the test gap is 150 ohms.

Resistance in series with irradiator gap is:-

a) Rig. = 0 b) Rig. = 66 c) Rig. = 132 d) Rig. = 198 ohms.

As resistance is added in series with the irradiator gap a given value of P is moved to an earlier irradiator time.

The experimental results set out in table 4 and illustrated in figure 17 show the result of the effect of irradiator series resistance. Again the explanation of the observed movement of given P values to earlier irradiator pulse times is sought in the RC change in the irradiator circuit.

The irradiator capacitance of 165 micro-microfarads, including leads, together with an increment in resistance of 66 ohms gives an RC change of 10.9×10^{-9} sec. The movement of a given P value to an earlier setting of the irradiator gap recorded for this increment of resistance was from 8 to 16 $\times 10^{-9}$ sec. For example, in figure 17, for the same test pulse setting at 30 line units a value of P of one half (50%) was recorded for the irradiator at 50 line units (for no irradiator series resistance) and for the irradiator at 40 line units with 66 ohms in series. In the latter case the pulse applied to the irradiator gap lagged behind the pulse reaching the RC combination at the gap by the equivalent of 10 line units, a delay approximately equal to that change in RC introduced by the resistance.

3.2.8. The effect of the termination of the delay line on sparking probability.

The calculated value of the characteristic impedance of the delay line used in these experiments, presuming negligible resistive losses, was 173 ohms, after measurement of the average value of the capacitance of an individual line section to be 3,5 micro-microfarads. It was necessary to ensure that any reflection of the applied voltage pulse at the line termination of this order would be so small as to have a negligible effect on the nature of the probability curves which would be obtained if the true characteristic impedance was used. A count of P using a set of irradiator pulse times and a fixed test pulse time was therefore made for six values of line termination. Table 5 shows the results for this count.

The conclusion reached was that the reflection from the termination, slightly mis-matched, was not seriously distorting the probability results. The nearness of the theoretical proper termination to the best possible was confirmed by the later oscillographic records.

Table 5. Variation of P with irradiator pulse time for fixed test pulse time. The effect of delay line termination is shown.

Gas - Dry air. Pressure 76 cm. Hg. Applied volts 20 Kv.
Fixed test pulse time at 30 line units.

Termination. (Ohms across the end capacitance).	Position of irradiator on delay line B. (line units)								
	10	15	20	25	30	35	40	45	50
0	39	+	+	+	+	50	0	0	0
100	36	96	+	+	+	46	0	0	0
150	35	95	+	+	+	45	0	0	0
200	36	95	+	+	+	45	0	0	0
1000	41	+	+	+	+	50	0	0	0
Infinite.	51	+	+	+	+	55	2	0	0

100 % indicated by +.

3.2.9. The effect of the size of the pulse forming condenser (Figure 4) on sparking probability.

All of the experimental work carried out, except that described in this section, was with the condenser at the input to the line of value 150 micro-microfarads. The shape of the pulse which travelled down the line was as shown in figure 29 in the section on oscillographic recording. It was thought that the size of this condenser might be one of the

many possible variables which could contribute to the value of P for a given setting of the irradiator and test pulse leads. A brief investigation was made of this possibility, using in succession three values of capacitance C₂, namely, 60, 150, and 190 micro-microfarads. The result for different irradiator pulse times and a fixed test pulse time using 20 Kv. pulses is shown in table 6, where it is seen that the larger condenser value gave generally a larger value of P. This may be due to the larger condenser forming a longer duration pulse, but without extended oscillographic investigation of the shape of the pulse for the 60 and 190 micro-microfarad condensers no definite statement on this point can be made.

Table 6. Variation of P with irradiator pulse time for fixed test pulse time. The effect of line input condenser value is shown.

Gas - Dry air. Pressure 76 cm. Hg. Applied volts 20 Kv.
Fixed test pulse time at 30 line units.

Line input capacitance.	Position of irradiator on delay line B. (line units)								
	10	15	20	25	30	35	40	45	50
$\times 10^{-12}$ farads.	P \times 100								
60	5	82	+	+	+	14	0	0	0
150	34	96	+	+	+	45	0	0	0
190	40	+	+	+	+	70	10	0	0
	100 % indicated by +.								

It is quite conceivable that the larger C_2 the slower will be the rise of potential on the electrode of the line input trigatron and also the slower will be the discharge of the condenser into the delay line subsequent to the breakdown of the trigatron gap.

3.3. Mechanical count records in gases.

3.3.1. Conclusions from the early experiments.

Results quoted so far were all taken using dry air at atmospheric pressure, brass irradiator electrodes (which gradually deteriorated as a result of the relatively heavy discharges of the short gap) and with the largest collimator aperture consistent with the shielding of the test electrodes from the irradiator beam. They served to show that an effect in the gas of the test gap, directly attributable to the irradiator spark, was triggering the test spark. The effect of increase in probability has been shown to vary in a systematic way with the manner in which the short duration irradiator and test pulses were applied.

1. Only a very limited range of times separating the time of application of the test pulse and the time of

irradiation of the test gas resulted in an increase in P above the value 0 obtained when the test gas was un-irradiated. The change in P from 0 to 1 occurred for a change in the time separating irradiator and test pulses of less than 10^{-8} sec.

2. Increase in overvoltage of the test gap increased the range of irradiator times, for any fixed test pulse time, for which an increase in P was observed.

3. The range of times over which P was increased depended not only on the delay line settings of the pulse leads, but also on the RC value of both the irradiator and test gap capacitances, together with the resistances in series with them.

4. The value of P was shown to increase with the size of the input condenser to the delay line for the limited number of capacitances tried.

5. P did not appear to be critically affected by a mismatch of the delay line by up to 25 % of the calculated characteristic impedance.

The work was next extended to cylinder commercial nitrogen, oxygen, hydrogen and argon, with the aim of deciding the form of the graph of P against irradiator time, for fixed test pulse times under conditions in each gas corresponding to

those in dry air.

3.3.2. Pre-set electrode arrangements and electrical circuit constants in experiments with various gases.

In all gases examined in the present section the following conditions of test were applied, unless specific data are given to the contrary:-

1. Separation of test electrodes,	mm. 2.1
2. Separation of irradiator electrodes, (tungsten),	1.0
3. Average diameter of irradiator spark, (estimated from tungsten diameter),	0.5
4. Collimator aperture near a) test gap, b) irradiator,	0.55 0.4
5. Distance from test gap to collimator,	22.0
6. Distance from test gap to irradiator,	95.0
7. Capacitance of test gap, Resistance in series with test gap,	97 uuf. 150 ohms.
8. Capacitance of irradiator gap, Resistance in series with irradiator,	195 uuf. 100 ohms.

3.3.3. Dry air.

The basic form of the graphs of sparking probability against irradiator time, for a fixed test pulse time, checked with the new irradiator and collimator conditions as listed above.

The general shape of these test curves, as already indicated,⁶ was not altered; a complete set of records for these new conditions of test is included in tables 7 to 16, for two values of pulse voltage and six set pressures. The range of irradiator times for which a finite value of P was recorded here is less than for the earlier exploratory measurements; the times at which the irradiator pulse started and ceased to affect P as the irradiator leads were moved down the delay line were also earlier than for former experiments. Both of these changes are reasonable when it is recalled that a) a reduction has been made in the size of the collimator apertures, + , and b) an increase of 30 micro-microfarads has been made in the irradiator capacitance and 100 ohms is now permanently included in the irradiator leads, so increasing the irradiator gap RC time.

A decrease in the pressure resulted in a general increase in the value of P for a given setting of irradiator and test pulse times; the range of values for which a finite value of P was obtained was also extended (see for example table 7). The results of that table are shown in graphical

⁶ See previous test results, pages 60 on.

⁷ Prowse and Jasinski have recorded a change in P with the flux of photons entering the test gas.⁷⁶

Table 7. Probability counts for dry air at six set pressures and applied voltage 24 Kv.

Pressure. mm. Hg.	Test gap position. Line units.	Position of irradiator on delay line. Line units.								
		10	20	30	40	50	60	70	80	90
		P x 100								
720	20	+	90	10	0	0	0			
	40	45	+	90	25	0	0	0	0	0
	50	0	50	+	50	0	0	0	0	0
	60	0	0	0	0	0	0	0	0	0
610	20	+	+	65	0	0	0			
	40	+	+	+	75	0	0	0		
	60	0	10	+	+	+	60	0	0	0
500	20	+	+	+	0	0	0			
	40	+	+	+	+	30	0	0	0	
	60	0	60	+	+	+	+	60	10	0
390	20	+	+	+	60	0	0	0		
	40	+	+	+	+	+	0	0	0	0
	60	0	+	+	+	+	+	+	+	+
280	20	+	+	+	+	+	+	70	40	0
	40	+	+	+	+	+	+	50	20	0
	60	+	+	+	+	+	+	+	+	+
180	20	100 % count for all settings, independent of irradiator.								
	40									
	60									

+ indicates 100 % count.

Table 8. Probability counts for dry air at six set pressures and applied voltage 20 Kv.

Pressure. mm. Hg.	Test gap position. Line units.	Position of irradiator on delay line. Line units.							
		10	20	30	40	50	60	70	80
		$P \times 100$							
720	20	90	10	0	0	0			
	40	20	30	0	0	0	0		
	50	0	40	50	0	0	0		
	60	0	0	0	0	0	0	0	
610	20	+	60	0	0	0			
	40	+	+	65	0	0	0		
	60	0	0	+	90	0	0	0	
500	20	+	70	0	0	0			
	40	+	+	+	+	10	0	0	0
	60	0	60	+	+	+	70	0	0
390	20	+	+	30	0	0	0		
	40	+	+	+	+	15	0	0	0
	60	0	+	+	+	+	+	0	0
280	20	+	+	+	0	0	0		
	40	+	+	+	+	+	0	0	0
	60	+	+	+	+	+	+	+	0
180	20	100 % count for all settings, independent of irradiator.							
	40								
	60								

+ indicates 100 % count.

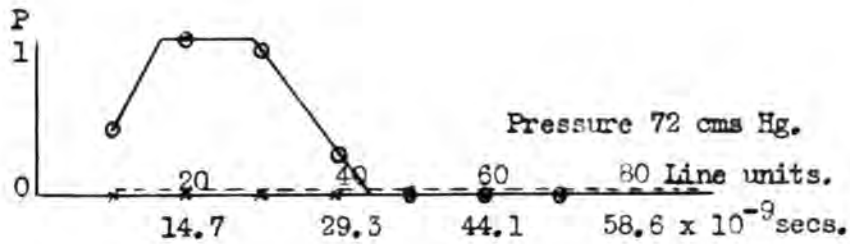
form of P against irradiator time, for each pressure, in figure 18; the full line graph is for the test pulse time 40 line units from the delay line input, while the broken line graph is for it at 60 line units. If the same type of graph is drawn from the results of table 8 for 20 Kv. pulses, no exact equivalence can be seen between the graph for any particular pressure with that for any other pressure in the 24 Kv. set. The following two sets are nearly equivalent, a) 610 mm.Hg. with 24 Kv. pulses, table 7, and 300 mm.Hg., with 20 Kv. pulses, table 8, and b) 500 mm.Hg. table 7, and 280 mm.Hg., table 8. They are sufficiently close in the value of P and range of effective irradiator times to suggest the possibility that there is an increase in overvoltage that will give the same change in P as a given change in pressure. Both increase in pulse voltage and decrease in pressure appear to have the same effect on P , probably attributable to an increase in what has been termed the effective pulse duration.

It may be, however, that an increase in P as pressure is reduced is not only a direct effect of increase in overvoltage. There is the possibility that the flux of photons

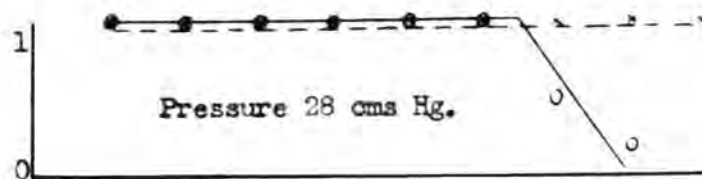
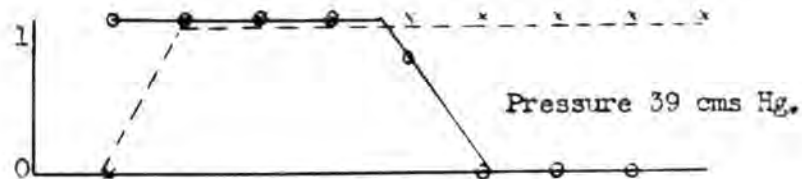
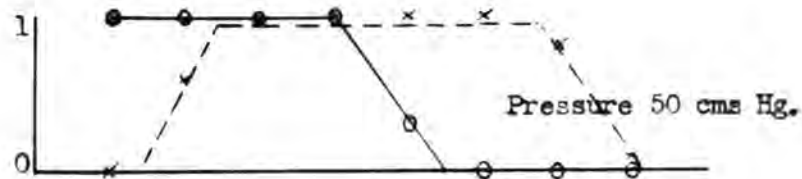
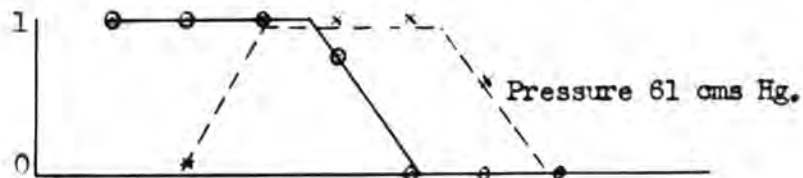
Fig. 18. Variation of sparking probability with irradiator pulse time for fixed test pulse time. The effect of change in pressure is illustrated.

Gas - Dry air.

Applied volts 24Kv.



Position of irradiator on delay line B.



Tg fixed at 40 line units •
Tg fixed at 60 line units x

At 18 cms pressure the test gap fired without irradiation.

penetrating to the test gap is increased as the mass of gas between the irradiator spark and the sensitive volume of the test gas is decreased.

With 24 Kv. pulses in air at 720 mm. Hg. a movement of the irradiator to a later time by 18 line units, (0.014 microsec.), was required to change P either from 0 to 1 when earlier than the test pulse, or from 1 to 0 again when applied after the start of the test pulse. As the pressure was reduced the movement of irradiator time to achieve the same change in P of unity decreased to a constant value not in excess of 0.009 microsec., indicating the high speed of onset of the particular mechanism responsible for the effect in the gas.

5.3.4. Nitrogen.

The sparking probabilities measured for nitrogen are shown in tables 9 and 10. They were generally higher than for the equivalent conditions in air. This may be simply an indication of the lower breakdown voltage in nitrogen, (increased effective pulse time), or it could indicate a change in the type of radiation active in the test gas from that active

Table 9. Probability counts for nitrogen at five set pressures and applied volts 24 Kv.

Pressure. mm. Hg.	Test gap position. Line units.	Position of irradiator on delay line. Line units.							
		10	20	30	40	50	60	70	80
		$P \times 100$							
725	20	+	+	70	15	0	0	0	0
	40	0	+	+	60	0	0	0	0
	60	0	0	0	90	+	50	10	0
	80	0	0	0	0	0	+	+	90
610	20	+	+	+	+	+	+	+	+
	40	0	+	+	+	+	+	+	50
	60	0	0	0	+	+	+	+	+
	80	0	0	0	0	30	+	++	+
480	20	+	+	+	+	+	+	+	+
	40	+	+	+	+	+	+	+	50
	60	0	0	+	+	+	+	+	+
	80	+	0	0	40	+	+	+	+
390	20	100 % independent of irradiator.							
	40	+	+	+	+	+	+	+	+
	60	0	0	+	+	+	+	+	+
	80	80	0	35	+	+	+	+	+
280	20	100 % independent of irradiator.							
	40	100 %	"	"	"	"	"	"	"
	60	100 %	"	"	"	"	"	"	"
	80	+	+	+	+	+	+	+	+

+ indicates 100 % count.

Table 10. Probability counts for nitrogen at five set pressures and applied volts 20 Kv.

Pressure. mm. Hg.	Test gap position. Line units.	Position of irradiator on delay line. Line units.							
		10	20	30	40	50	60	70	80
		P x 100							
725	20	+	+	60	0	0	0		
	40	0	30	20	0	0	0		
	60	0	0	0	30	30	0	0	0
	80	0	0	0	0	0	70	70	30
610	20	+	+	+	0	0	0		
	40	0	+	+	+	+	0	0	0
	60	0	0	0	+	+	+	50	0
	80	0	0	0	0	0	+	+	+
480	20	+	+	+	10	0	0		
	40	+	+	+	+	+	0	0	0
	60	0	0	+	+	+	+	+	0
	80	90	0	0	20	+	+	+	+
390	20	100 % independent of irradiator.							
	40	+	+	+	+	+	+	+	0
	60	0	0	+	+	+	+	+	+
	80	70	0	40	+	+	+	+	+
280	20	100 % independent of irradiator.							
	40	100 % " "							
	60	100 % " "							
	80	+	+	+	+	+	+	+	+

+ indicates 100 % count.

Table 11. Probability count for nitrogen for five set pressures and applied volts 16 Kv.

Pressure. mm. Hg.	Test gap position. Line units.	Position of irradiator on delay line. Line units.							
		10	20	30	40	50	60	70	80
		$P \times 100$							
725	20	+	0	0					
	40	0	0	0	0				
	60	0	0	0	0	0	0		
	80	0	0	0	0	0	0	0	
610	20	+	+	+	0	0	0	0	0
	40	0	+	+	+	0	0	0	0
	60	0	0	0	+	+	25	0	0
	80	0	0	0	0	0	+	70	50
480	20	+	+	+	0	0	0	0	0
	40	+	+	+	+	0	0	0	0
	60	0	0	+	+	+	30	0	0
	80	+	0	0	0	+	+	+	+
390	20	+	+	+	0	0	0		
	40	+	+	+	+	30	0	0	0
	60	0	40	+	+	+	+	0	0
	80	20	0	0	+	+	+	+	+
280	20	+	+	+	+	+	+	0	0
	40	+	+	+	+	+	+	+	0
	60	+	+	+	+	+	+	+	0
	80	+	+	+	+	+	+	+	+

+ indicates 100 % count.

in air. Consistent sparking of the irradiator was possible when a 16 Kv. pulse was applied and so this additional set of records is included in table 11.

The trend of the nitrogen records as pressure was reduced was very similar to that for air, but the stage at which the test gap fired independently without irradiation occurred at a higher pressure than for air. The movement of the time of the irradiator needed to give a change in P of unity was the same at the lower limit as that reached in air, 0.009 microsec.

At the lower pressures, below 500 mm. Hg. an unexpected but finite value of P was recorded when the irradiator was timed to be very early and the test pulse late, (see tables 9 and 10). This value of P was reduced to zero as the irradiator was moved to a later time; then when the irradiator was timed later still the usual and expected rise of P to a maximum occurred as the test and irradiator pulses were almost coincident in time. This same phenomena had been noticed in the early air results and is there illustrated in figure 13. A longer total delay time than 0.08 microsec. used here would be required for

a full investigation of the nature of this part of the P - irradiator time graph. Possible causes of it are considered tentatively in the later discussion.

3.3.5. Oxygen.

With the same test conditions as were used for the other gases it was difficult at the higher pressures to keep the irradiator firing regularly in oxygen. The 'bleeder' spark gap, arranged to give ionising radiation in the irradiator gap to ensure its breakdown, (described in section 2.2.5.), fired regularly but the irradiator did not. A continuous discharge was arranged between the electrodes of the bleeder gap but there was no improvement in the firing of the irradiator gap. It was presumed that sufficient pre-ionisation was not being produced in the irradiator gap to trigger the irradiator spark in every trial made. It was decided to continue the experiment with the electrode systems in exactly the same form as that used for the other gases air and nitrogen, as only the test pulses during which the irradiator actually fired were counted as trials and the counts required for a determination of P were still made. Even when the irradiator was firing regularly, at the lower pressures,

test sparks seemed to come in groups or bursts of consecutive sparking not experienced in the purely random nature of the test sparks counted in the other gases.

Probability counts were low in oxygen ; for pressures above 600 mm. Hg. unit value of P was not recorded for any setting of the times at which pulses were applied to the irradiator and test gaps. Fixed test pulse time settings were taken at intervals of 10 units (see table 12) and the irradiator time was moved through each test pulse time while counts of P were made in the usual way, before it was satisfactorily established that the pattern of the P - irradiator time graphs was not dissimilar to those already established for air and nitrogen. At 255 mm. Hg. pressure the test gap would not break down for 24 Kv. pulses independent of the irradiator, (in other gases it would), but when the irradiator was firing the test gap fired with unit probability for all time settings.

The change in P as the time of irradiation was moved through the test pulse time was comparatively slow; the least change in irradiator time recorded which would change P from 0 to 1 was 0.03 microsec.

Table 12. Probability counts for oxygen at four set pressures and applied volts 24 Kv.

Pressure. mm. Hg.	Test gap position. Line units.	Position of irradiator on delay line. Line units.							
		10	20	30	40	50	60	70	80
		P							
		x							
		100							
750	10	30	10	0	0	0	0	0	0
	20	75	25	30	20	20	0	0	0
	30	40	30	20	15	0	0	0	0
	40	0	50	20	0	0	0	0	0
	50	0	0	30	20	0	0	0	0
	60	0	0	0	0	0	0	0	0
660	10	75	65	20	20	0	0	0	0
	20	60	55	40	10	0	0	0	0
	40	15	20	30	20	20	0	0	0
	60	0	0	10	45	40	20	0	0
460	10	+	+	+	+	70	40	0	0
	20	+	+	+	+	+	+	40	0
	40	+	+	+	+	80	80	70	0
	60	10	20	50	+	90	60	50	50
255	10	Still dependent on irradiator but 100 % count for all settings.							
	20								
	40								
	60								

+ indicates 100% count.

Table 13. Probability counts for oxygen at four set pressures and applied volts 20 Kv.

Pressure. mm. Hg.	Test gap position. Line units.	Position of irradiator on delay line.							
		10	20	30	40	50	60	70	80
		Line units.			Line units.				
		P			x			100	
750	10	0	0	0	0				
	20	55	25	0	0				
	30	40	25	0	0				
	40	0	0	0	0				
660	20	30	15	0	0	0			
	40	20	20	20	15	5	0	0	
	60	0	0	0	25	15	10	0	
460	20	90	70	15	0	0	0	0	
	40	80	80	80	40	50	10	0	
	60	0	10	30	70	80	20	0	
255	20	Still dependent on irradiator but							
	40	100 % count at all settings.							
	60	100 % count at all settings.							

+ indicates 100 % count.

3.3.6. Hydrogen.

Hydrogen was, at the other extreme from oxygen, very easy to work with. The irradiator spark was singularly vigorous and the sparking probability could be examined using pulse voltages as low as 12 Kv. Results of the probability counts are shown for 24, 20 and 16 Kv. in tables 14, 15 and 16 respectively.

P had a remarkable short, sharp cut-off region; an additional separation in the time of the test pulse and irradiator pulse of four line units (0.0028 microsec.) being sufficient for the probability to $\frac{90}{\wedge}$ from 1 to 0 even at atmospheric pressure.

In hydrogen unexpected spark counts, as recorded in nitrogen and the very early experiments in air, again appeared for late test pulses with the irradiator timed very early. They appear to occur, for any given applied voltage, at pressures just above those at which the test gap sparking becomes independent of the irradiator. At atmospheric pressure in hydrogen (table 14) this unexpected count was particularly apparent, a fact which led to further investigation with the oscilloscope to make absolutely certain that it was not an effect of reflections on the delay line.

Table 14. Probability counts for hydrogen with applied volts 24 Kv.

Pressure. mm. Hg.	Test gap position. Line units.	Position of irradiator on delay line. Line units.							
		10	20	30	40	50	60	70	80
					P	x	100		
739	10	+	+	+	Part radiation independent.				
	20	+	+	+	+	+	+	+	+
	30	+	+	+	+	+	+	+	+
	40	0	+	+	+	+	+	+	+
	50	80	50	+	+	+	+	+	+
	60	+	+	50	0	90	+	+	+
	70	+	+	80	20	50	+	+	+
	80	+	+	+	55	0	+	+	+
	90	+	+	+	+	70	0	0	30
650	20	For test gap positions up to 30, 100 %							
	40	count made independent of irradiator.							
	60	For test gap positions 40, 60 and 80 still							
	80	dependent on irradiation but 100 % for all							
		settings.							
550	For pressures of 550 mm. Hg. and less								
	sparking probability becomes quite								
independent of irradiation and 100 %									
is recorded for all settings.									

+ indicates 100 % count.

Table 15. Probability counts for hydrogen at four pressures and applied volts 20 Kv.

Pressure. mm. Hg.	Test gap position. Line units.	Position of irradiator on delay line.							
		10	20	30	40	50	60	70	80
					Line units. P x 100				
739	20	+	+	+	80	20	0	0	0
	40	+	+	+	+	+	+	50	0
	60	0	0	+	+	+	+	+	+
	80	60	20	0	0	0	+	+	+
650	20	+	+	+	+	+	+	60	0
	40	+	+	+	+	+	+	+	+
	60	0	80	+	+	+	+	+	+
550	20	+	+	+	+	+	+	+	60
	40	+	+	+	+	+	+	+	+
	60	+	+	+	+	+	+	+	+
450	20	Still dependent on irradiator but 100 % count for all settings.							
	40								
	60								
	80								

+ indicates 100 % count.

Table 16. Probability counts for hydrogen at five pressures and applied volts 16 Kv.

Pressure. mm. Hg.	Test gap position. Line units.	Position of irradiator on delay line.							
		10	20	Line units. P x 100			60	70	80
739	20	+	+	+	0	0	0	0	0
	40	+	+	+	+	+	60	0	0
	60	0	0	+	+	+	+	+	0
	80	0	0	0	0	0	+	+	+
650	20	+	+	+	+	0	0	0	0
	40	+	+	+	+	+	0	0	0
	60	0	0	+	+	+	+	+	0
	80	0	0	0	0	0	+	+	+
550	20	+	+	+	+	0	0	0	0
	40	+	+	+	+	+	0	0	0
	60	0	30	+	+	+	+	+	60
	80	+	60	0	0	+	+	+	+
450	20	+	+	+	+	30	0	0	0
	40	+	+	+	+	+	0	0	0
	60	+	+	+	+	+	+	+	+
	80	+	+	+	+	+	+	+	+
350	20	Still dependent on irradiator but							
	40								
	60	100 % count for all settings.							
	80								

+ indicates 100 % count.

3.3.7. The facility for sparking of the gases tested with the same experimental conditions.

The minimum sparking potentials of the gases used in this work, for the application of direct voltage with no time limit, are in ascending order of magnitude, hydrogen, oxygen, air and then nitrogen.⁷⁷ At ultra high frequency the order in which the gases break down as the voltage is increased is hydrogen, nitrogen, air then oxygen⁷⁸. With short duration direct voltage pulses the gas hydrogen again breaks down most readily. The facility for sparking found for the other gases examined seems to be in the same order as that found in the U.H.F. work rather than in the order found in experiments with extended direct voltage, i.e. nitrogen, air then oxygen.

In tables 17 and 18, which follow, the irradiator lead positions have been given at which a probability of 0.5 was recorded. This has been done for each pressure, voltage and test gap time position at which the four gases could be compared. Under each gas heading two columns of symbols are shown. The column on the left indicates the earliest irradiator position (in line units from the delay line input) where P was 0.5 and the slope of the P - irradiator time curves was positive. The

Table 17. Irradiator positions at which a sparking probability of 0.5 was recorded in hydrogen, nitrogen, air and oxygen; 20Kv.pulses.

Pressure.	Test gap position.	Hydrogen	Nitrogen	Air	Oxygen
750 739 725 720	20	E 45	E 31	E 16	E 12
660 650 610		E 70	E 35	E 21	U U
550 500		E 82		E 22	
480 450 390		E L	E 55 I I	E 28	E 23
750 739 725 720	40	E 70	U U	15 23	U U
660 650 610		E L	15 55	E 31	U U
550 500		E L		E 46	
480 450 390		E L	E 55 E 75	E 47	E 40
750 739 725 720	60	25 L	U U	25 25	U U
660 650 610		15 L	35 70	25 44	U U
550 500		E L		19 62	
480 450 390		E L	25 75 25 L	15 65	36 55

Table 13. Irradiator positions at which a sparking probability of 0.5 was recorded in hydrogen, nitrogen, air and oxygen; 24Kv. pulses.

Pressure.	Test gap position.	Hydrogen	Nitrogen	Air	Oxygen	
750	20				E 15	
739		E L				
725			E 35			
720				E 25		
660						E 21
650		I I				
610			E L	E 52		
550						
500					E 35	
480				E L		
450					E 68	
390			I I	E 41		
750		40				20 20
739			E L			
725				15 42		
720				11 36		
660						U U
650		E L				
610			15 80	E 45		
550						
500					E 48	
480				E 60		
450					E 73	
390			E L	E 55		
750		60				U U
739			30 L			
725				55 60		
720				U U		
660			E L			U U
650			35 L			
610				24 61		
550						
500					9 75	
480				25 L		30 70
450						
390			25 L	5 L		

right hand column gives the irradiator position with P again equal to 0.5 where the slope of the same graph was negative. Where no early irradiator time gave a value as low as 0.5 a letter E is used. A letter L indicates that no late irradiator time where P was as low as 0.5 was observed on the length of delay line available. The letter I indicates that for all irradiator times the test spark occurs independent of irradiation. U indicates that the irradiator never has sufficient effect to give a probability of 0.5.

The range of irradiator times for which a sparking probability in excess of 0.5 was recorded here was, for each pressure and test pulse time, greatest in hydrogen, less in nitrogen, air and oxygen in that order.

SECTION 4.Photographs of test gap sparks.4.1. Introduction.

While checking visually the operation of the mechanical test spark counter it was noticed that certain extremely faint sparks, only observable in a blacked out room, were not recording counts. This indicated that the current through the test gap was not sufficiently in excess of the displacement current through the balancing capacitance of the detector circuit, figure 10, to trip the thyatron of the spark counter circuit. But the balancing capacitance was essential if the displacement current through the test gap capacitance, for an applied pulse failing to give a spark, was not to record a count. The counter system was not sufficiently sensitive to record the difference, if any, that there might have been between a capacitive pulse through the test gap and a very faint spark. It was therefore decided to photograph the test gap with conditions such that faint sparks could be compared with strong ones.

The camera, (fitted with an astigmatic glass lens of

focal length 1.25", f 1.9), was arranged above the test chamber to take an exposure for each voltage pulse applied to the test gap. A pulse applied was indicated on the side of the film by an auxiliary light spot. This, together with a later count of the sparks photographed, gave a measure of the value of P . As the photographs were taken through the Pyrex glass chamber walls, which were a centimeter thick, the lower wavelength limit of the light able to activate the H.P.3 film was about 3700 Å. The photographs of sparks taken with test conditions where relative irradiator and test pulse timing or gas pressure were varied showed changes in diffuseness, intensity and multiplicity more than could be noted visually.

The test gap width, the distance of the test gap from the irradiator and other distances in the test chamber were retained the same as those used in the previous section of work. Close links were noticed, in examining the spark photographs between the type of spark channel developed and the value of P recorded. This value of P found from the photographs, as near as could be estimated from 10 exposures for each setting of the time separating the irradiator and

test pulses, was a little in excess of the mechanical count where low values of P occurred. Where test and irradiator pulses were sufficiently close in time to give high values of P the same value was recorded by photographic and mechanical means, for then no faint sparks occurred. Photographs of sparks in air, oxygen, nitrogen and hydrogen are shown in the figures from 19 to 25. Viewing the photographs directly, a) the plane of the electrode surfaces was perpendicular to the surface of the paper and parallel to the side edges, b) the irradiating photons entered the test gap in a direction from the top edge of the paper to the bottom one. Conditions of test peculiar to each photograph are indicated below it, using the abbreviations set out in figure 19. To keep the length of the film reasonably short for a large number of trial photographs, a) the camera was made to move on sliders in the time between one pulse trial and the next, so that two exposures could be made on the width of the film and b) the film was moved only a fraction of a frame by hand after every two exposures. The order of the images as they appear in the photographs is :-

1 3 5 n
 2 4 6 n + 1 for successive trials.

4.1.1. Dry air spark photographs.

The general shape of the air spark was that of a waisted dumbbell ∞ (see figures 19 to 21). At atmospheric pressure this shape was fairly clearly defined, but using the camera stopped down to f 3.1 showed that the dumbbell consisted of a fine filament connecting bright spots on the electrodes, (figures 19.3 and 20.1), surrounded by a more diffuse glow. This glow spread further from the core of the spark channel as the pressure was reduced.

The way in which the type of spark channel changed with irradiator time at a fixed test pulse time is of interest.

a) Irradiator very early.

It was found that where values of P were small the density of the images of spark channels was correspondingly low. Occasional extremely weak channels occurred as if of a partly developed spark, (figure 20.4), and it is possible that these channels did not completely bridge the gap.

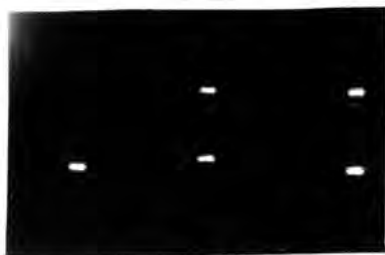
b) Irradiator just early.

Figure 19. Photographs of sparks formed in air.

Test gap distance, in line units, from input to delay line A is indicated by Tg

Irradiator distance from input to delay line B is indicated by Ig ..

Pressure in cm.Hg. is p ... Camera lens stop is f 1.9 or f ...



19.1 Tg 30, Ig 20,
p 76, f 1.9.
6 trials; 3 single,
2 double, 1 failure.



19.2 Tg 30, Ig 20,
p 76, f 1.9.
6 trials; 4 single,
2 failures.



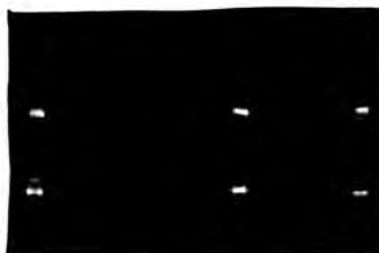
19.3 Tg 40, Ig 40
p 76, f 3.1.
2 trials showing spots
at electrodes.



19.4 Tg 60, Ig 40,
p 66, f 1.9.
6 trials; 4 single,
2 double, 2 diffuse.



19.5 Tg 30, Ig 30,
p 56, f 1.9.
6 trials; 4 single,
1 double, 1 diffuse.



19.6 Tg 30, Ig 30,
p 56, f 1.9.
6 trials, 4 single,
1 double, 1 diffuse.

Fig. 20. Photographs of sparks formed in air, continued.

20.1 Tg 30, Ig 40,
p 56, f 3.1.
4 trials; 4 sparks
differing in intensity,
shape and multiplicity.



20.2 Tg 60, Ig 45,
p 56, f 1.9.
8 trials; 8 sparks with
multiple or diffuse
channels.



20.3 Tg 40, Ig 20, p 46, f 1.9.



Tg 40, Ig 40.



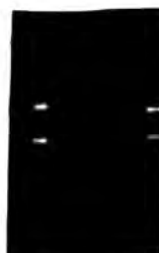
Tg 40, Ig 60.



20.4 Tg 60, Ig 45,
p 46, f 1.9.
10 trials; 3 single,
(2 faint), 7 failures.

20.5 Tg 40, Ig 60,
p 56, f 1.9.
6 trials, 3 singles,
(1 faint), 3 failures.

Fig. 21. Photographs of sparks formed in air, nitrogen, oxygen and hydrogen under similar test conditions.



Air **Nitrogen** **Oxygen** **Hydrogen**
21.1 4 trials, Tg 60, Ig 50, p 66, f 1.2.



Air **Nitrogen** **Oxygen** **Hydrogen**
21.2 2 trials as for 21.1 but enlarged prints.

b) Irradiator just early.

As irradiator time was moved to be just earlier than test pulse time the brightness of the spark channel image increased to a maximum. Here at the higher pressures, (680 mm. Hg. and over), a very occasional double spark occurred,

(figures 19.1 and 19.4). These multiple sparks, often with more than two channels, occurred much more frequently as the pressure was reduced. Usually one of the multiple channels was of the same normal shape and brightness as the single sparks occurring at the same delay line setting of the leads to the irradiator and test gaps, (figures 20.2 and 20.3). This strong channel occurred most often on the side of the test gap near to the source of radiation. On the side of the strong spark, remote from the irradiator and into the test gap, were the one or more fainter channels, many of which did not appear to reach the electrodes with the bright spot that was usual for the stronger sparks. Occasionally double spark channels were of equal brightness, (figure 20.2, trial 8 and some trials in 20.3). Sometimes a single dense channel had an area of diffuse radiation into the gas of the test gap on the side remote from the irradiator, (figures 19.4, 19.5 and others).

c) Irradiator late.

With late irradiator times the occasional faint sparks, described in a) above, began to appear again, as if the radiation

in the gas of the test gap had insufficient time to be effective, (figure 20.5).

A set of spark photographs taken for three different irradiator times, with fixed test pulse time, at 46 cm. Hg. pressure, is shown in figure 20.5, illustrates the differences of channel and multiple channel development.

A set of photographs with the same set conditions in air, oxygen, nitrogen and hydrogen is shown in figures 21.1 and 21.2.

Fig. 22. Photographs of sparks formed in nitrogen.




22.1. Tg 30, Ig 10, p 76, f 1.9.
15 trials with 0 ohms in series with the irradiator gap.



Tg 30, Ig 10, p 76, f 1.9.
10 trials with 66 ohms in series with the irradiator gap.

4.1.2. Nitrogen spark photographs.

The spark photographs in this gas showed dense bushy oval images  . Removing the image diffuseness by using the camera lens stopped down to f 3.1, the spark, if really bright remained oval shaped, but if less bright resolved into a dash shape with no sign of ball ends. Changes in spark type with relative irradiator and test pulse times were as follows :-

- a) Irradiator much earlier than test pulse; dash shaped faint single spark channels occurring with the same probability as medium density oval shaped spark images, (see figures 23.1).
- b) Irradiator just early; bulbous very dense single sparks, often 'winged', (see figures 23.1 and 23.3). Frequently at these pulse settings multiple channels developed as in air, (figure 23.1).
- c) Irradiator just later than the start of the test pulse gave less dense oval sparks, sometimes winged, but less frequently multiple.
- d) With a very late irradiator pulse setting, giving low values of P, medium density oval shaped single sparks developed with

Fig. 23. Photographs of sparks formed in nitrogen, continued.

23.1. Tg 60, Ig 30, p 66, f 1.9. 10 trials.



Tg 60, Ig 40.



Tg 60, Ig 50.



Tg 60, Ig 60.



Tg 60, Ig 80.



23.2. Tg 60, Ig 20, p 46, f 1.9. Diffuse sparks.



23.3. Tg 30, Ig 30, p 56, f 1.9. Winged diffuse sparks.

about the same frequency as dash shaped faint spark channels. Again a very rare type of spark occurred in delay line settings where its type was not the general rule, indicating the statistical nature of the development of spark channels.

A set of particularly diffuse sparks is shown in figure 23.2. Figure 23.1 shows the effect on the type of spark channel formed of introducing a resistance in series with the irradiator gap. This has already been attributed to the time effect of making the irradiator spark later by an interval RC where R is the resistance introduced and C is the irradiator gap capacitance.

4.1.5. Oxygen spark photographs.

Definite ball ended filament spark channels were the rule in oxygen for the fully developed spark, (figures 24.1). A larger proportion of angular spark irregularities occurred in this gas than in air, nitrogen or hydrogen, (figures 24.1, 24.2, 24.3 and 24.4). The spark images were denser than for air sparks and tended to be narrower in the waist, (figures 21.1 and 21.2). The f 3.1 stop at the camera lens revealed the ball ended filament channels more clearly, (figure 24.2).

Fig. 24. Photographs of sparks formed in oxygen.

24.1. Tg 20, Ig 30,
p 76, f 1.9.
6 trials; 4 singles,
2 failures.



24.2. Tg 20, Ig 30,
p 76, f 3.1.
6 trials; 4 singles,
2 failures.



24.3. Tg 20, Ig 30,
p 66, f 1.9.
Another irregular spark.



24.4. Tg 20, Ig 30,
p 76, f 1.9.
6 trials; 3 single,
(1 faint irregular),
3 failures.



24.5. Tg 30, Ig 30,
p 56, f 1.9.
6 trials; 5 single
with the only double
spark observed in oxygen.

No change in the density of the channel image on the photographic film could be detected for cases where the irradiator pulse time was moved through test pulse time. Even when the recorded values of P were low only occasional faint single sparks were observed, (figure 24.4). Only one double spark channel was photographed in oxygen for all the trials made and that was at a low pressure, (figure 24.5).

4.1.4. Hydrogen spark photographs.

Hydrogen sparks were extremely fine filaments with very small spots on the electrodes. They were similar to those of oxygen but with much less intense brightness. A slight increase in brightness occurred with a decreasing pressure, but the sparks were never diffuse. As in the other gases, except oxygen, an increase in brightness could be noticed in the records as the irradiator pulse time was moved in time through the test pulse time, with a subsequent fall off in brightness of image as the irradiator pulse became late, (figs. 25.1 to 25.3). But in only one case, even with pressures down to 46 cm. Hg., was a double spark recorded.

Fig. 25. Photographs of sparks formed in hydrogen.

25.1. Tg 60, Ig 70,
p 76, f 1.9.
8 trials, all
single filamentary sparks.



25.2. Tg 60, Ig 70,
p 76, f 3.1.
6 trials, all
single sparks.



25.3. Tg 60, Ig 80,
p 76, f 1.9.
6 trials; 4 single sparks,
less dense than those of 25.1. above.

4.1.5. Summary of spark photograph phenomena.

The general pattern of the changes brought about by the radiation incident in the gas of the test gas at different times relative to the time of the applied test pulse is shown in figure 23.1. for nitrogen. This gas showed the greatest amount of change in spark form with irradiator timing. Points of comparative interest in the gases examined are as follow:-

a) With irradiator pulse time earlier than test pulse time, but giving a finite value of P , single sparks showing low density of image were recorded in air, nitrogen and hydrogen. Oxygen showed strong single sparks. In all gases examined occasional very faint single sparks were recorded; no double sparks appear to occur here.

b) With irradiator pulse just earlier than test pulse time, so that there is considerable overlap of the effective irradiator and test pulses, an increase in the density of single spark channels occurs which is observable in the gases examined, except oxygen. Multiple spark channels occur in air and in nitrogen, the latter gas in particular showing a diffuse glow in the gas surrounding the main spark channel;

the occurrence of secondary faint channels, more frequently on the side of the main channel away from the irradiator, is the rule. Oxygen and hydrogen show little tendency to the formation of multiple spark channels at the pressures used.

c) The brightness of the spark channels falls off, from those observed in the conditions b) above, when the irradiator pulse is applied during the later stages of the test pulse. Also a smaller proportion of multiple channels occurs for these conditions of irradiation than in the conditions of b) for gases air and nitrogen. With irradiation very late in the test pulse and probability of sparking low, the intensity of sparks falls off further and occasional faint sparks are observed as in the conditions of a) above.

The appearance of very sharp angular bends in occasional spark channels, especially in oxygen, seems to be an indication that, even in a short gap, the spark development is not always completed in a single stage between the electrodes. The apparent failure of the weaker spark channels to completely cross the gap indicates that the sparks initiated in the region of the gas irradiated by the ultra-violet light

from the irradiator spark and that the discharge starts in mid-gap, spreading to the electrodes from there.

Due to the lower value of the minimum sparking voltage in hydrogen the records in that gas were taken at 18 and 14 Kv. rather than the 24 and 18 Kv. used in the other gases. One set of records taken of hydrogen sparks at 24 Kv. is still of interest. Here, at atmospheric pressure, P was unity independent of the irradiator spark. However, as irradiator pulse time was moved through test pulse time an increase in the spark image density to a maximum was recorded as the time of separation of the irradiator and test pulse was diminished, showing that even here radiation could make a contribution to spark development to a degree which depended on the time at which the radiation was applied.

SECTION 5.5.1. Methods of recording the shape and duration of the test pulse used in the sparking probability experiments.5.1.1. Data required.

The final characteristics of the test pulse (i.e. duration and envelope shape, together with the actual time separating the irradiator and test pulse for a particular experimental setting) were in part determined by the pulse forming unit and in part by the nature of the artificial delay line. The data required were as follow :-

- a) the velocity of the voltage wave in terms of line sections.
- b) the attenuation and consequent pulse distortion.
- c) the value of the proper termination for the line.

It was thought that these data could best be obtained by oscillographic examination taking the number of LC sections and the line termination as possible variables.

5.1.2. The oscillograph.

The oscillograph was built round a sealed off cathode ray tube, type VCRX 294, operated at a post deflection

accelerating potential of 4 Kv. The Y plates of this tube were brought out to side terminals on the glass envelope to reduce inductive loops. It was found necessary to keep the Y plates without direct earth connection. The capacitance between one plate and the other, including the leads out of the metal case of the unit, was less than 10 micro-microfarads.

The trace was photographed using an Avimo camera with a lens of focal length 1.25 inches at f 1.9, recording on H.P.3 film. As the tube was operated with a single stroke trace, the shutter was left open throughout each record; the film was moved on manually by a part of a frame between pulse trials which started the trace.

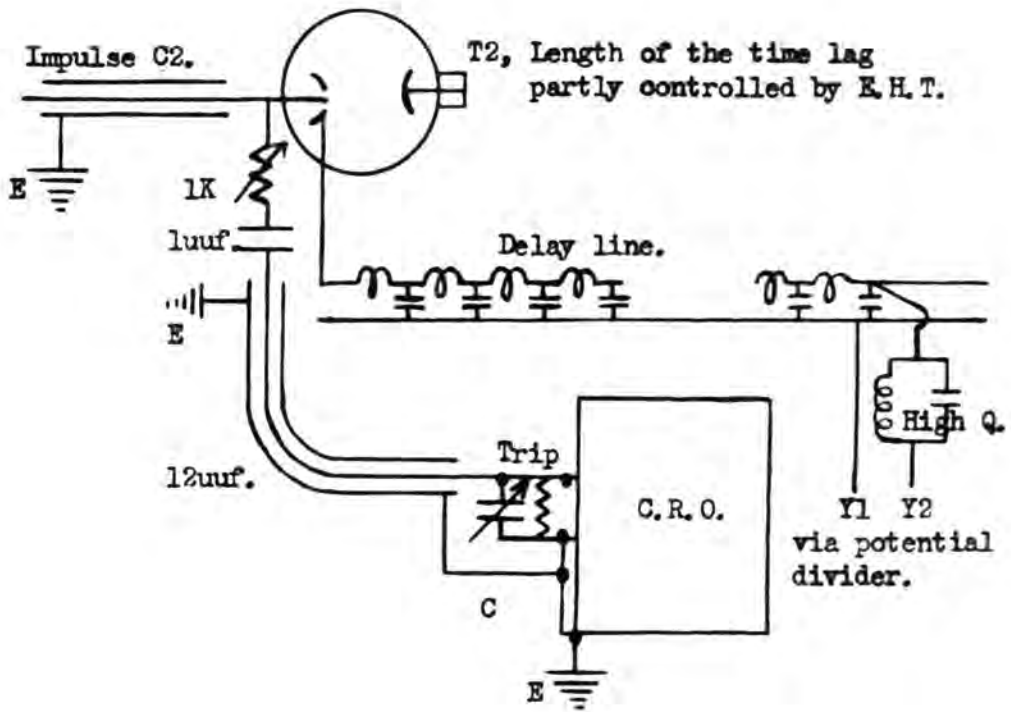
5.1.3. Recording methods.

The oscillograph was designed to record impulsive voltage changes on one of three set time ranges, for which the spot was deflected across the screen with velocities of a) 11.5 cm. per microsecond, high speed, b) 6.4 cm./microsec., medium speed and c) 1.34 cm./microsec., slow speed. Each time range could be calibrated by switching onto the Y plates the output from a built in 5 Mcs. crystal controlled oscillator.

To trip the oscilloscope time base an early warning pulse of 50 volts was required. The most suitable place from which this could be obtained was found to be at the junction of condenser C2 and the trigatron T2 of figure 4. A sufficiently early warning pulse could not be obtained from any point on the delay line to record the test pulse with the Y plate leads connected to a later stage on the line. This gave a first indication that the delay of the line was less than the inherent delay of the high speed oscilloscope trip circuits. Synchronisation of the trace and the voltage to be displayed, by means of an early warning pulse from any point before T2, was bound to be difficult because of the statistical lag preceding the breakdown of the trigatron. The method adopted, for any setting of the leads from the delay line to the Y plates, was to insert a high Q oscillatory circuit in the leads, figure 26. It was then possible to arrange a warning pulse delay system so that the start of at least one train of oscillations in five in the oscillatory circuit was displayed.

A major delay in the arrival of the warning pulse

Fig. 26 . Early warning pulse circuit for high speed
oscillograph.



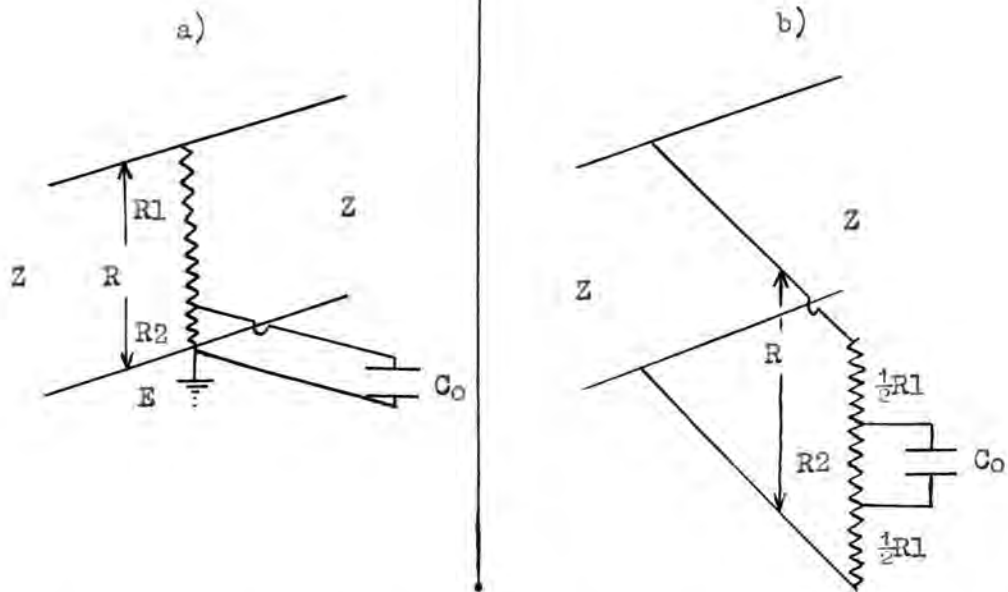


Fig. 27 . Potential dividers. For accurate reproduction of the wave-form the rise time of the pulse must be greater than the time constant of the C.R.O. circuit, $T_0 = C_0 \cdot R_1 \cdot R_2 / (R_1 + R_2)$. Also, $R \gg Z / 2$.

at the oscilloscope trip leads was introduced by means of the variable condenser C, figure 26. A further control of timing, to bring the time base and the display into synchronization to the best possible extent, was achieved by the insertion of a variable resistance of 1000 ohms in the leads from the trigatron T2 to the potential divider, (made up of a 1 micro-microfarad coaxial cable condenser, in series with the condenser C and a 12 micro-microfarad coaxial lead in parallel). Re-adjustment of this warning pulse circuit had to be made each time the voltage of the applied pulse was changed, as the overvoltage applied to the line input trigatron was a deciding factor in the time before breakdown of that gap.

When the trip circuit was adjusted to give a display of one pulse in every five that were applied to the Y plates from the delay line the high Q oscillatory circuit was short circuited. A fraction of the pulse voltage on the line, determined by the potential divider resistance ratio, was then applied to the Y plates. It was found that, by placing the oscilloscope close to the delay line, the leads to the

divider and from there to the Y plates could be kept short. It was not found necessary to use screened leads as the aerial pick-up on the Y plates, divider and leads was negligible compared with the voltage wave passing the pick up points on the delay line. Just before the beginning of the leading edge of each pulse record there was a slight indication on the trace of the firing of the line input trigatron but this was reduced to negligible proportions by placing an earthed screen round that tube.

The literature⁷⁹ shows that resistive potential dividers are satisfactory for recording impulsive waves with rise times of 6 milli-microsec. and greater, so the measurements were made using this type for the feed from line to Y plates. The sharpening gap in the line input trigatron was not expected to achieve such a high speed for the leading edge of the pulse. Using a simple divider of the type shown in figure 27a, a wave on the line of voltage V_1 will give across the resistance R a voltage V_2 such that

$$V_2 = V_1 R / (R + Z/2), \quad \text{where } Z \text{ is the surge}$$

impedance of the line. If reflections at the point of

connection are to be avoided R must be greater than $Z/2$. For the shape of the wave to be accurately reproduced on the oscilloscope trace the time constant of the divider-C.R.O. capacitance combination must be short compared with the time changes it is desired to record. This time constant T_0 is equal to $C_0(R_1R_2/(R_1 + R_2))$; thus if the capacitance across the Y plates C_0 is 5 micro-microfarads and $R_1 + R_2 = 11000$ ohms, taking the ratio of R_2 to R_1 as 1 : 10 we have $T_0 = 0.5 \times 10^{-9}$ sec., which is sufficiently short to record the shape of any voltage wave of duration 10^{-6} sec. or longer.

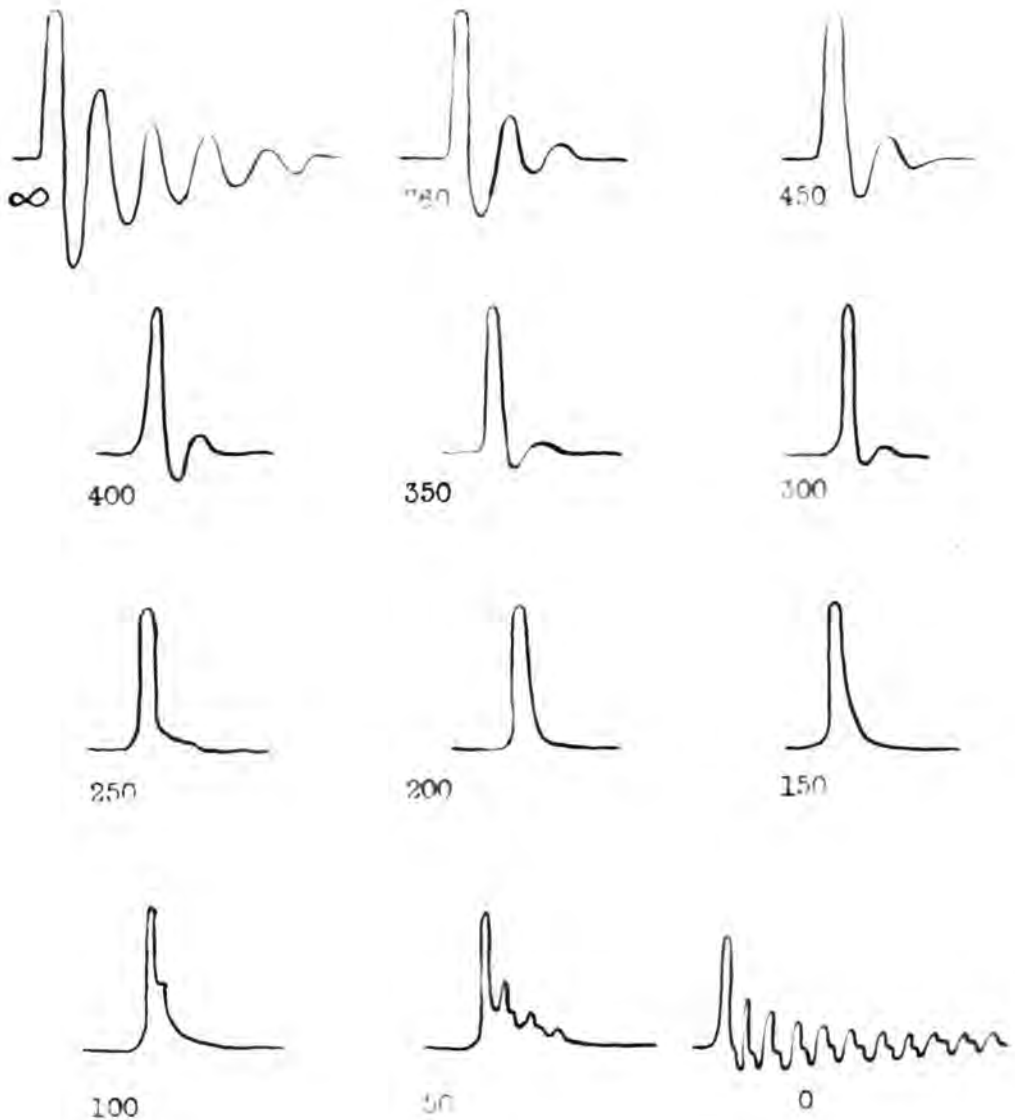
It was desired to record the potential difference between the two plates of one of the delay line condensers, from which the true earth connection was remote during the passage of the surge along the line. The Y plates of the C.R.O. tube were therefore left without earth connection. In that condition it was found that it was best to treat the divider symmetrically and the resistance R_1 was equally shared between the two leads from the line condenser as in figure 27b. This form of divider was used for all of the work to be described, with values of R_1 and R_2 chosen as the experimental best after trials over a wide range. The actual divider resistances were situated at the case of the C.R.O. where the Y plate leads were brought out.

5.1.4. The shape and duration of the pulse on the delay line; reflected waves from the theoretical proper termination do not appear to be appreciable.

First the slow speed time base of the oscilloscope was used to display the voltage variations at a point 150 IC units from the input, on a delay line made up of 218 sections. The potential divider used had R_1 and R_2 equal

to 8,000 and 1,000 ohms respectively. A series of tube displays were photographed with a sequence of resistive line terminations from zero to infinity across the last line capacitance. The oscillograms are traced out in figure 28. With the line terminations of 150 and 200 ohms the down stroke of the wave form returns to the base line without any succeeding oscillation. For increasingly large values of terminating resistance R_t reflected waves develop at the termination which return to the line input and are further reflected there. Successive reflections of the wave at the termination also occur when the value of R_t is less than 100 ohms. The oscillogram for R_t infinite and for R_t zero show the two extreme conditions of mismatch of the delay line. They correspond to the least absorption of energy and give rise to a large number of return journeys of the wave on the line.

It appears that, provided the value of R_t is kept within the limits from 150 to 250 ohms, the reflections, if any, occurring there will not be of any consequence in the sparking probability measurements. The leading edge of

Fig. 28 . Choice of the best value of line termination.Only $R_t = 150$ and 200 ohms give no reflection.(The value of R_t in ohms is given beneath each trace.)

Potential divider, $R_1 = 50k$, $R_2 = 1k$.
 Line length = 718 LC units.
 Leads to C.R.O. at 150 units.



5 M/cs.

Slow speed calibration trace.

the pulse for those values of R_t is steeper than the trailing edge. The pulse duration, by comparison with the calibration trace, also shown in figure 28, is about 0.4 microsec.

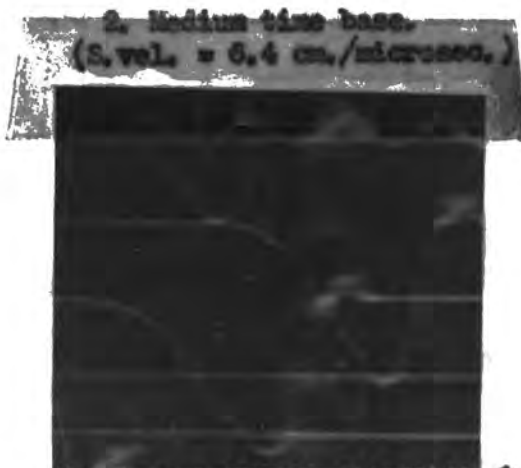
Photographs of the pulse recorded on the slow, medium and high speed traces, together with a calibration trace for each, are shown in figure 29. These give the pulse duration as 0.35 microsec. The actual rise time to the peak is in the ratio of 1 : 5 to the time of the tail of the pulse. For figure 29 see page 137.

Fig. 29. The test pulse used in the sparking probability experiments.

Conditions of display on the C.R.O. :-

- a) Delay lines as used in experiment and illustrated in figures 4 and 5, using a terminating resistance of 200 ohms.
- b) Leads to C.R.O. from a point 50 IC units from the line input taken by way of a potential divider (fig. 27b) with $R_1 = 8,000$ ohms and $R_2 = 1,000$ ohms.

1. Slow time base.
(Sweep velocity = 1.34 cm./microsec.)



In each case a calibration trace (5 Mc/sec.) has been included in the lower part of the print.

5.2. Determination of the time taken for a wave to travel down the artificial delay line and the delay incurred by one LC section.

5.2.1. Theoretical consideration of oscillations on the artificial line.

The repetitive patterns of figure 28, where R_c is infinite or zero, offer a method for the determination of the time taken for a wave to travel down the delay line. A pattern recorded with the oscilloscope leads at the end of the line can give the attenuation of the line. The method followed here in the theoretical argument is principally that used by Tropper⁶⁰, in his mathematical treatment of the errors introduced by the measuring circuit in recording of impulse voltages, though the final equation for the natural oscillation of a line can be arrived at by other methods.

Expressed operationally, for a unit impressed voltage (written '1') at the input to a delay line, the voltage and current at a point r units from the input are, instantaneously:-

$$V = (A \exp.ar + B \exp.-ar)L \quad (1)$$

$$I = (-A \exp.ar + B \exp.-ar)L \quad (2)$$

Where A and B are functions only of the operator 'p' which is

a simple multiple of the time constant of the input circuit. They do not depend on the characteristics of the line. The surge impedance, Z_s , and the propagation constant 'a' do depend on the line constants. Where R , G , L and C are the usual line parameters of resistance, conductance, inductance and capacitance per unit line section; where Z_0 is the characteristic impedance of the loss free line and $(LC)^{\frac{1}{2}}$ is the reciprocal of the velocity of transmission of the wave on the line ;

$$\begin{aligned} \text{The surge impedance, } Z &= (R + pL)^{\frac{1}{2}} / (G + pC)^{\frac{1}{2}} \\ &= Z_0 (R/L + p)^{\frac{1}{2}} / (G/C + p)^{\frac{1}{2}}. \end{aligned} \quad (3)$$

The propagation constant,

$$a = (LC)^{\frac{1}{2}} (R/L + p)^{\frac{1}{2}} (G/C + p)^{\frac{1}{2}}. \quad (4)$$

To determine the integration constants A and B take the two conditions :-

- i.) When the time $t = 0$, $x = 0$, then $V_0 = A + B$ at the line input.
- ii.) When $x = x'$, $I = 0$ for all values of t if the line is 'open' and there are x' sections to complete the line.

Thus from (1) and (2) we obtain :-

$$\begin{aligned} A &= V_0 \exp.ar' / (\exp.ar' + \exp.-ar'), \\ B &= V_0 \exp.-ar' / (\exp.ar' + \exp.-ar'). \end{aligned} \quad (5)$$

For the voltage at the x^{th} section, from (1) and (5),

$$V_r = V_0 (\exp. -ar + \exp. -a(2r'-r).) / (1 + \exp. -2ar'). \quad (6)$$

To demonstrate the repetitive nature of this expression, assume for simplicity that the voltage required is at the end of the line. Then,

$$\begin{aligned} V_{r'} &= 2V_0 (\exp. -ar') / (1 + \exp. -2ar'). \\ &= 2V_0 (\exp. -ar' - \exp. -3ar' + \exp. -5ar' - \exp. -7ar' \\ &\quad + - + - \dots) \quad (7) \end{aligned}$$

From the value of the propagation constant in(4), $\exp. -ar' = \alpha \exp(-br'/v)$, where the velocity of transmission is v and the time τ for a surge to travel down the line is r'/v ;

α is the attenuation factor for that length r' of the line and $\exp. (-br'/v$ is the transfer operator effective at each reflection of the wave at the termination.

Equation (7) can now be written,

$$\begin{aligned} V_{r'} &= 2V_0 (\alpha \exp. (-br'/v) - \alpha^3 \exp. (-3br'/v) + \alpha^5 \exp. (-5br'/v) \\ &\quad - + - + \dots) \quad (8) \end{aligned}$$

The above equation represents the natural oscillation of the line when a sustained voltage is suddenly applied to it.

The transfer operators bring successive terms into operation after times τ , 2τ , 3τ and so on.

The expression for an impulsive voltage applied to the line is

obtained by subtracting the voltage V_0 from the right hand side of equation (8), thus,

$$V_p' = -V_0 + 2V_0 (\alpha \exp.(-2\tau'/v) - \alpha^3 \exp.(-6\tau'/v) + \dots) \quad (9)$$

In figure 30 it is shown how successive terms of the equation (9) contribute to the build up of natural oscillation, each individual term coming into effect at a time 2τ after the previous one.

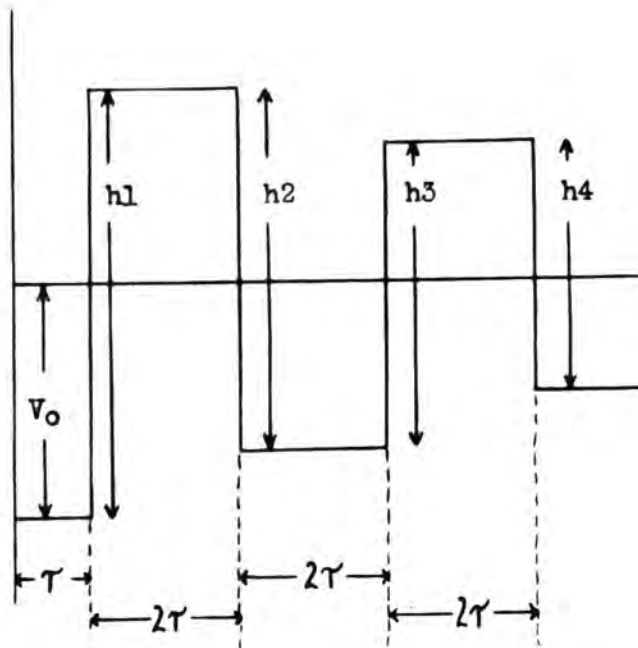


Fig. 30 . The natural oscillation of
of a line in the absence of distortion
but with attenuation.

The ratio of the successive amplitudes h_2/h_1 , h_3/h_2 , h_4/h_3 etc. could give the attenuation of two lengths of the line, but would include the attenuation at reflection at the termination as well as the attenuation in travelling down the line itself, unless a unit reflection coefficient is assumed.

The time for a complete cycle of the pattern is seen to be 4τ . A similar equation can be developed for the line with a value of R_t not infinite and the pattern repetition time for $R_t = 0$ is 2τ , using the initial condition for $r = r'$ that $V = 0$ at all times.

5.2.2. Value of the delay time for 109 IG units. Oscilloscope determination.

The oscilloscope patterns were examined for the two terminations of the line $R_t = 0$ and R_t infinite as photographed on the three writing speed ranges. It was found that the shape of the patterns depended on the position at which the leads to the Y plates were connected to the delay line. Some of these patterns are shown traced in figure 31. For the purpose of measurement the patterns were projected onto a

cine screen from the film and the distance separating successive oscillations was taken. From the measurement of many such traces it was possible to obtain a consistent value for the delay to the pulse caused by a unit LC section of the delay line. The change in shape of the patterns with the position at which the Y plates were connected to the line and with terminating resistance (R_t) used was in good agreement with the shape achieved in the graphical construction illustrated in section 5.4 below.

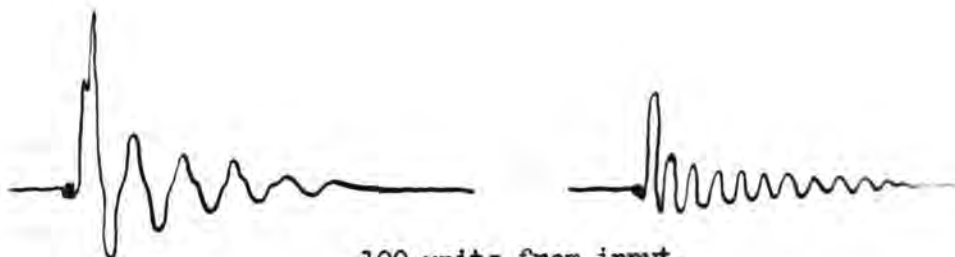
A further check was made using different numbers of LC sections to make up the line and photographing the natural oscillation as before with an open and then short circuited termination. Some of these traces are shown in figure 33. Again the same consistent value for the delay caused by one section of the delay line was obtained from the repetition measurements. A typical set of results for these measurements is shown in figure 34. The average value for the delay of one section of the delay line was found to be equal to 0.735×10^{-9} sec.

This gives the value for the total delay of a pulse in

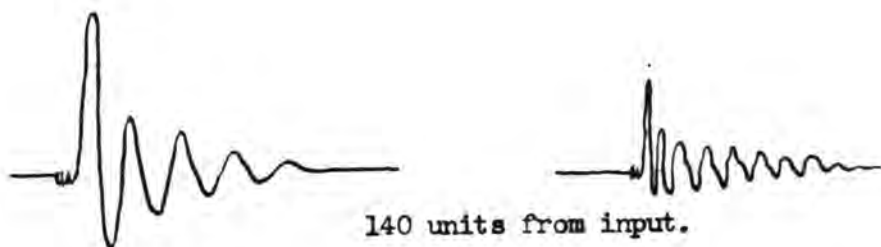
Fig. 51 . The nature of the repetitive pattern with
 $R_t = 0$ or ∞ depends on the point of connection of the
leads to the oscilloscope.



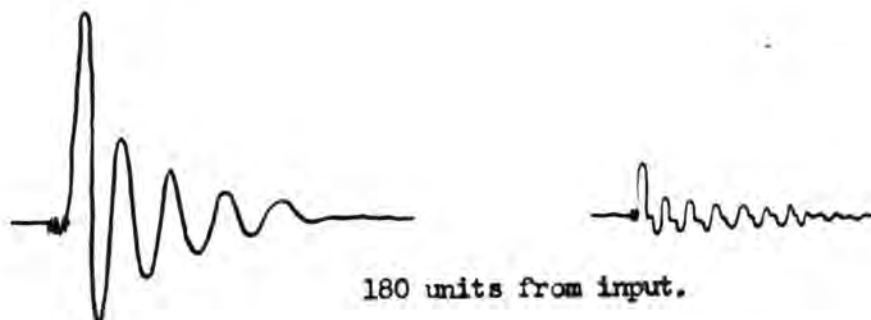
Leads 50 units from line input.
 (Length of the line 218 units)



100 units from input.



140 units from input.



180 units from input.

↑
 $R_t = \infty$.

↑
 $R_t = 0$

Slow time-base traces.... 1 cm \equiv 4/5 microsec. as enlarged.

Fig. 32 . The repetitive pattern of line oscillations for two points of connection of the oscilloscope leads, as displayed using the medium and high speed time bases.

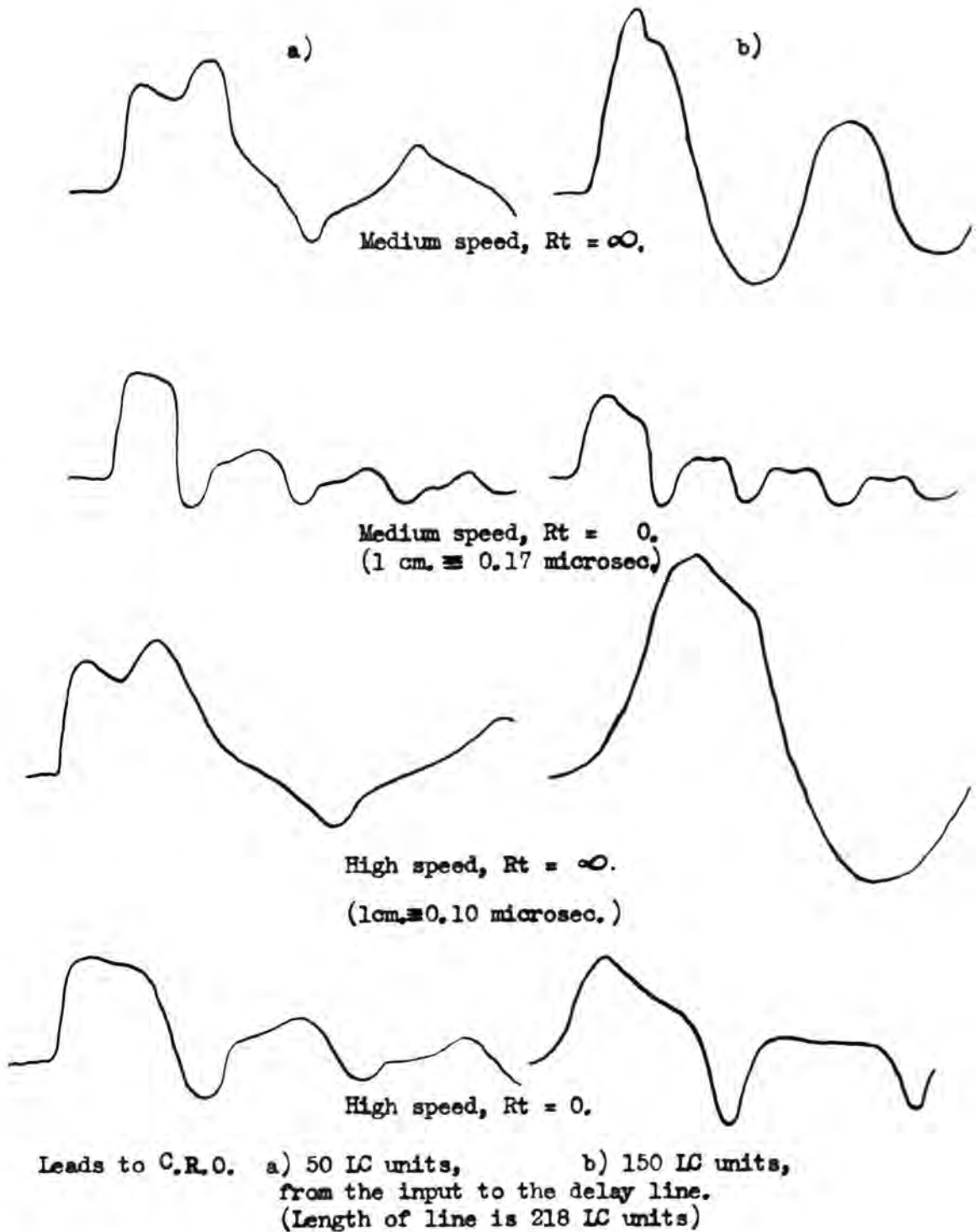
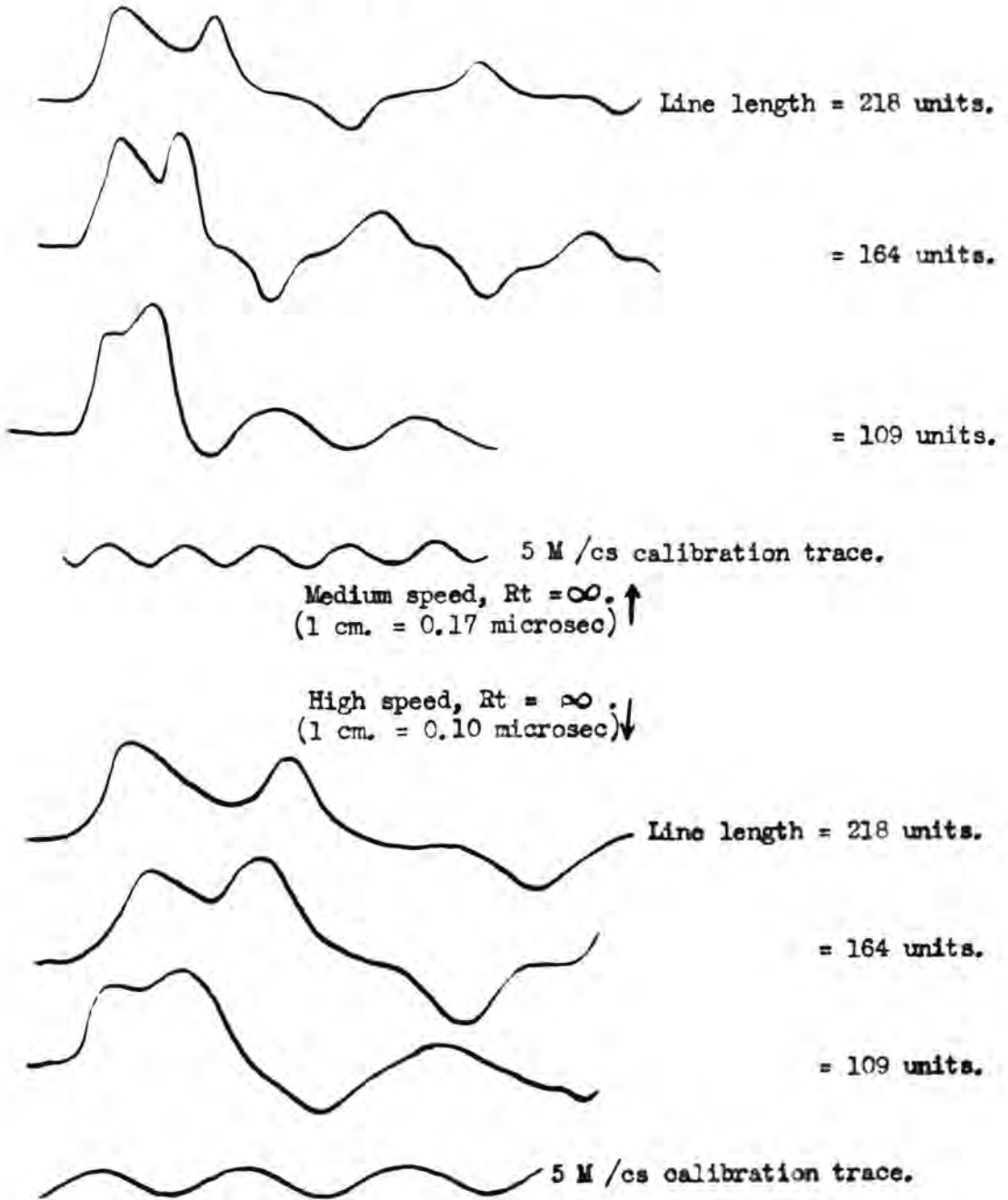


Fig. 33. . The repetitive pattern of line oscillations for three different line lengths, as displayed using the medium and high speed time bases.



Leads to the C.R.O. are at 10 units from the input to the line.

N.B. Halving the length of the line doubles the frequency.

Fig. 34 . Typical set of measurements on the repetitive line oscillations to obtain the delay resulting from one LC section of the line.

Time base - High speed.

Calibration trace projected on cine screen - 70 cms / microsec.

C.R.O. leads connected at 50 LC units from the input to the line.

Line length used. (LC units)	Value of Rt. (ohms)	Distance per pattern repetition. (cms)	Time per pattern repetition. ($\times 10^{-6}$ secs)	Time per LC unit. ($\times 10^{-9}$ sec)
218	∞	42.2	0.6	0.69
	0	21.0	0.3	0.69
164	∞	34.0	0.49	0.72
	0	17.3	0.25	0.76
109	∞	21.5	0.31	0.71
	0	11.0	0.16	0.73

The average value obtained from a large number of determinations of the type above gives the following :-

a) Time for a single journey of the pulse down a 109 unit

$$\text{delay line} = 80 \times 10^{-9} \text{secs.}$$

b) Delay resulting from a unit LC section = 0.735×10^{-9} secs.

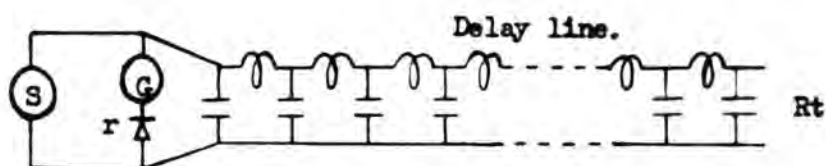
travelling once down the line as used in the probability measurements, i.e. 80×10^{-9} sec. for a line of 109 LS units.

In making copies of these traces, especially those on the higher writing speed ranges, it was necessary to build up from two or more successive photographs; a complete pattern rarely filled exactly the 8 cm. of tube screen, a fact entirely due to the impossibility of synchronising more than approximately two events, each lasting less than half a microsecond, when an uncontrollable event (the firing of the line input trigatron) could introduce a variation up to five times that amount.

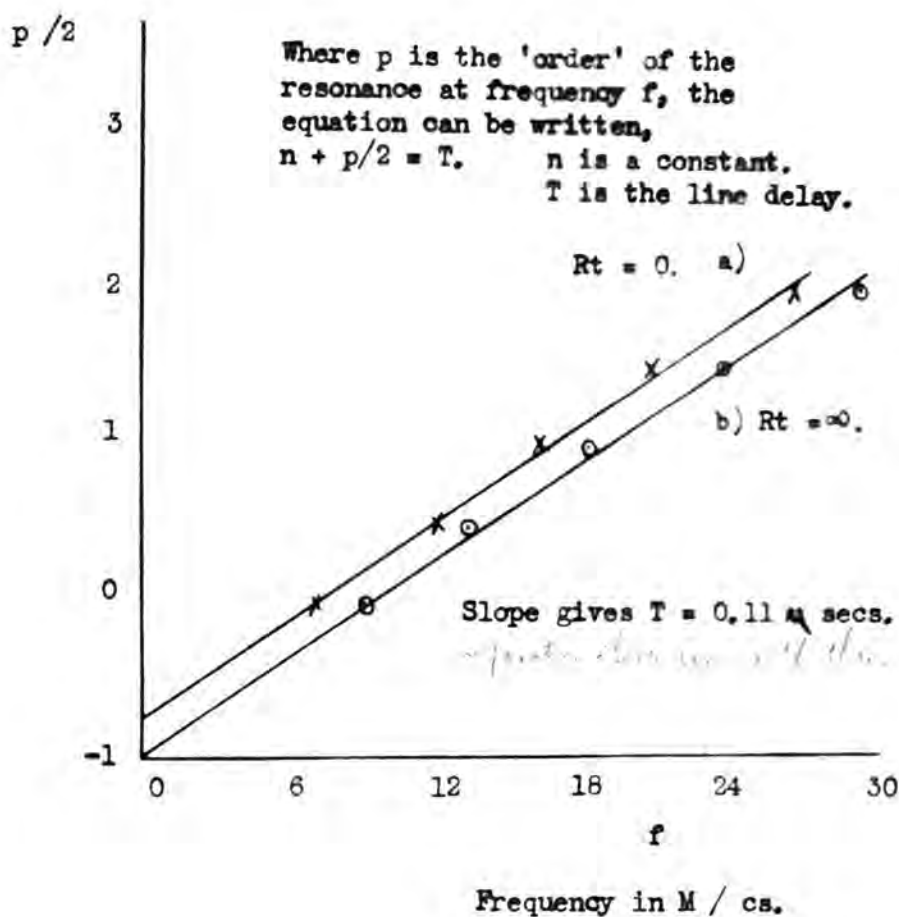
5.3. Check on the length of the delay line by a resonance method.

The circuit of figure 35 was used to determine the length of 160 units of delay line by a non-pulsed method. The two conditions of the line termination $R_t = 0$ and R_t infinite were again taken. For each condition the voltage as read by the galvanometer G (with a series crystal rectifier) was plotted against the frequency applied to the line from the generator at S. The graphs show a series of voltage

Fig. 35 . Determination of the length of a delay line of 160 LC units by a method of resonance detection.



S Variable frequency source. r Crystal rectifier.
G 40 ohm galvanometer. Rt Terminating resistance.



resonances. When a voltage maximum occurs at the detector, in the case of an open ended line (R_t infinite), it can be written for the standing wave pattern, $n \lambda / 2 = M$,

where n is integral, λ is the wavelength of the oscillation applied and M is the equivalent air length of the line.

In terms of the frequency applied and the time taken for a given condition to travel once down the line, $n/2f = T$.

For two different frequencies, f_1 and f_2 , each giving line resonance, $n_1/2f_1 = T = n_2/2f_2$.

Since n_1 and n_2 are both integral the general equation giving the resonant frequencies is $(n_1 + p)/2f = T$, where p is also integral.

Plotting $p/2$ against f the slope of the graph, shown in figure 35, gives T .

A similar expression can be derived for the line with $R_t = 0$ at resonance, $(N + p)/2f = T$, where p is again integral, but where N is integral plus a half.

The slope of the graphs plotted gave $T = 0.111 \times 10^{-6}$ sec. for the time of travel for a wave down 160 LC units of line.

For the 109 unit line this gives the delay time as 75.5×10^{-9} sec.
 This is in satisfactory agreement with the value of 80×10^{-9} sec.
 determined oscillographically. It also corresponds closely
 with the value obtained from the measured values of L and C;
 where C = 3.3 micro-microfarads and L = 0.13 microhenry, T is
 theoretically 70.8×10^{-9} sec. *Verified*

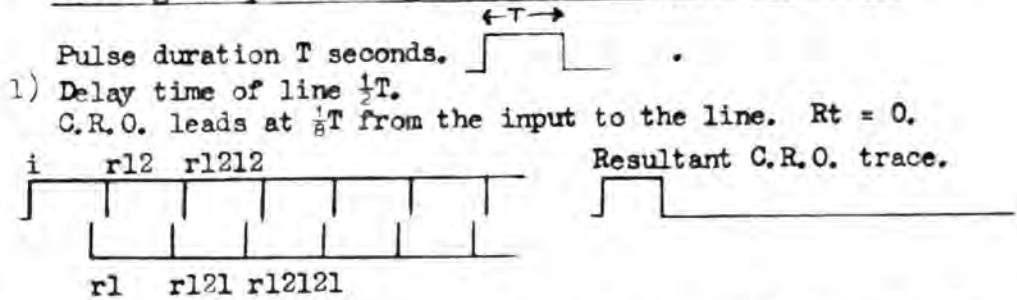
5.4. Correspondence of the oscillographically recorded traces
 of line oscillations with those by graphical construction.

A voltage wave incident at the open end of a delay
 line (R_t infinite) gives rise to a reflected wave without
 change of phase. At a closed end (R_t zero) a π change of
 phase occurs. The oscillograms traced out in figures 28 and
 31 show that the frequency of repetition of the line oscill-
 ations where R_t is zero is twice the frequency for R_t infinite.
 This is only possible if a further change in phase of π
 occurs at the input to the line each time the wave is reflected
 there. The maximum operating frequency for the type of
 trigatron used at the input to the line is specified as 3,000
 pulses per second, which allows a de-ionisation time much in
 excess of the time taken for a complete train of reflections

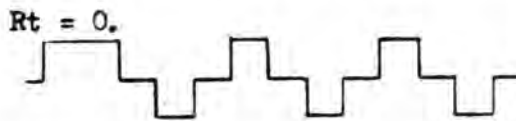
as indicated on any C.R.O. trace recorded here. The impedance of the line input condenser (C2, figure 4), which is of order 80 ohms is a sufficient mis-match and near enough to zero to give the condition required to account for the observations.

Another point of interest seen in the oscillograms of figure 51 is that, as the position on the line at which the variations in potential difference are examined is moved towards the line termination with $R_t = \text{infinity}$ the peak amplitude of the first half cycle of the repetitive pattern increases because the reflected wave reaches the Y plates before the direct wave is removed. With the Y plates connected to a point more than half way down the line the first incident and reflected pulses are not separately distinguishable. For the termination condition R_t zero the first half cycle of the oscillatory pattern is reduced in amplitude as the later positions on the line are reached with the Y plate connections, because the reflected wave, π out of phase with that incident, has the effect of removing the Y plate voltage and reversing it.

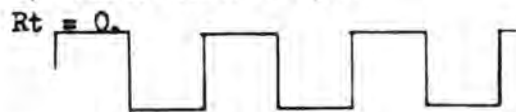
Fig. 36 . Addition of incident and subsequently reflected rectangular pulses to give the resultant C.R.O. trace.



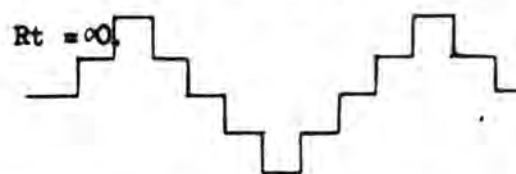
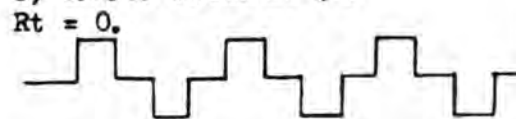
- 2) Delay time of line T .
a) C.R.O. leads at $\frac{1}{2}T$.



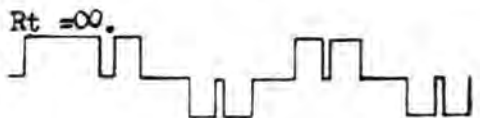
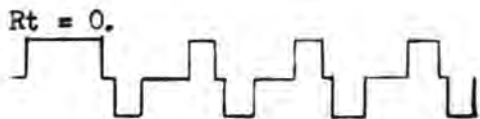
- b) C.R.O. leads at $\frac{1}{2}T$.



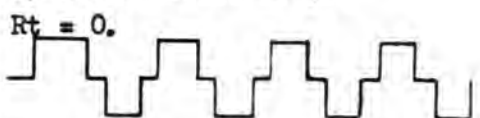
- c) C.R.O. leads at $\frac{3}{4}T$.



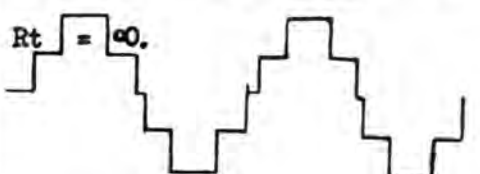
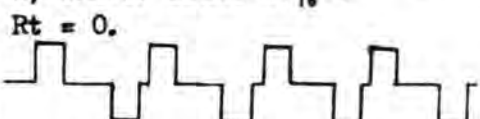
- 3) Delay time of line $\frac{3}{4}T$.
a) C.R.O. leads at $\frac{3}{16}T$.



- b) C.R.O. leads at $\frac{3}{8}T$.



- c) C.R.O. leads at $\frac{9}{16}T$.



With the delay time of the line between 0.5 and 1.0 times the pulse duration the traces constructed in part 3) above and experimentally recorded previously are most likely.

The effect of changing the point of connection on the line of the leads to the C.R.O. Y plates is shown by means of a simple reconstruction of rectangular voltage pulses in figure 36. It is also shown that a graphical diagram is similar to that recorded in practice only if the test pulse time is taken to be between one and two times the delay time of the line. In actual fact the pulse duration, including the rise time and the tail, was measured as 0.55 microsec. while the delay line unit of 216 sections (on which the repetitive patterns for comparison were made) had a delay time of 0.16 microsec.

In the first illustration of figure 36 a rectangular pulse of duration T sec. is taken to be incident on a delay line of length $0.5T$. The line is presumed to be effectively short circuited and the wave incident (shown by the symbol i) is reflected with π phase change at the termination, (returning as r_1). At the line input a further reflection and phase change takes place and r_2 travels down the line. For the purpose of demonstration the attenuation and distortion of the pulses are deliberately

neglected. The addition of the incident and reflected waves effective at the oscilloscope plates at each instant gives the resultant waveform, which in this case is shown on the right hand side of the diagram. Whatever the point of connection of the Y plates to the delay line the resultant for an incident pulse of duration T and line length a half T is always a single pulse and not a repetitive pattern. As this was not observed in the oscillograms photographed a second and third set of conditions have been chosen, where line lengths are T and $0.75 T$; the graphical patterns drawn out for them are in more satisfactory agreement with the experimental patterns. Condition 5) in figure 36, with line length $0.75 T$ very closely resembles the oscillograms of figure 31 where successive points of connection for the Y plates are taken. This is accepted as confirmatory evidence that the duration of the test pulse and the delay of the 218 unit line have been correctly determined as described earlier in this section.

5.5. Determination of the attenuation constant for a voltage pulse travelling down the delay line.

The attenuation constant required was that for a

wave travelling on the line, not including consideration of any reflection, as oscillograms have shown that reflected waves do not develop with the line terminated by the resistance as used in the probability experiments. The method of measurement of the height of successive waves of the natural oscillation of the line was not adopted as it involves the inclusion in the attenuation constant of the termination reflection coefficients, which are not necessarily unity except for an ideal line. Instead of this the heights of the oscilloscope traces were measured, with the line properly terminated, for a series of points of connection of the Y plate leads to the line.

The peak voltage of the pulse, measured at any point n sections from the input to the line can be taken as

$$V_n = V_0 \exp.(-kn), \text{ where } V_0 \text{ is the input voltage and } k \text{ is the attenuation constant.} \quad (1)$$

Similarly, for any two points of connection of the Y plates, n_1 and n_2 unit sections from the input to the delay line, the equation can be written,

$$\log_e V_1 / V_2 = (n_2 - n_1)k. \quad (2)$$

Fig. 37 . Determination of the attenuation constant
for a unit section of delay line.

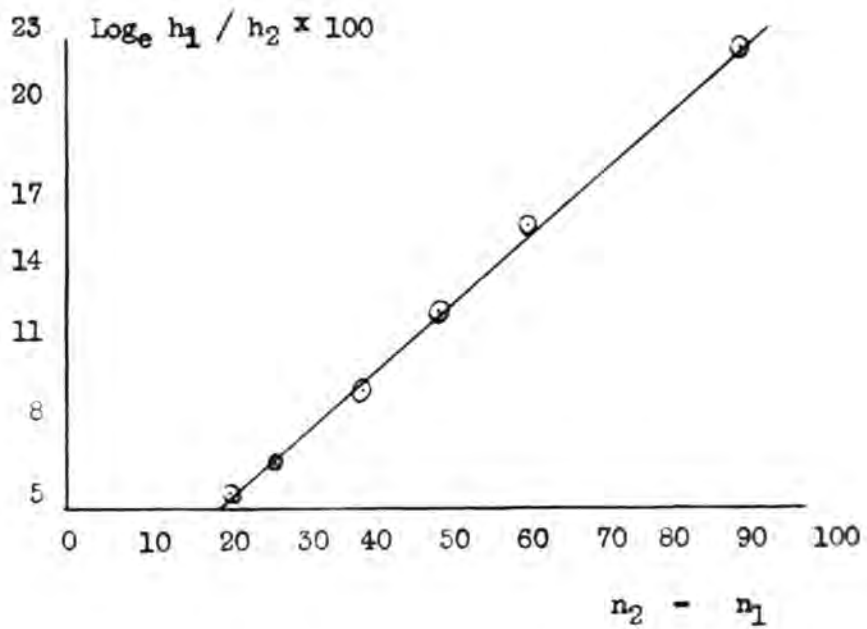
Length of line 218 LC units.

$R_t = 200$ ohms.

C.R.O. leads connected to delay line at, in LC units,

$n = 10 \quad 38 \quad 60 \quad 100$

Peak height of pulse, in cms, 15.35 14.3 13.5 12.2
 (Measured on cine screen)



$$\text{Log}_e h_1 / h_2 = \text{Log}_e V_1 / V_2 = k (n_2 - n_1)$$

Slope of graph gives $k = 0.0026$ per unit section.

If h_1 and h_2 are the heights of the traces recorded for pulses of voltage V_1 and V_2 at points n_1 and n_2 respectively,

$$\text{Log}_e h_1 / h_2 = (n_2 - n_1)k. \quad (3)$$

The graph of figure 37 was drawn from values of pulse height recorded at different pick-up points. The resulting straight line represents equation 3 above and the slope gives k .

The value of k from the graph was 0.0026 per unit line section.

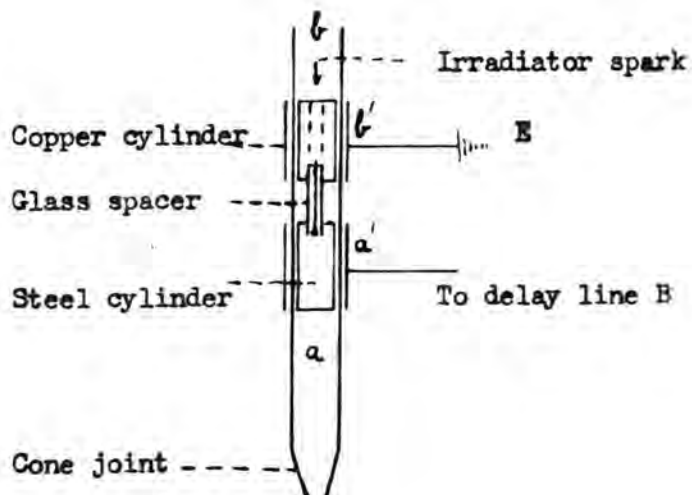
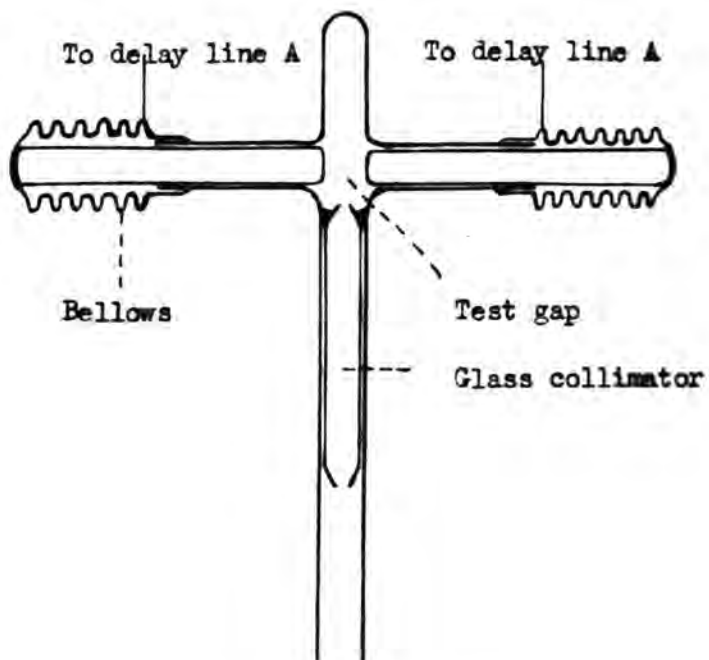
SECTION 6.Measurement of the absorption coefficient for the active radiation in argon, air, oxygen, nitrogen and hydrogen.6.1. Introduction.

The term absorption coefficient can be applied strictly only to monochromatic radiation. The atomic absorption coefficient is defined as,⁸²

$$= \frac{\text{Ions formed per atom}}{\text{Number of quanta incident per cm}^2}.$$

The radiation from a naked spark used as irradiator in the sparking probability experiments is not monochromatic; it is thought, however, that it is the radiations of shorter wavelength which are responsible for the photo-excitation and possibly photo-ionisation of the inter-electrode gas of the test gap and that it is these radiations that lead to the particular event that triggers a spark. The sparking probability measured for successive displacements of the irradiator spark from the test gap offers the possibility of determining a 'mean absorption coefficient' for the radiations active. This is the coefficient which must be considered in the theory of the development of spark channels⁸³, rather than one for monochromatic radiation only.

Fig. 38. . Apparatus for determination of
absorption coefficients.



Preliminary tests on the change in sparking probability with the distance separating the irradiator and test gaps showed that the value of P would not decrease from 1 to 0 in all of the gases it was desired to use, over the range of distances that was possible in the test chamber used in the previous experiments. So that a greater range of distances could be employed the following apparatus was devised.

6.1.1. Apparatus and method.

The test electrodes, of similar material and shape to those used in the chamber experiments, were mounted in the short limbs of a cross made of 1 cm. diameter glass tube, (figure 38). By adjustment of the bellows, sealed at their open ends to the glass limbs, the electrodes could be adjusted to give a suitable test gap with the sensitive volume of gas centred in the main part of the cross. Also in this main limb of the cross ran the irradiator mechanism, adjustable for distances between 10 cm. and 50 cm. from the test gap by means of a magnet applied from outside the glass.

The type of irradiator was adapted to give initial

collimation of the irradiation it emitted. Two steel cylinders, each 2 cm. long, fitted closely in the glass tube. They were separated by a 3 cm. long glass spacing piece, down the centre of which ran a steel needle in direct electrical contact with one cylinder a. The high voltage energising pulse was fed capacitively to a from an outer copper cylinder a' through the glass as dielectric. A discharge took place between the point of the needle and the second steel cylinder b, which again was capacitively connected to earth through the glass via a copper cylinder b'. The spark was arranged to take place inside a 2.2 mm. diameter cylindrical hole in b, 1.5 cm. from the end, giving the desired initial collimation.

Further collimation was provided by a glass tube 8 cm. long with the ends drawn out to a diameter of 1.7 mm. The tube was laid coaxial with the line of the radiation between the irradiator and the test gap. The end of this collimator near to the test gap (2 cm. from it) was sealed to the outer tube. In the time separating the irradiator and test pulses photo-electrons could not, even if they were

to be produced at the edge of the collimating holes, drift into the sensitive volume of the test gap. Thus only the effect of the radiations in the test gas could be responsible for the increase in sparking probability observed. To check the faint possibility that particles from the irradiating spark might accompany the photons and actually be the cause of the triggering mechanism a magnetic field of about 4,000 oersteds was applied across the tube down which the irradiator beam passed, but there was no change in the probability observed.

6.1.2. Theory of the method of measuring absorption coefficients.

The magnitude of the absorption coefficient is obtained from the values of the sparking probability, P , for distances of the irradiator from the test gap, $x_0, x_1, x_2 \dots \dots x_n$ as follows.

Let there be G photons emitted by the irradiator at S (figure 39) which are of sufficient energy to contribute to the production of a test spark if they enter the test gas. The number of these photons which travel in a direction such that they would, if unabsorbed in the intervening gas, enter the sensitive

volume of the gas through the collimator aperture of area A , situated at a distance d from the source, is GA/d^2 .

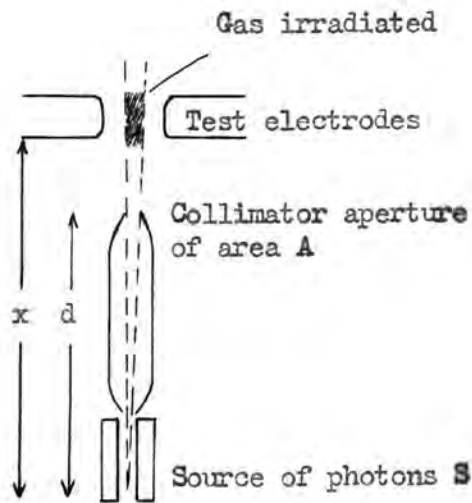


Fig. 39 . Showing the beam of photons restricted to the sensitive volume of gas between the electrodes.

The number of these photons which travel to actually enter the sensitive region (shaded in figure 39), after passing

through x cm. of gas of mean absorption coefficient μ , will be

$$(GA/d^2) \cdot \exp.(-\mu x).$$

Let the probability that this flux of photons will give the requisite triggering event in the gas in unit time be p . Then the probability of a spark starting in the small time Δt is $p \Delta t$. The probability that there will be no breakdown in N such intervals Δt , which make up the duration of the pulse t , is given by:-

$$(1 - p \Delta t)^N = \exp.(-pt).$$

Where P is the observed sparking probability,

$$1 - P = \exp.(-pt).$$

p is essentially proportional to the flux of photons given by

$$(GA/d^2) \cdot \exp.(-\mu x).$$

Therefore $\log_e(1 - P) = (NGA/d^2) \cdot \exp.(-\mu x)$,

$$\text{or } \log_e \cdot \log_e(1 - P) + 2\log_e d = K' + \mu x,$$

where K and K' are constants, independent of x .

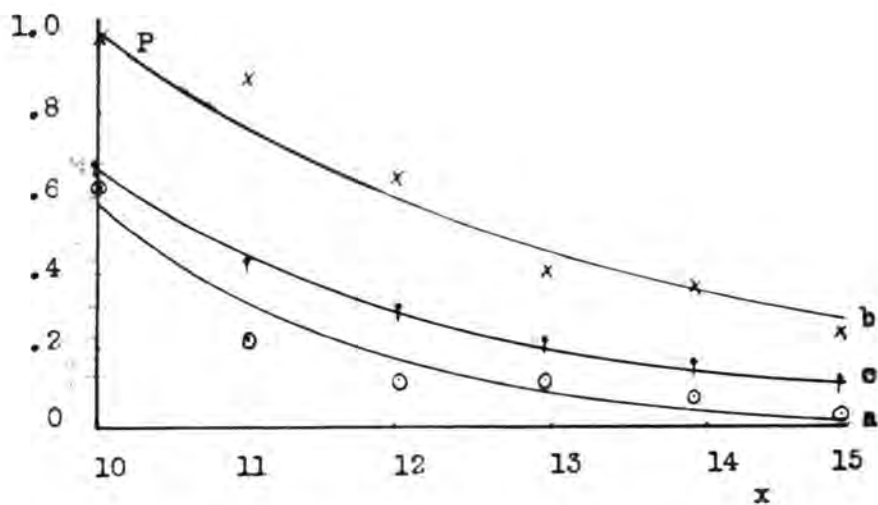
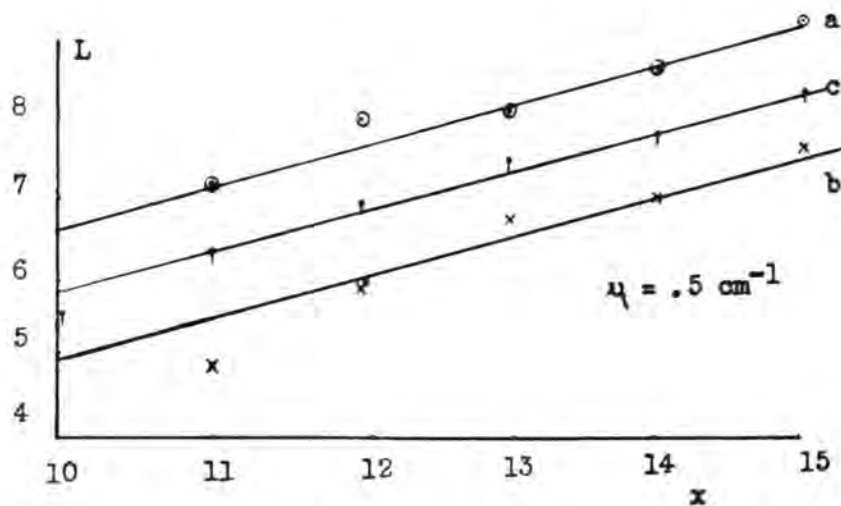
The graph in which $\log_e \cdot \log_e(1 - P) + 2\log_e d$ is plotted against x will have the absorption coefficient μ as slope.

6.1.3. Absorption coefficient for argon.

The gas argon was examined to determine whether the

Fig. 40. Absorption coefficient of argon.

No change with applied voltage.



Pressure 76 cms Hg.

Gap length 7.5 mms.

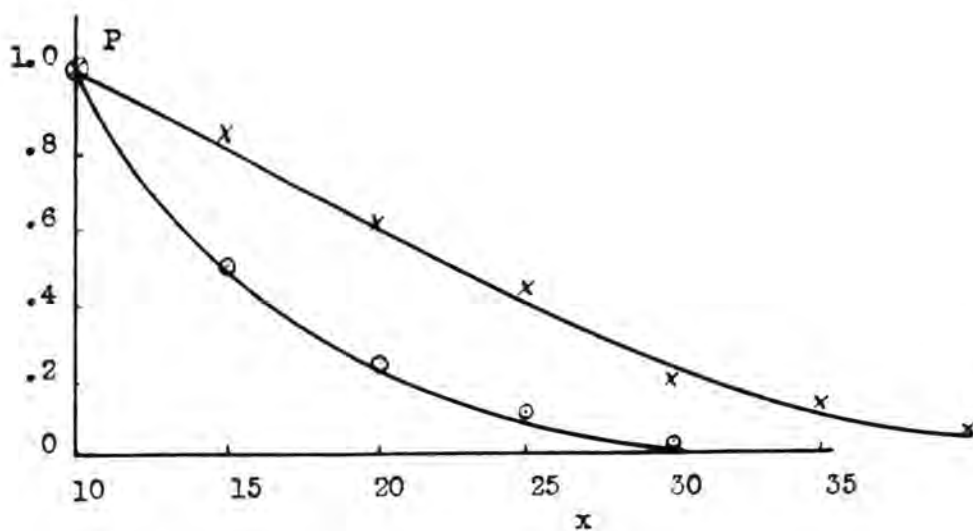
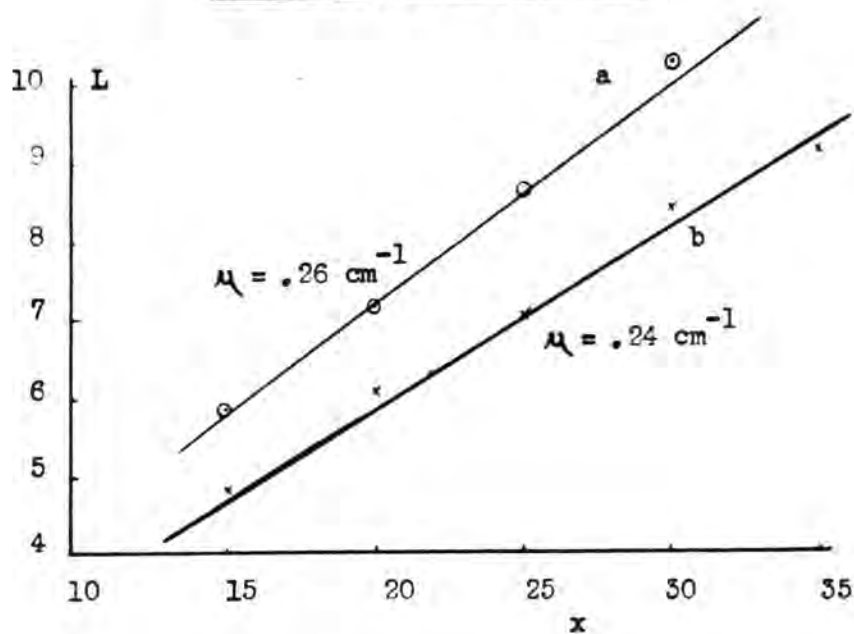
	Voltage	Tg	Ig	Symbol
a	16Kv	40	20	●
b	18	40	20	x
c	20	20	20	↑

effect of radiation was restricted to the diatomic gases or not. The behaviour of argon was very similar to that of hydrogen and if anything it was more subject to the radiation effects.

The lower part of figure 40 shows the points plotted for experimentally observed values of P at different irradiator distances x and for three different pulse voltages, using argon as the test gas. The test electrodes were 7.5 mm. apart and the gas pressure was 76 cm. Hg. For the two lower pulse voltages P was reduced to zero, for all settings of the irradiator and test pulse leads on the delay lines, by 15 cm. of gas between the irradiator and test gap. This was also the case for the particular line setting T_g 20, I_g 20, for 20 Kv. pulses. Plotting the graph of $\text{Log}_e \cdot \text{Log}_e(1 - P) + 2\text{Log}_e d$ (abbreviated to L) against x , for these three sets of measurements, the result is in each case a straight line; the slopes of the three straight lines, drawn in the upper part of figure 40, are the same, giving a value for the absorption coefficient in argon of 0.5 cm^{-1} .

This value applies only to radiations which affect

Fig. 41 . Absorption coefficient of argon.

Small change with gap length.

Pressure 76 cms Hg.

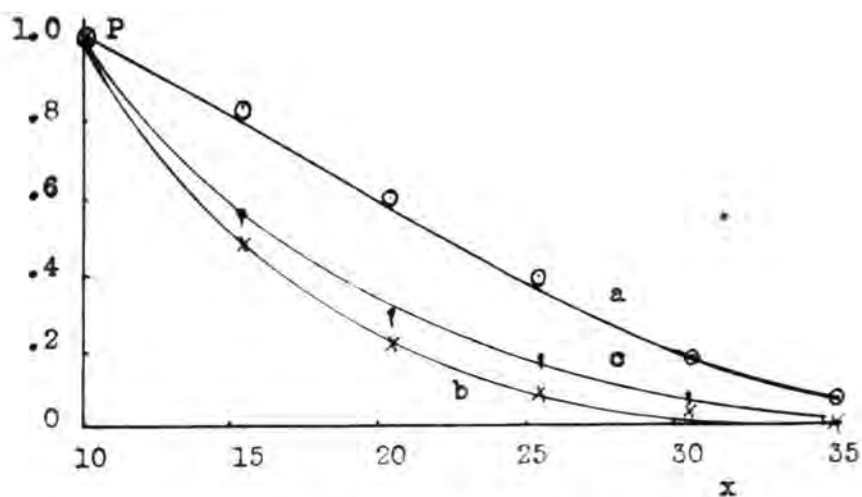
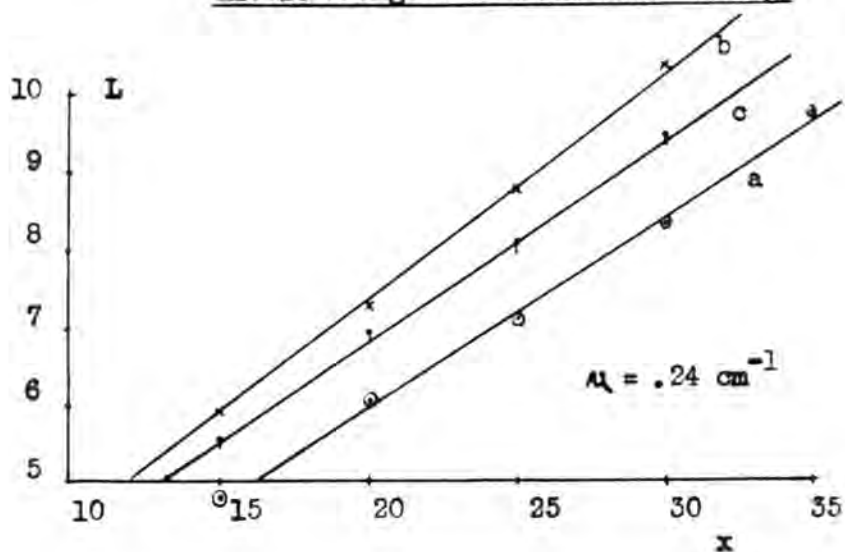
Voltage 20Kv.

	Gap length	Tg	Ig	Symbol
a	7.5mm.	40	30	○
b	6.0	40	30	x

P with the irradiator at a distance from the test gap of between 10 and 15 cm. It was expected that if measurements could be made over some other range of irradiator distances the mean value of γ would be different⁸⁴. Some of the radiations able to effect sparking of the test gap from a distance of 10 cm. would be filtered out to negligible flux density if they travelled a much greater distance in the gas. Measurements over long irradiator distances should give γ for the less strongly absorbed radiation only, while over short irradiator distances the value of γ measured should be for the more highly absorbed type of radiation.

For 20 Kv. pulses, with delay line settings of irradiator and test pulse times more favourable to sparking than those used above, finite values of P were recorded with the irradiator at much greater distances from the test gap. Two typical sets of results are shown in figure 41. The value of γ for the 7.5 mm. gap at distances from 10 to 35 cm. from the irradiator was 0.24 cm.^{-1} ; for the 6 mm. gap with otherwise identical conditions γ evaluated was slightly greater at 0.28 cm.^{-1} . From many sets of measurements in which

Fig. 42. Absorption coefficient of argon.

Little change with irradiator timing.

Pressure 76 cms Hg.

Gap length 7.5 mms.

	Voltage	Tg	Ig	Symbol
a	20Kv.	40	20	o
b		40	30	x
c		50	10	†

overvoltage, gap length and time separating irradiator and test pulse were varied the average value of absorption coefficient for this range of irradiator distances was determined as 0.25 cm.^{-1} . At a lower pressure of 46 cm. Hg. a value of 0.14 cm.^{-1} for μ was obtained over irradiator distances 10 to 45 cm.

6.1.4. Absorption coefficients in air, nitrogen, oxygen and hydrogen.

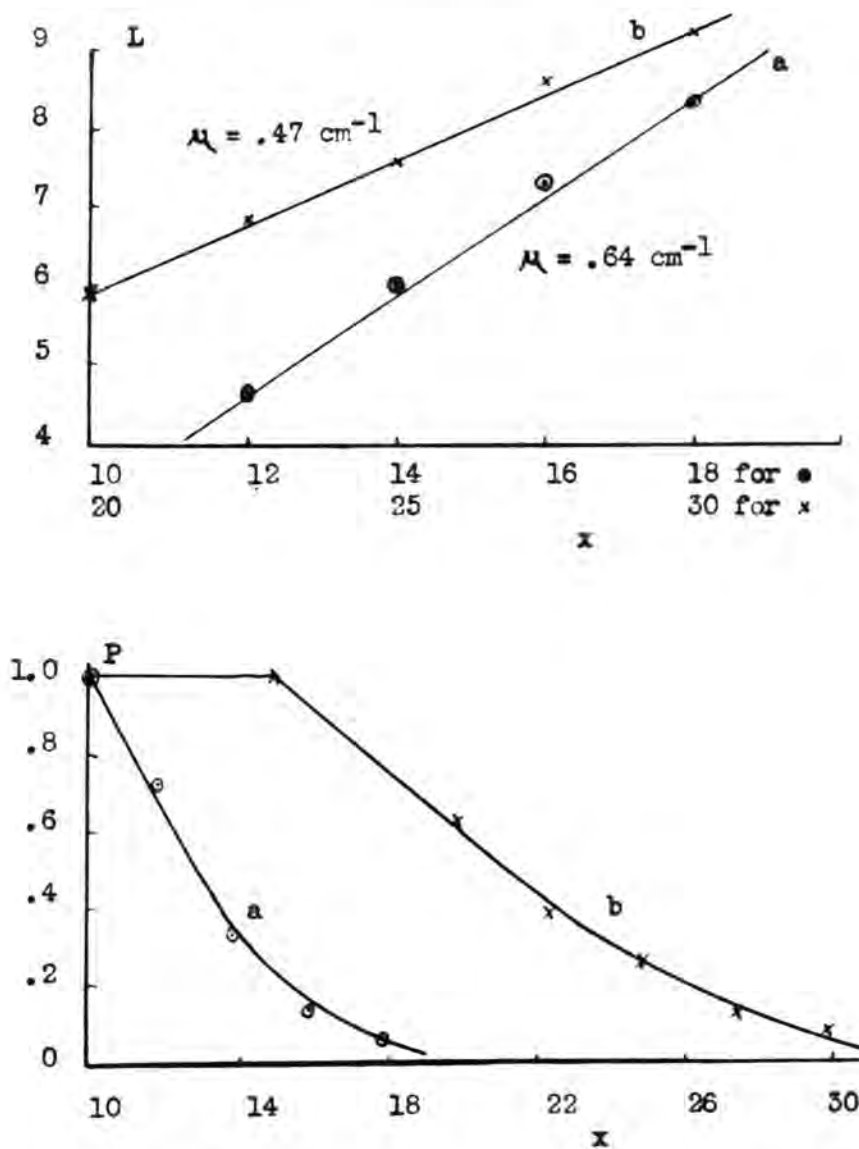
It was confirmed that in air, as for argon, there was little change in measurement of absorption coefficient value because of :-

- a) change in test gap length, (graphs for argon, figure 41).
- b) change in irradiator timing, (graphs for air, figure 42).
- c) change in overvoltage, (graphs for argon, figure 40).

There was, however, a definite change as had been expected with the range of irradiator distances over which the measurement was made, (compare graphs 40c and 41a) and with the pressure of gas used, see figure 43.

To obtain a comparison between the values of absorption coefficient for different gases used extensively

Fig. 43. Absorption coefficient of air.



Voltage 20Kv.

Gap length 3.5 mm.

	Pressure	Tg	Ig	Symbol
a	61 cms Hg.	40	20	●
b	46	40	20	×

in the earlier sparking probability experiments the method was repeated in each gas in turn at 61 cm. Hg. pressure and at one lower pressure. The higher pressure was chosen because this was the greatest at which a measurement could easily be made in air with a 3.5 mm. test gap. Two of the graphs of 'L' against x used to determine the absorption coefficient of air at different pressures are shown in figure 43, with the experimentally observed variation of P with x plotted in the lower half of the figure.

The table 19 is a summary of the experimental values obtained for μ in all the gases examined. The second column shows the pressures at which the determination was made; column three gives the gap length used and the fifth column gives the range of irradiator distances over which the measurement applies. The fact that no determination was possible in nitrogen at 46 cm. Hg. pressure, or in hydrogen at atmospheric pressure, simply indicates that the gases were so transparent to the effective radiation at these pressures that even with the irradiator at the greatest distance from the test gap that was possible with this apparatus, 50 cm.,

the value of P recorded was still unity. No value of γ could be assessed with these conditions.

Table 19. Experimental values for the absorption coefficients in the gases examined.

Gas	Pressure cm. Hg.	Gap length mm.	Mean γ cm. ⁻¹	Range γ at 76 cm. cm. Hg.
Argon	76	7.5	.5	10 to 15 .5
		7.5	.28	10 to 55 .28
	46	6.0	.24	10 to 35 .24
		6.0	.14	10 to 45 .23
Air	61	3.3	.64	10 to 18 .80
	46	3.3	.47	17 to 30 .78
Nitrogen	61	3.3	.20	10 to 35 .25
	46	No determination,		10 to 50, $P = 1$.
Oxygen	61	3.3	1.0	10 to 14 1.24
	46	3.3	.62	10 to 18 1.18
Hydrogen	76	No determination,		10 to 50, $P = 1$.

6.1.5. Summary of absorption coefficient results.

To provide a basis on which the results of the measurements of γ made in these experiments could be compared the values of the mean absorption coefficient in the fourth column of table 19 were converted to an equivalent

coefficient at atmospheric pressure, given in the last column of the table. For example, the coefficient for argon at 46 cm. Hg. pressure, 0.14 cm.^{-1} , gives an equivalent of $76/46$ times that value, 0.23 cm.^{-1} . This is found to agree very well with the actual value of absorption coefficient determined at atmospheric pressure over the same range of irradiator distances. Reasonable agreement is also found for the values of the equivalent in all the gases where such a comparison could be made. At the same pressure and over the same range of irradiator distances the measured absorption coefficient was greatest in oxygen, followed in order of magnitude by air; argon and nitrogen indistinguishable; then hydrogen.

Previous work done in measuring absorption coefficients of gases for short wavelength radiations is difficult to correlate with the present findings because of the wide variety of methods used, the uncertainty of the actual wavelength groups for which the measurements were made and the wide scatter of results recorded. The table 20 has been drawn up to indicate the situation in this field.

In general the equivalent value of absorption coefficient at atmospheric pressure seems to increase as the pressure at which the determination was made decreases, e.g. see hydrogen. This is a trend that might be expected when it is recalled that at the lower pressures the band of wavelengths to which the measurements apply is much wider than at higher pressures, where much of the radiation might be filtered out in a distance small compared with the range of distances used in the measuring experiment.

Table 20. Survey of work determining the absorption coefficient for photons in some gases.

Absorp. Coeff., cm. ⁻¹ (76 cm. Hg.)					Working pressure cm. Hg.	Worker	Method
Argon	Air	Nitrogen	Oxygen	Hydrogen			
	0.55		3.0		76	Prose & Jasinski	Microsec. Pulses.
	2.0		5.0	0.84	14 to 50	Raether	Cloud chamber.
				1.36	10	Greiner	Geiger Counter.
	0.99			0.91	2.5 to 10	Craggs	"
	50.0			27.0	1.5	Christoph	"
				50.0	0.1	Geballe	Photocell.
	50.0				0.1	Schneider	Vac. Spectr.
0.25 to 0.5	0.8	0.25	1.2	-	46 to 76	Present work.	

Considering the wide variety of the methods used, there is reasonable agreement between the work with micro-second pulses (Prowse and Jasinski), the recent Geiger counter work (Craggs) and the present work. In none of these sets of work was a window in the irradiating beam; irradiator and detector systems in all three cases operated in the same gas. The slight differences, for example between the Craggs result for Argon and the present one are quite within reason when the difference in working pressure and type of irradiating discharge are realised.

There is a need for an exhaustive examination, by a method which can be used for a variety of gases, of this problem of absorption coefficients. The present work is placed on record as an indication of one of the methods from which a choice could be made. Slight modification of the apparatus to lengthen the tube down which the radiation passes to the test gap would give conditions for the determination of the absorption coefficient for hydrogen.

SECTION 7.Discussion of the results of experiments.7.1. The broad theory of spark initiation.

The basic theories which have been postulated to account for the development of a direct voltage spark in a gas are included in the general Townsend⁹⁰ and the Meek⁹¹ streamer theories. All theories require at least an initial electron to trigger the discharge. For two main reasons the possibility of a Townsend type of discharge development has been eliminated from this discussion. The experiments described above in sections 3, 4 and 6 were conducted with, a) the time for which the voltage was maintained on the electrodes too short for the movement of positive ions or metastable atoms, travelling with 10^{-2} and 10^{-5} of electron velocities respectively, to contribute to the discharge by their action at the electrodes; b) the product of pressure of gas and electrode separation always in excess of 200 mm. Hg. x cm. Although Llewellyn Jones's recent paper¹¹¹ makes doubtful the upper limit of the range of pd values to which the Townsend theory may apply, special attention still attaches

to high speed breakdown where the Townsend mechanism is too slow. For example in very long sparks such as lightning discharges the complete traverse of contra streams of ions and electrons between the ends of the system, before breakdown, is improbable.

Common to both theories the first fundamental question which must be answered concerns the source of the triggering electron. The possibilities which must be considered are, assuming an ionising agent :-

- a) that casual electrons may appear at random in the gas even in the absence of any applied electric stress, have a short life and then revert into some neutral condition again,
- b) that electrons in small numbers may be continuously available in the gas, and
- c) that electrons may only be released during an electric stress which exceeds a certain minimum value.

Subsequent to the appearance of an electron in the gap the streamer theory requires three overlapping stages to account for the high speed of spark development.

- a) First the initiating electron must increase in

velocity, while acted on by the electric field, to give cumulative ionisation in inelastic collisions with neutral molecules. The number of new electrons liberated by one electron in moving a distance d in the field direction is expressed by $\exp. \left(\int_0^d \alpha dx. \right)$ where the coefficient α represents the number of new electrons liberated by any electron in moving one cm. This group of electrons is termed an electron avalanche; its occurrence was demonstrated in the cloud chamber experiments of Raether⁸⁵. As a result of diffusion, and possible some mutual repulsion of the electrons⁸⁶ perpendicular to the field direction as they progress, the avalanche is broader towards the anode. Due to the electron velocity being much greater than that for positive ions the concentration of electrons far exceeds the concentration of ions in this broad head of the avalanche.

b) For each centimeter advance of an electron there must also be produced w photons, so that for each new electron there w/α new photons. This ratio of electrons to photons will vary with the electron energy for any particular value of photon energy created. For a particular photon energy,

w/α first increase with electron energy and subsequently decreases.⁸⁷ It is not known what form the action of emitting photons takes. It may be the direct result of excitation of neutral molecules in multiple or high energy transfer collisions with electrons⁸⁸, or it may be the result of recombination of positive ions and electrons⁸⁹. Photon emission is given quantitative expression in the term w merely to put it on a basis where it can be compared with electron production. Breakdown of a long gap in a time less than the electron crossing time cannot be accomplished by a single avalanche. Photographic and photo-multiplier evidence^{61,65} indicates a wide zone of feeble luminosity before a narrow spark channel develops. This suggests multiplicity of avalanches ascribed to the generation of new initiating electrons by ultra-violet radiation.

c) In any high speed discharge secondary processes must operate in conjunction with the primary ones stated above. The speed of discharge development depends on the type of high speed process which is operative. The Meek streamer theory postulates a rapid completion of an ionised

path for the main discharge because, as the positive ion core of the developing streamer has a field comparable with the applied field, photon triggered avalanches feed in laterally. The actual speed of transfer of ionisation through the stressed gas will depend on many factors, among which are:- electric stress applied to the gas, pressure and type of gas, electric circuit and voltage timing arrangements. In the experiments described above (section 2), the timing arrangements were such that discussion of the possible processes at the cathode can be limited to those dependent on photons incident there as secondaries from the irradiated gas once the discharge has been triggered.

7.2. Time lags before sparking.

Experimental evidence indicates that, in direct voltage^{51 to 38} and ultra-high-frequency discharge⁷⁶ development, there is a measurable delay from the application of a potential in excess of the minimum sparking voltage between the electrodes of the test gap to the actual breakdown. This delay can theoretically be divided into two parts, a statistical lag and a formative lag. The statistical lag (t_s) is that

part of the total delay which is not common to all observations and has usually been taken to indicate the time from the start of the voltage application to the appearance of the pre-requisite condition for breakdown in the gap. This is possibly the time for the appearance of a casual electron in the sensitive volume of the gas. The formative time (t_f) is the time needed, after the establishment of the pre-requisite condition, for the growth of ionisation to the point of instability at which a spark passes.

Considering the special case where the formative time is negligibly small, the equation can be deduced⁶, $\text{Log } n_p / n = 0.434 t/t_g$, where for n applied voltage pulses, each of duration t sec., n_p result in no spark before a time t_g from the start of the pulse. The type of curve to be expected experimentally is that shown in figure 44, where t_f , the constant part of the formative time, is represented by the intercept of the graph on the time axis. It is known that the values of both t_f and t_g are measurably reduced by a) an increase in overvoltage of the gap, b) the use of ultra-violet irradiation⁹⁵ or other ionising agencies in the gap

during the time that the test voltage is maintained there.

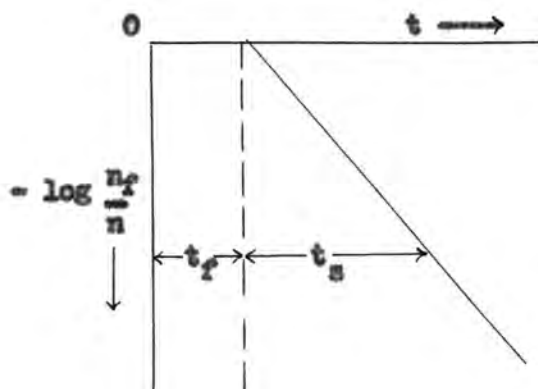


Fig. 44. Expected experimental curve for $\text{Log } n_f/n = 0.454 t/t_s$

If the possibility is to be acceptable that free electrons might be continuously available, then to conform with the observations of time lags the statistical lag must be interpreted a) as the wait for a particular electron density in the gap, or b) to be more in keeping with the low electrical conductivity of dry gases, as the wait for one of the electrons to drift into the sensitive volume of the gap.

An experiment was tried in which a direct voltage was applied to the test electrodes continuously while a short

duration test pulse was superposed. The change in sparking probability with irradiator timing with this condition was of the same form as when the direct voltage was not sustained. A slight increase in P was noted when the sustained voltage, of order 500 volts, was added to the impulsive stress and a slight decrease when the sustained and impulsive voltages were opposed, which was the least to be expected. Until an experiment can be carried out in which the gas can be effectively cleared of any long lived electrons before the test voltage is applied it is impossible to distinguish between electrons of this type and electrons which have only a fleeting life in the gas... Thus the possibility that a) the discharge is triggered by a particular event in the life of a long lived electron, or that b) triggering occurs with the appearance in the gas of a casual short lived electron must be grouped together and weighed against the possibility c) that electrons are only freed by the direct action of an electric stress.

7.3. The time lag test curves and pulse length.

Using voltage pulses of sufficient duration to ensure

a high sparking probability the experimental curves of $100 n_p / n$ plotted against time from the start of the pulse should be of the form shown in figure 45 ; there t_s includes any part of the formative time that is not constant, e.g. the variation in the formative time that could arise with the appearance of the triggering electron in different parts of the gap in successive trial pulses. The slope of the right hand part of the graph will depend either on the number of electrons present in the gas at the start of the test pulse, or on the rate of electron production thereafter.

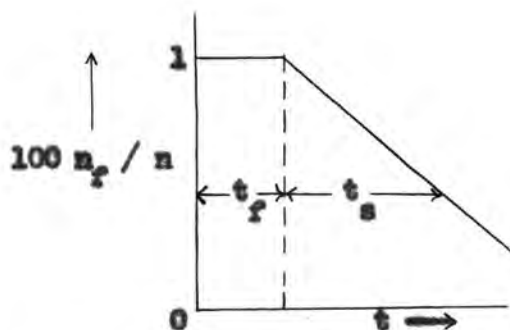


Fig. 45. Expected experimental curve for $100 n_p / n$ against time.

If the duration of the test pulse is chosen, in a particular set of working conditions, so that it considerably

exceeds the sum of the formative time and the largest measured value of the statistical lag for those conditions, (as measured with steady direct voltage), then almost unit sparking probability will result. If, at the other extreme, the duration of the test pulse is taken small, (as in the experiments described in sections 3, 4 and 6), so that a voltage in excess of the sparking value is applied only for a time of the same order as the normal formative time, a spark will not occur unless the triggering electron appears, or is present in the gas, right at the beginning of the pulse.

7.4. Effect of radiation or ionisation in the test gap.

Working with such a short pulse (page 48 on) it was found that, if the gas between a pair of electrodes was irradiated from another spark gap at an appropriate time before the completion of the test pulse applied to those electrodes, there was observed an increase in sparking probability. The amount of the increase in P depended on the time of irradiation relative to the time of the test pulse.

The immediate interpretation might be that ultra-violet irradiation of the test gas ensures the presence of

the pre-requisite electron in a suitable part of the test gap sufficiently early in the test pulse for the formative stages of the spark development to be completed. This would appear to be justified in view of the evidence that a) a radium source placed near to the test gap, or b) the gases from a piece of burning wood, in the earlier exploratory part of the work, were sufficient to considerably increase the sparking probability. Both of these are, however, spasmodic producers of ionisation, and it is possible that during the pulses that resulted in sparks with them electrons were freed which triggered the discharge. When short pulses of radiation preceded the test pulse by times as little as a few hundredths of a microsecond there was little increase in P in most gases at atmospheric pressure, requiring that the above interpretation should be examined more closely.

7.5. The expected effect of time of irradiation on sparking compared with that observed.

The persistence of electrons in the common gases is believed to exceed 2 microseconds⁹⁴. If then the effect of the ultra-violet irradiation of the test gas is to free

electrons it should not matter whether the release occurs one or two microseconds before the test pulse. The statistical distribution of electrons should improve in the time between the irradiator and test pulses. The result of this should be to ensure breakdown on average earlier in the test pulse than would be the case with irradiator and test pulses starting simultaneously. Thus the test graphs of $100n_p/n$ plotted against delay time should appear in the form of figure 46 rather than as in figure 45. The actual form of this curve depends not only on the time separating irradiator and test pulses but on the stage at which the electrons begin to appear in the test gas subsequent to the rise of the irradiator pulse.

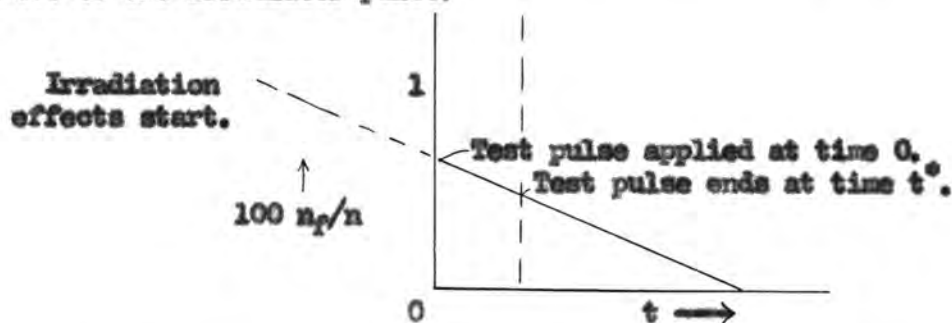


Fig. 46. Expected curve for $100 n_p/n$ against time with early irradiation of the gas.

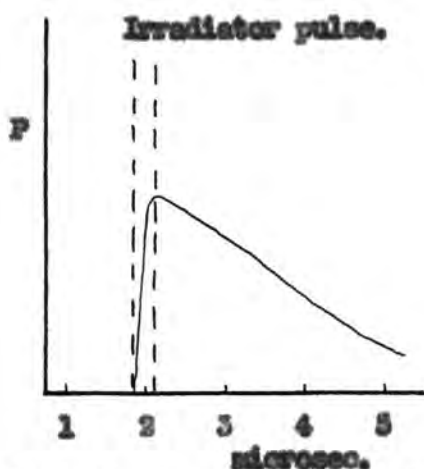
Three of the possibilities are taken here for consideration, namely, the release of electrons,

- a) in a batch almost simultaneously with the rise of the irradiator pulse,
- b) in a batch some time after the rise of the irradiator pulse,
- c) at random over an extended period subsequent to the start of the irradiator pulse. Whichever form the release of electrons does take, the spread of irradiator times for which an increase in P can be expected extends for a few microseconds.

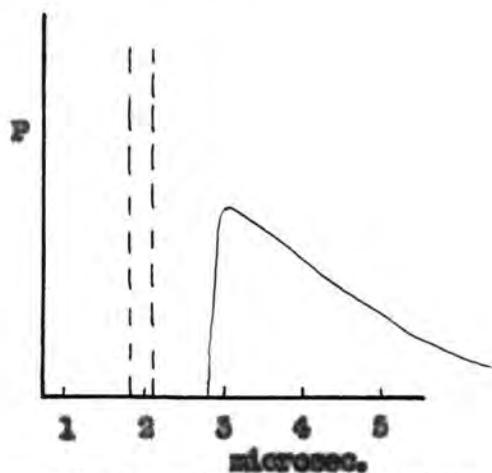
If a time t^* is taken to be the time at which the test pulse is terminated, as shown in figure 46, then n_f^* represents the number of failures to spark before this time. P for a given irradiator time is then given by $P = 1 - n_f^*/n$ and hypothetical curves can be plotted as in figure 47 to illustrate the effect of the time of release of electrons. The major difference to be expected in the curves for the three cases taken is in the position of the centre of the band of irradiator times which would give a finite value of P .

Figure 47. Expected test curves, assuming 2 microsec. electron life.

P plotted against test pulse time, with irradiator time fixed.

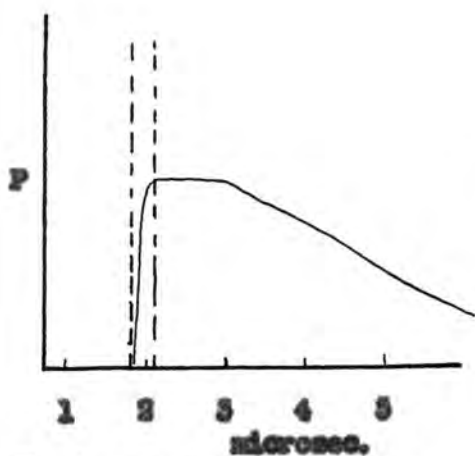


a) Instantaneous batch of electrons.

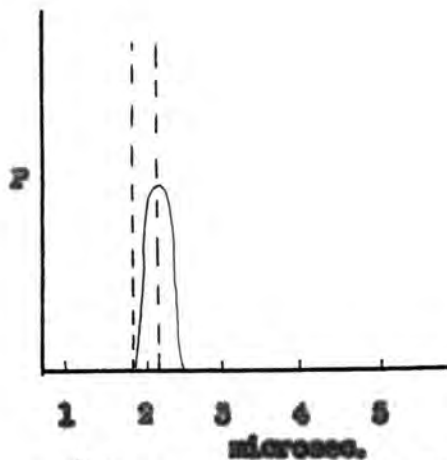


b) Delayed batch electrons.

The full line in each case depicts the rise and subsequent fall of concentration in the test gap, therefore the form of the expected sparking probability.



c) Electrons generated for a period of order 1 microsec.



d) Experimentally observed form.

7.6. The unexpected failure of irradiation.

Beside the curves of P against test pulse time shown in figure 47 for three possible modes of rise and fall of electron concentration in the gas is drawn a typical experimental curve, as it was obtained using air at atmospheric pressure. It can be seen that the range of times for which an increase in P was obtained experimentally is very small compared with the expected range. Experimental values for the range of irradiator times giving finite values of P under comparable conditions at 74 cm. Hg. pressure follow :- air, nitrogen and oxygen, 0.029 microsec., hydrogen 0.05 microsec., (for the band adjacent to the test pulse time only). All of these are much less than the duration of the test pulse, but of the same order as that which, in section 3 was termed the 'effective pulse time'. Even with the pressure of gas reduced, the range of irradiator times effective in increasing P did not extend to values as large as 0.1 microsec., before the pressure was reached at which the test spark fired independent of irradiation.

An examination is needed of the possible sources of

electron production and removal to try to account for the following observations :-

1) At atmospheric pressure in air, nitrogen and oxygen no irradiator pulse which precedes the test pulse by more than 0.02 microsec. triggers the spark. This was found to be true to the limit of the time separation of irradiator and test pulses possible with the delay lines used, 0.06 microsec.

2) Between 0.02 microsec. early and 0.01 microsec. late irradiator pulses are very successful in triggering test sparks.

7.6.1. Occasional appearance of finite sparking probability for widely separated pulses.

Hydrogen showed an abnormal rise in sparking probability for irradiator times which were much earlier than those generally found to give a finite value of P. From coincidence with the test pulse to times 0.03 microseconds earlier the irradiator caused the expected rise in P in hydrogen at atmospheric pressure; from 0.03 to 0.045 microsec. early the irradiator was quite ineffective, but from 0.045 microsec. to the early limit for the irradiator it again caused a finite P.

This unusual rise to finite sparking probability for widely separated irradiator and test pulses appeared for the higher values of X/p in nitrogen. It was also observed in the first experiments in air as is seen in figure 15. A longer delay time and further special study will be required before it can be determined whether the curve of P against irradiator time for the higher values of X/p in these gases has a second earlier irradiator time limit giving zero value of P .

7.7. Processes of removal of electrons from the gap.

a) Loss by diffusion.

The process of diffusion of electrons from the test gap is a slow one when the time for an electron to do so is compared with the least lag between irradiator and test pulses which fails to give an increased P value. In air at atmospheric pressure an electron takes about 100 microseconds to diffuse 0.5 cm. without any applied field. In the time of the pulses used here the transverse movement of electrons from the gap due to diffusion alone is less than 0.001 cm.

b) Loss by attachment.

Attachment will be of greatest importance in oxygen

and to a much smaller extent in air in discharges where the rate of growth of ionisation required is slow. In nitrogen and hydrogen the consideration of attachment can be neglected. It has been calculated that electrons can exist freely in a gas where attachment is the only process of removal for an average time given by L_0/vh ,⁹⁴ where L_0 is the electron mean free path, v the random velocity and h the normal attachment coefficient for electrons to molecules of the gas considered. The resulting value for the mean life of an electron in air at atmospheric pressure, using data of Bradbury⁹⁴ for h and Townsend's⁹⁷ values for v and L_0 , is about 2 microseconds. The life in oxygen is only one thousandth part of this. If normal attachment was likely to be an important process during short pulse discharge production then some difference ought to appear between the probability curves for oxygen and for the other common gases used, (h for air is 4×10^{-6} whereas for oxygen it is 350×10^{-6} for an electron of 2 electron volts energy). No difference between the probability curves for air and oxygen appears which is attributable to so large a factor.

c) Loss of electrons by recombination.

The number of electrons and ions distributed at random in the gas which are able to recombine depends on the square of the electron density. This process, while it might be of importance in the second stage of spark development where energetic photons are required, is not likely to exercise appreciable effect in the early stages of electron avalanche development where the number of electrons is small. There is, however, a possibility of preferential recombination between electron and parent atom if the process of production is one in which the electron does not move out of the influence of the parent atom when there is no electric field applied.

7.8. Processes of electron production that might be initiated by photons in the gas. a) Direct photo-ionisation.

Where a gas contains only one species of molecule it is not to be expected that photons, arising in another part of the gas, will be able to ionise the molecules in a single stage so as to increase the total number of ions in the gas. In a mixed gas it is evident that photons emitted

by excited molecules of the gas of higher ionising potential will possibly be sufficient in energy to ionise molecules of the other species.^{98,71} For example in air the nitrogen molecule excited to a level at 15 electron volts would, on return to the ground state, emit a quantum of 800 \AA , sufficient to ionise either the atom or molecule of oxygen. Even where gases are originally homogeneous in molecular content it has been shown that it is possible for new species of molecules to be built up in discharges. There is the possibility of dissociation of the molecular gases O_2 , H_2 and N_2 . Also in the cases of oxygen and hydrogen there can be built up the tri-atomic states.⁹⁹

b) Stepwise ionisation and auto-ionisation.

If, in the test gas, molecules are excited by photons from the irradiator spark, most of them will radiate and return to the ground state again in 10^{-7} sec. or less¹⁰⁰. The chance that an excited molecule will receive a second quantum to ionise it in this time is small, as is the chance of a collision between a pair of excited states to complete the release of an electron. Studies of Holstein and McCoubrey

have shown that for some gases there is the possibility of trapping 'resonance' radiation, which can delay the return of the excited state to normal for up to 10^{-4} of a second.¹⁰¹ Thus the probability of occurrence of a second impact to ionise the excited state, whether it occurs between another photon and the excited state or between a pair of excited states, is increased. There is no direct evidence in favour of, or against, ionisation by successive photon impacts but this is the only one of these stepwise processes which could operate in a gas which retained its homogeneity. There is evidence to show that ionisation by collision between excited states can occur.¹⁰² The mechanism here can be either the transfer of energy from one colliding atom or molecule to the other, or it can be the combination of two excited atoms to give an ionised molecule.

The case of an excited discrete state of an atom having energy in excess of ionising energy has been discussed by Burhop.¹⁰³ This can be so if more than one electron of an atom is raised above its normal energy level. A two electron radiationless transition is then possible, in which

one electron is ejected from the atom and another makes a transition to a lower energy level. This is an Auger type process¹⁰³ applied to the outer levels of the atom which determine atomic spectra and is known as auto-ionisation. While there is a high transition rate for auto-ionisation from the doubly excited states of helium the importance in gaseous discharges of this process must not be over-rated. The cross-section for double excitation of helium in electron collisions turns out to be small, only 10^{-2} of that for direct ionisation.¹⁰⁴ No measurements are known to the author of the cross-section for double excitation of other gases by electrons or photons. There is only the evidence of Beutler and Junger¹⁰⁵ that auto-ionisation occurs in the hydrogen molecular spectrum, both in emission and absorption.

Mohler, Lawrence, Edfson and Houtermans¹⁰⁶ have all observed positive ions in the alkali vapours when photons well below the long wavelength limit for direct photo-electric ionisation were used, (also see page 7). In potassium vapour up to 20 % diatomic molecules were observed, any of which could be ionised by photons emitted from the reversion of the

higher excited states of a single atom. In caesium the yield of Cs_2^+ ions was such as to indicate that resonant states of monatomic caesium were active. The probability of this action is quite large, as is suggested by the evidence of dissociative recombination of Cs_2 already available.¹⁰⁷ The studies of Hornbeck¹⁰⁸ indicate that for lower values of X/p , the production in the rare gases of He_2^+ and A_2^+ ions by collision between excited states of single atoms can be as large as the production of atomic ions by direct electron impact.

7.9. The action of the applied field and photons together.

7.9.1.

The release of an electron and recapture.

At the lower values of X/p in air, oxygen and nitrogen it appears from the test curves that irradiation and the test pulse must occur almost simultaneously if in the gas the release of a triggering electron is to occur. The failure of early irradiation at the lower values of X/p might be interpreted in several ways, namely,

a) the photons alone might be insufficient in the high pressure gas to release electrons, or

- b) the photon excited atoms in their subsequent lives might not form a sufficient fraction of the molecular population to make an ionising collision likely, or
- c) an electron, if released by the impact of a photon, might be quickly recaptured by the parent atom in a form of preferential recombination. That the application of an electric stress in the gas while it is being irradiated by a pulse of photons is sufficient to give a high sparking probability requires special consideration.

The life history of an electron immediately after its release from an atom, whether by photon impact or in some other way, has been the subject of considerable discussion.⁹⁸ Langevin's¹¹⁰ original theory contains the assumption that ions of opposite sign are at all times attracted towards each other by the Coulomb force e^2/r^2 , where r is their distance apart and e the electronic charge. Thomson¹⁰⁹ showed that if Brownian motions of the ions are considered the Coulomb force is ineffective except within a distance of ionic separation d equal to about 4×10^{-6} cm. at N. T. P. This distance is 12 times the average molecular separation

and half the molecular mean free path. The Thomson criterion is that for two ions of opposite sign to recombine after mutual attraction they must first come within the critical distance d of each other. A collision between the faster moving ion and a neutral molecule is desirable within this distance d if the ions are not to separate again on open orbits.

Preferential recombination ensues after the original pattern set by Langevin and modified by Thomson if an electron collides with a neutral molecule and attaches to form a negative ion within a distance d of the parent atom. However, the low rate of electron attachment does not permit preferential recombination in this way, except in the gases such as oxygen and then only at pressures greater than five atmospheres. At the lower pressures only a considerable reduction in the rate of diffusion of an electron near the parent atom, accompanied by a large increase in the coefficient of attachment could make preferential recombination possible.

Bradbury⁹⁵ has shown that high energy electrons sufficient to give inelastic impacts with, or perturbation of, the molecule can rapidly increase h . If an increase of 10^4

could be achieved, a one hundredfold decrease in the electron diffusion rate within the critical distance of the parent atom would give the probability of recombination finite value.

Information on the behaviour of a nascent electron within the critical distance d of the parent atom is negligible. The classical recombination theories of Langevin and Thomson, with dependence on electron attachment before a drift together to recombine, has not the speed of the mechanism required to explain the appearance of an electron only when photons in the gas and applied field coincide in time. The mechanism to be examined is one which requires a two stage removal of an electron from the influence of the nucleus of the atom. The action of photons and the applied field separately have been found to be insufficient to give the electron to trigger a discharge. But applied field and photons together have been shown to be singularly effective in supplying the initiating electrons.

7.9.2. Release of photo-electron only if an electric stress is also applied.

If there is incident upon an atom or molecule of a gas a photon of energy exactly corresponding to the ionisation energy, then an electron is removed to occupy, theoretically an orbit at infinity. If the incident quantum exceeds the ionisation energy, then the surplus energy appears as kinetic energy of the electron removed, which corresponds to a reversal of the recombination process in discharge afterglows (which gives rise to spectral lines in a wide range of wavelengths shorter than the series limit). A quantum of lower energy than that required for a complete removal of an electron to an orbit at infinity is normally considered to excite the atom, raising at least one electron to a bound orbit higher than the one it usually occupies. We usually think of the bound electron as being close to the nucleus of its parent atom compared with the distance separating adjacent atoms. But is there an outer radial limit to the position of a bound electron in an excited atom? Can electrons be raised to high order bound levels and then be

ejected by perturbations arising from a) a collision with a neutral molecule, or b) the application of a strong external electric field? The usual result of a) would be for the neutral molecule to gain some energy and the electron to lose some causing it to fall to a lower energy bound level. If the orbit of the electron is so large that the nuclear field at the orbit, computed on the ordinary inverse square law basis, is no greater than the applied field, then it is reasonable to suppose that there will be a fair chance of ejection of the electron.

The objection to this possibility b) is that the energy difference between a pair of remote orbits, e.g. of 10^{-5} and 10^{-4} cm. in diameter, is small compared with that between those of 10^{-7} and 10^{-6} cm. In fact all of the orbits where the nuclear field could be neutralized by an applied field of 30 Kv. per cm. cover a large range of diameters for a small change in excitation potential energy.

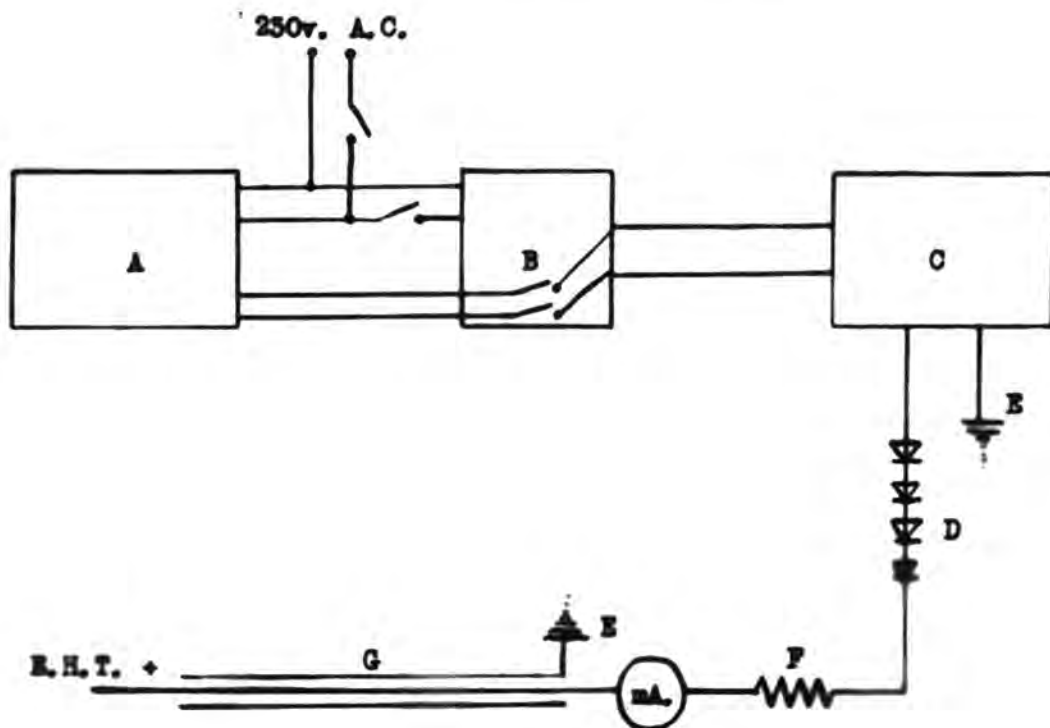
No sound reason is apparent for non-release of electrons by photons in the gas before the test field is applied. The simplest picture of the mechanism is that

on the kinetic theory. A photon incident on an atom might cause an electron to move away from the parent nucleus by a distance L_p . If at this stage the electron, in the absence of an applied field, is influenced by a neutral molecule there is the possibility that it will drop back toward the nucleus and 'recombine'. The electron so energized by a photon does not appear to be likely to make an inelastic collision of this sort unless the energy it has is almost that to remove it altogether from the parent atom. The energy it would lose in elastic collision would be so small that, according to Thomson, it would have too great a velocity of return to the parent atom and would pass it by on an open orbit. The electron would therefore begin a wandering life among the atoms and would be available to trigger a discharge during a test pulse applied in the next microsecond or so. The observation has been made that a triggering electron only appears to act when irradiation is applied at the same time as the electric field. An explanation of the non-activity of electrons, if produced by early irradiation, must be left as a further research problem.

Appendix 1.High voltage supply unit.

The diagram of figure A1 illustrates the layout of the apparatus to give a controlled supply of direct voltage up to 50 Kv. The positive output lead of the E.H.T. transformer was connected to a bank of forty metal rectifiers in series and at the negative output lead was earthed. The rectified output was then fed by way of a limiting resistor and milliammeter to a storage condenser of 500 micro-microfarads capacity, which acted as the lead from the high voltage platform to the pulse forming unit. The limiting resistor construction was done according to one of the Gemant⁷² formulae for high value liquid resistances:- 25 % Amyl Alcohol, 24 % Phenol, a drop of picric acid and Carbon Tetrachloride to make 100 %. The current drawn during a direct short circuit of the output side of the resistor to earth was 2 m. amp. and under normal working conditions the current drawn by the pulse forming circuit was never in excess of 0.5 m. amp.

Fig. A1 30 Kv. D. C. Supply Unit.



A Calibrated control.

B Contactor.

C E. H. T. Transformer.

D Rectifiers.

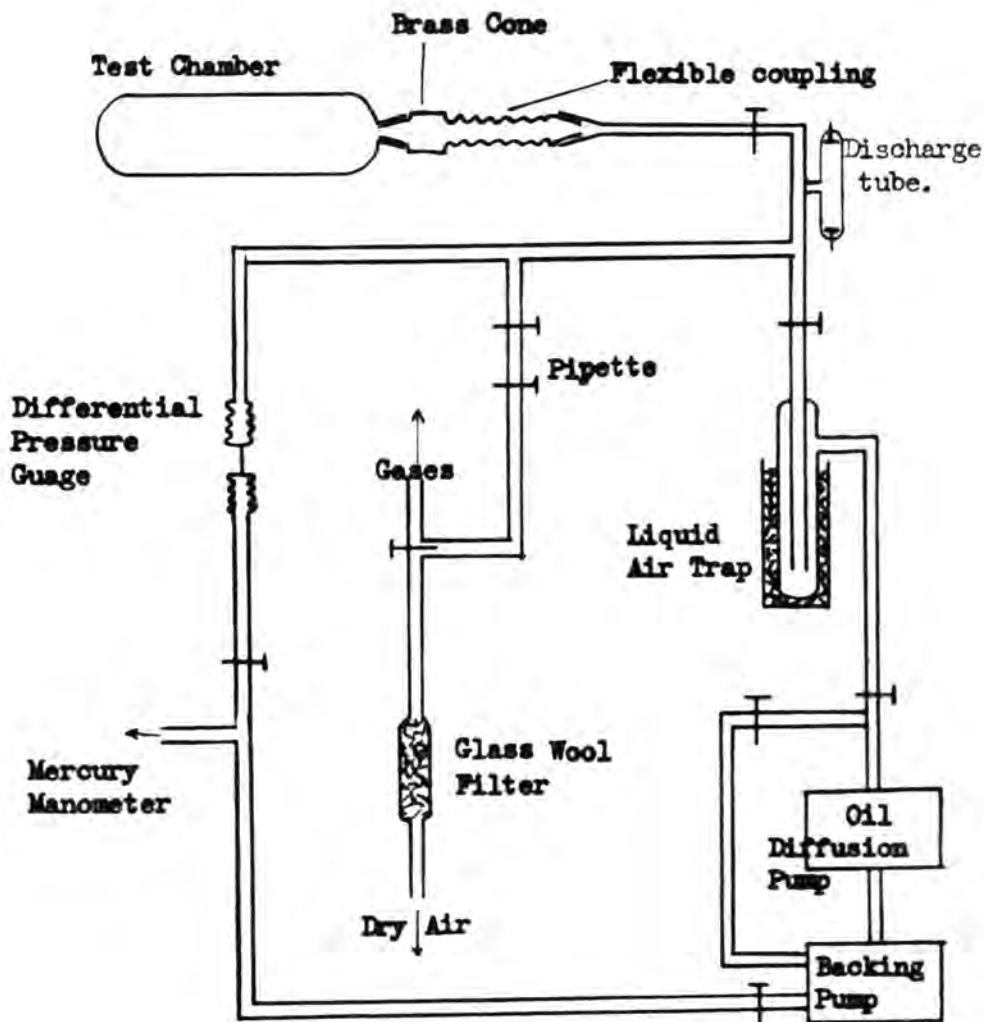
F Liquid resistor.

G Cable condenser.

Appendix 2.Ancillary vacuum plant.

A simplified layout diagram of the vacuum plant built to work in conjunction with the test chamber is shown in figure A 2a. The main requirements of the system were :-

a) that the test chamber could be quickly evacuated to a stage at which only deeply occluded gases in the metallic parts of the test apparatus remained in the system. This was indicated by the complete blackness of a discharge tube while the pumps remained cut off for an hour. At the relatively high working pressures used it would be unlikely that such gas as remained occluded would make a reappearance in sufficient quantities to diminish the purity of the cylinder commercial gases used in these exploratory experiments. A Metro-vac oil diffusion pump, with a backing pressure provided by an Edwards Speedivac rotary pump, was therefore incorporated to give a combined pumping speed of six litres/sec. at 10^{-5} mm. Hg. pressure. A tap system was arranged to allow filtered dry air, or cylinder gases, to be pipetted into the test chamber as required. The

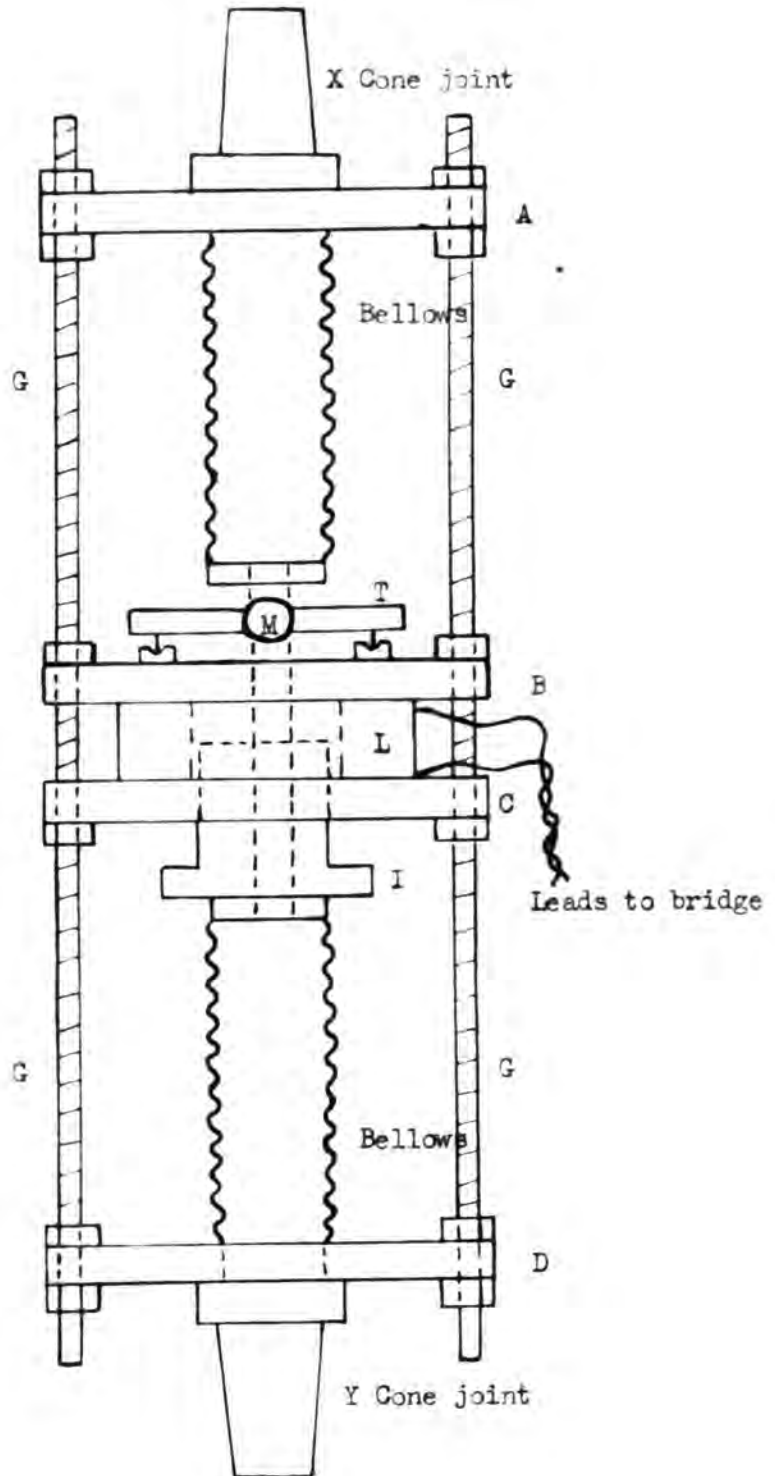
Fig. A2a. High Vacuum System.

chamber was directly coupled to the vacuum plant by way of a flexible copper tube about eight inches long, which also allowed the cone joint to the chamber to be rotated freely. This was necessary to move the irradiator mechanism without breaking vacuum.

b) There was a second requirement that the pressure in the test chamber should be easily and quickly measurable without introducing mercury contamination⁹³. It was required for this purpose to design or adapt a robust differential pressure gauge and the following kind, illustrated in figure A 3b, was constructed.

A pair of flexible metal bellows, 4.5 cm. long and 2 cm. in diameter, were connected at their sealed ends by half cm. diameter brass rod, 4 cm. long. The bellows were rigidly mounted between two Tufnol discs, A and B, which were supported by four guide rods, G. The open ends of the bellows were connected on cone joints, at X to the test vacuum and at Y to a Speedivac pump and mercury manometer. The setting of the bellows connecting rod thus depended on the degree of pressure difference between the enclosure at

Fig. A2b. Bellows differential pressure gauge.



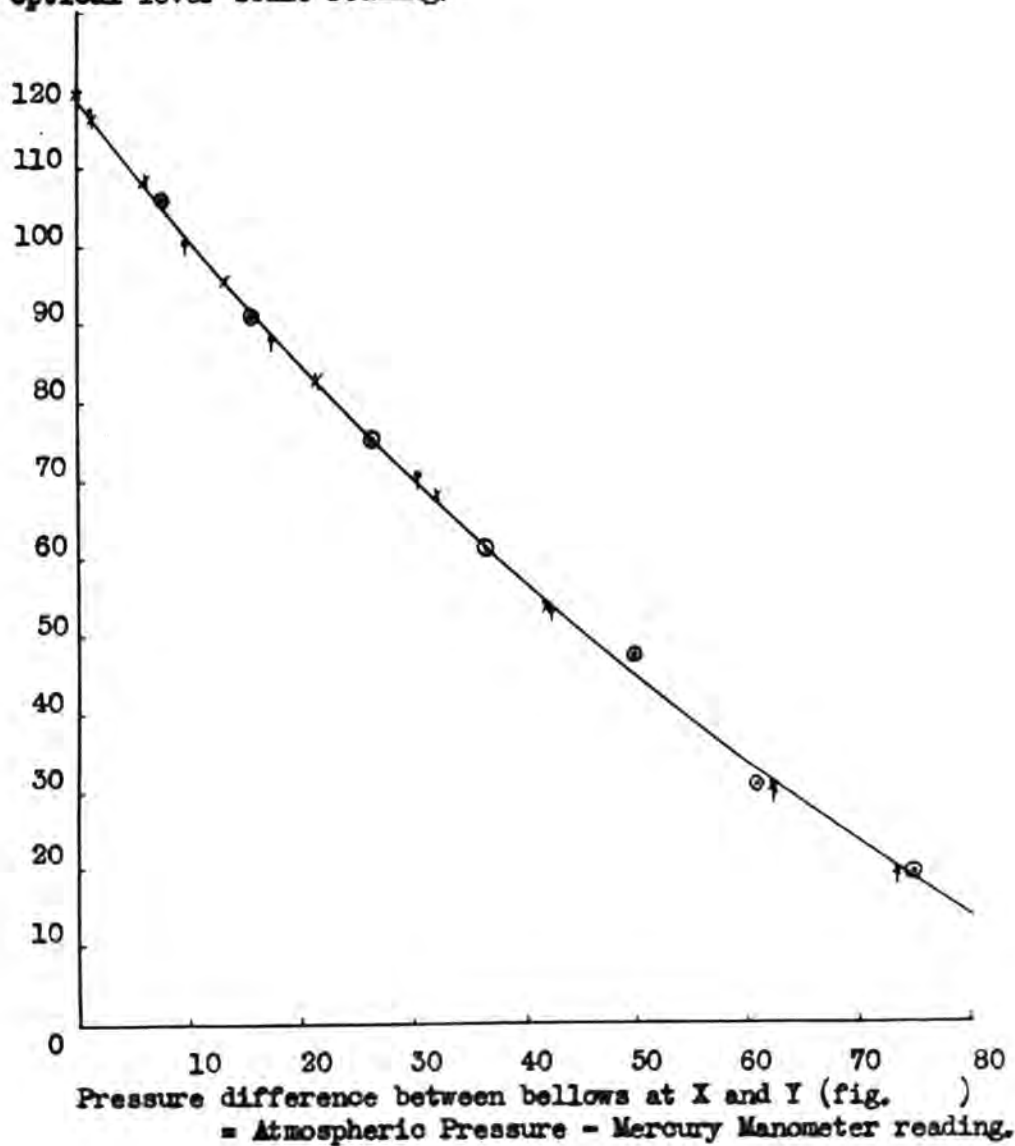
X and that at Y. This difference in pressure was indicated by an optical lever arrangement at M. The scale could be calibrated to read pressure directly provided that an initial volume of gas at known pressure was locked in the reference side of the bellows, Y. The pressure in the chamber was thus readable to half a mm. Hg.

An alternative method of calibration of the manometer more generally adopted, as it required no regular check on the vacuum tightness of the bellows, is now outlined. First both sides of the gauge were evacuated to the limiting vacuum that could be obtained by the respective pumps. In this condition the scale indication of pressure difference between the two bellows could be taken as the zero of the instrument. The mercury manometer, with one limb connected to Y and the other to the atmosphere read atmospheric pressure to check with the Fortin barometer. Air was then let into the bellows Y slowly and the difference in height of the manometer columns was plotted against the reading of the gauge. A calibration graph is shown in figure A2c. At a later stage, when the unknown pressure in the test chamber was to be

Fig. A2c. Calibration graph for the differential pressure gauge, as completed on three occasions separated by several months.

a)	Atmospheric Pressure = 75.4 cms Hg.	x
b)	" " = 75.9 cms Hg.	o
c)	" " = 76.0 cms Hg.	†

Optical lever scale reading.

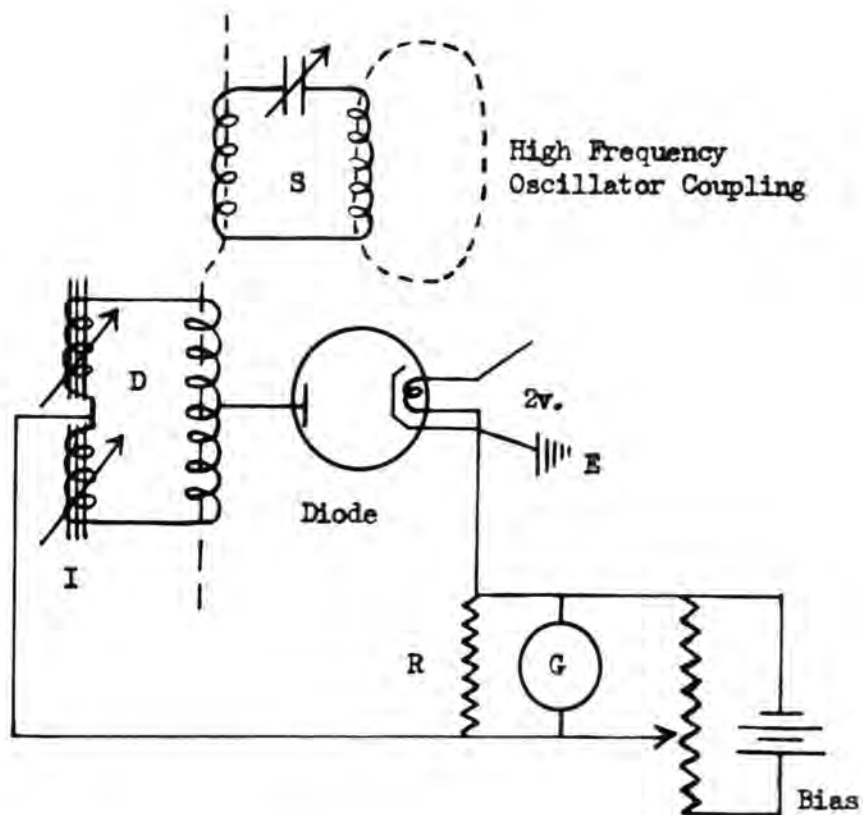


Pressure in test chamber = Atmospheric Pressure - Mercury Manometer reading - Pressure difference equivalent to Optical lever scale reading as taken from the above graph.

determined, or a gas pressure there pre-set, the side Y was left open to the atmosphere. The gauge calibration then gave the pressure difference between the bellows, which when subtracted from the current barometer pressure reading gave the value of the test chamber pressure.

Another method for indicating the movement of the connecting rod between the bellows is worthy of note. It proved rather more sensitive than was required for the present work and would have required more work to stabilise it against the electrical impulsive surges in the laboratory than was felt to be worth its immediate advantage. The position of an iron dust core, I, locked to the connecting rod, partly determined the self inductance of a small fixed coil L in the centre of which it moved. The preliminary circuit used is shown in figure A 2d. The coil was in one arm of a differential transformer bridge operated just off balance. This was supplied from a high frequency source. The additional amount out of balance of the bridge developed by the movement of the dust core, which changed L, was indicated by a galvanometer in series with a rectifying diode across the bridge arms as shown.

Fig. A2d Movement detector circuit for bellows
differential gauge.



- S Step-over tuned circuit.
- D Differential transformer bridge.
- I Iron cored inductance at bellows gauge.
- G 40 ohm galvanometer.
- R Range shunts.

BIBLIOGRAPHY.

1. Meek, J. M., *Phys. Rev.*, 57, 722, 1940.
2. Loeb, L. B., & 'The mechanism of the electric spark',
Meek, J. M., Stanford University Press, 1941.
3. Weisaler, G. L., *Phys. Rev.*, 63, 93, 1943.
4. Kerff, S. A., 'Electron and nuclear counters',
Van Nostrand, N. Y., 1946, pps. 45-48.
5. Jaffe, A. A., *Proc. Phys. Soc.*, 62, 39, 1949.
Craggs, J. D., &
Balakrishnan, G.
6. Frowse, W. A., & *Inst. Elec. Eng.*, Monograph 32, 4, 1952.
Jasinski, W.,
7. Massey, H. S. W., 'Negative ions',
Cambridge University Press, 1938, p 84.
8. Sayers, J., *Rep. Prog. Phys.*, 9, 52, 1943.
9. Appleton, E., *Proc. Roy. Soc.*, A 150, 685, 1935.
Proc. Inst. Rad. Eng., 23, 655, 1935.
10. Hughes, A. L., & 'Photoelectric phenomena',
Dufridge, L. A., McGraw-Hill, 1932, p 275.
11. Price, W. C., *Rep. Prog. Phys.*, 9, 10, 1943.
12. Hopwood, W., *Proc. Phys. Soc.*, 62, 657, 1949.
13. Craggs, J. D., & *Research*, 4, 5, 1951.
Meek, J. M.,
14. Hertz, H., *Wied. Ann.*, 51, 935, 1887.
15. Thomson, J. J., 'Conduction of electricity in gases', 2 ed.,
Cambridge University Press.

BIBLIOGRAPHY.

16. Lenard, P., *Ann. d. Phys.*, 1486, 1900., 3, 298, 1900.
17. Wilson, G. T. R., *Phil. Trans. Roy. Soc.*, 192, 403, 1899.
18. Hughes, A. L., *Proc. Camb. Phil. Soc.*, 15, 463, 1910.
19. Lyman, T., *Astrophys. Jour.*, 25, 45, 1907.
20. Palmer, F., *Phys. Rev.*, 32, 1, 1911.
21. Lenard, P., & Remusat, C., *Sitz. ber. d. Heidelberg Akad. d. Wiss.*, 1910-11.
22. Martin, M. J., *Ibid.*, 10, 1918.
23. Mohler, F. L., *Phys. Rev.*, 28, 46, 1926.
Proc. Nat. Acad. Sci., 12, 492, 1926.
24. Thomson, J., *Phil. Mag.*, 7, 970, 1927.
25. Mackay, C. A., *Ibid.*, 46, 828, 1923.
26. Morris, J. C., *Phys. Rev.*, 32, 456, 1928.
27. Varney, R. N., & Loeb, L. B., *Ibid.*, 48, 822, 1935.
28. Oldenberg, O., *Z. Physik.*, 58, 37, 1926.
29. Brode, R. B., & Neuman, L. J., 'Seminar in discharge through gases', University of California, 1928.
30. Townsend, J. S., *Phil. Mag.*, 5, 557, 1902., 6, 398 & 598, 1903.
31. Pedersen, P. O., *Ann. d. Phys.*, 71, 571, 1923.
32. Turck, J. J., *Trans. A. I. E. E.*, 47, 177, 1928., 48, 46, 1930.
33. Beams, J. W., *Jour. Frank. Inst.*, 206, 809, 1928.

BIBLIOGRAPHY.

34. Tama, R., Arch. Elektrotech., 16, 14, 1926.
35. Rogowski, W., Ibid., 20, 99, 1928.
36. Lawrence, E. O., & Dunnington, F. G., Phys. Rev., 35, 396, 1930.
36. Dunnington, F. G., Ibid., 39, 1935, 1931.
37. White, H. J., Phys. Rev., 46, 99, 1934., 42, 507, 1936.
38. Tilles, A., Ibid., 46, 1015, 1934.
39. Loeb, L. B., 'Fundamental processes of electrical discharge in gases', Wiley, 1939, p. 448.
40. Greiner, E., Z. Physik., 91, 543, 1933.
41. Gravath, A. M., Phys. Rev., 47, 254, 1933.
42. Dechens, C., J. de Phys. et Rad., 7, 533, 1936.
43. Jones, F. L., Proc. Phys. Soc., 62, 371, 1949.
44. Howell, A. H., Elec. Eng., 59, 195, 1939.
45. Trichel, G. W., Phys. Rev., 55, 382, 1939.
46. Kip, A. F., Ibid., 55, 549, 1939.
47. Flegler, E., & Raether, H., Z. Physik., 103, 305, 1936.
48. Raether, H., Z. Physik., 110, 611, 1938.
48. Costa, H., Ibid., 113, 531, 1939.
49. Schonland, B. F. G., & Collens, H., Proc. Roy. Soc., A 168, 645, 1934., A 152, 595, 1935., A 164, 132, 1938.

BIBLIOGRAPHY.

50. Allibone, T. R., & Meek, J. M., Proc. Roy. Soc., A 166, 97, 1938., A 169, 246, 1938.
51. Meek, J. M., Phys. Rev., 55, 972, 1939.
52. Cravath, A. M., & Loeb, L. B., Physics, 6, 125, 1935.
53. Loeb, L. B., See ref. 59, p. 404.
54. Loeb, L. B., & Meek, J. M., Jour. App. Phys., 11, 458, 1940.
55. Raether, H., Z. Physik., 112, 464, 1939., 117, 575 & 524, 1944.
56. Fisher, L. H., & Bedersen, B., Phys. Rev., 81, 109, 1951.
57. Loeb, L. B., Ibid., 74, 210, 1948.
58. Loeb, L. B., & Wijsman, R. A., Jour. App. Phys., 19, 797, 1948.
59. Etepian, J., & Tarok, J. J., Elec. Jour., 26, 106, 1929.
60. Tarok, J. J., Trans. A. I. E. E., 47, 177, 1928.
61. Flowers, J. W., Phys. Rev., 64, 225, 1943.
62. Dunnington, F. G., Phys. Rev. 58, 1535, 1931.
63. Komelkov, V., Bull. Akad. Sci. U. S. S. R. Dept. Tech. Sci., 8, 955, 1947. (E. R. A. Translation).
64. Komelkov, V., Doklady. Akad. Nauk., 68, 56, 1947. (E. R. A. Translation).

BIBLIOGRAPHY.

65. Saxe, R. F., & Meek, J. M., Nature, 162, 263, 1948.
66. Allibone, T. E., Jour. I. E. E., 82, 513, 1938.
67. Allibone, T. E., & Meek, J. M., Proc. Roy. Soc., A 166, 97, 1938., 169, 246, 1938.
68. Allibone, T. E., Nature, 161, 970, 1948.
69. Loeb, L. B., Jour. App. Phys., 19, 862, 1948.
70. Hemsalech, G. A., 'Recherches sur les Spectres d'Etincelles', Hermann, Paris, 1901.
71. Jones, F. L., Dutton, J., & Hayden, S. G., Proc. Roy. Soc., A 215, 185, 1952., 218, 206, 1953.
72. Gemant, A., 'Liquid Dielectrics', Wiley, N. Y., 1933, p. 66.
73. Fletcher, R. G., Rev. Sci. Instr., 20, 861, 1949.
74. & 75. See 70.
76. Prowse, W. A., & Jasinski, W., I. E. E. Monograph, 30, 7, 1951.
- 77.
78. Prowse, W. A., & Jasinski, W., See ref. 6, p. 6.
79. Strigel, R., 'Elektrische Stossfestigkeit', Edwards Bros., 1944, p. 153. See also ref. 73.
80. Tropper, H., 'Recording of Impulse Voltages', (I. E. E. Technical report).

BIBLIOGRAPHY.

82. Hughes, A. L., & Ref. 10, p. 273.
 DuBridge, L. A.,
83. Frowse, W. A., & Ref. 76, p. 8.
 Jasinski, W., Ref. 6, p. 4.
 Loeb, L. R., Ref. 39, p. 379.
84. Frowse, W. A., & Ref. 76, p. 6.
 Jasinski, W.,
85. Raether, H., Phys. Zeits., 530, 530, 1936.
86. Tessner, S., Bull. Soc. franc. des Elec., 6, 61, 1946.
87. Loeb, L. R., Jour. App. Phys., 3, 541, 1952.
88. Loeb, L. R., Ref. 87, p. 542.
 Ref. 39, p. 379.
89. Hopwood, W., Proc. Phys. Soc., 62, 657, 1949.
90. Loeb, L. R., & Ref. 2 gives a full exposition of the
 Meek, J. M., Townsend theory.
91. Ref. 2 gives a full exposition of the
 Streamer theory.
92. Wilson, R. R., Phys. Rev., 50, 1032, 1936.
93. Loeb, L. R., Ref. 39, p. 696.
94. Bradbury, M. R., Phys. Rev., 44, 865, 1933.
95. Loeb, L. R., Ref. 39, p. 280.
96. Loeb, L. R., Ref. 39, p. 86.

BIBLIOGRAPHY.

97. Townsend, J. S., 'Electrons in gases,'
Hutchinson, 1947, p. 72.
98. Penning, F. M., Naturwiss., 15, 618, 1927.
99. Penning, F. M., Phil. Mag., 11, 961, 1931.,
See also ref. 39, p. 513.
100. Loeb, L. B., Ref. 87, p. 343.
Frowse, W. A., Ref. 76, p. 10.
101. Webb, H. W., & Phys. Rev., 35, 519, 1929.
Messenger, H. A.,
101. Zemansky, M. W., Phys. Rev., 29, 513, 1927.
101. Holstein, T., Phys. Rev., 76, 1257, 1949., 85, 995, 1952.,
Alpert, D., & 72, 1212, 1947., 83, 1159, 1951.
McCoubrey, A. O.,
102. Hughes, A. L., & Ref. 10, p. 273-4.
DuBridge, L. A.,
103. Burhop, E. H. S., 'The Auger Effect',
Cambridge University Press, 1952, p. 171.
104. Burhop, E. H. S., Ref. 103, p. 173-4.
105. Beutler, H., & Z. Physik., 100, 80, 1936., 101, 285, 1936.
Junger, H. O.,
106. Loeb, L. B., 'Atomic Structure', Wiley, N. Y., 1938.
Summary of photoelectric phenomena in
Hg. and alkali vapours, Ch. 13, p. 266.
Also ref. 10, p. 249.
107. Loeb, L. B., Ref. 87, p. 348, in particular references
29.

BIBLIOGRAPHY.

108. Hornbeck, J. L., & Molnar, J. P., *Phys. Rev.*, 84, 621, 1951.
 Hornbeck, J. L., *Phys. Rev.*, 80, 297, 1950., 83, 574, 1951.,
 84, 615, 1951.
109. Thomson, J. J., *Phil. Mag.*, 47, 557, 1924.
 'Conduction of Electricity Through Gases',
 McGraw-Hill, N. Y., 1934, 2 Ed., p. 598.
110. Langevin, P., *Ann. chim. Phys.*, 28, 289 & 433, 1903.
111. Jones, F. L., & Morgan, C. G., *Proc. Roy. Soc.*, 218, 88, 1953.
- Addenda.
 106. Houterman, G., *Z. Physik.*, 41, 619, 1927.
 See also ref. 82, p. 249.